

Republic of Iraq
Ministry of Higher Education
and Scientific Research
University of Babylon
College of Engineering
Mechanical Engineering Department



Dynamic Vibration Absorber Effect on the Characteristics of Beam Vibration for Different Boundary Conditions

**A Thesis Submitted to the
College of Engineering / University of Babylon in
Partial Fulfillment of the Requirements a ward of Degree of
Master in Engineering / Mechanical Engineering / Applied**

By

Teeb Basim Abbas Hamza

Supervised By

Prof. Dr. Salwan Obaid Waheed Khafaji

2023A.D.

1444A.H.

بِسْمِ اللَّهِ الرَّحْمَنِ الرَّحِيمِ

هُوَ الَّذِي جَعَلَ الشَّمْسَ ضِيَاءً وَالْقَمَرَ نُورًا وَقَدَرَهُ مَنَازِلَ

لِتَعْلَمُوا حَدَدَ السِّنِينَ وَالْحِسَابِ مَا خَلَقَ اللَّهُ ذَلِكَ إِلَّا

بِالْحَقِّ يُفَصِّلُ الْآيَاتِ لِقَوْمٍ يَعْلَمُونَ

صدق الله العظيم

سورة يونس آية رقم ﴿٥﴾

Dedication

*To all people who light a candle in their bare hands to
make that deep darkness tunnel less lonely, and carry me to
the light.*

To my guardian angel,

My one and only ...

My Father and my Mother.

To My lovely family .

Certification

we certify that this thesis entitled “**Vibration Characteristics of Spring Resonator-metamaterial Structures**” was prepared by **Teeb Basim Abbas** Under our supervision at the University of Babylon in a partial fulfillment of the requirements for the degree of Master of Science in Mechanical Engineering (Appleid).

we recommend that this thesis be forwarded for examination in accordance with the regulation of the University of Babylon.

Signature

Prof. Dr. Salwan Obaid Waheed Khafaji

(Supervisor)

Acknowledgment

Firstly, I would like to express my gratitude and thanks to ALLAH (be glorious) for all the blessings bestowed upon me. I wish to express my deepest thanks and sincerest gratitude to my supervisor Prof. Dr. Salwan Obaid Waheed Khafaji for his guidance comments invaluable instructions, help and continuous encouragement during the preparation of my study. I would like to take this opportunity to thank Prof. Dr. Sameer jasem Al-mareb , Babylon University. for his advices and support.

Special thanks to the staff at Babylon University, mechanical engineering department for their support and teaching especially Mr. Hussein H. Rashid. last but not least special thanks and gratitude goes out to my support father and my lovely mum, my beautiful sister, and my brother, also to all my friends for their help during this work.

Teeb 2023

Abstract

Dynamic Vibration Absorbers are commonly used to reduce vibrations in mechanical systems. This work investigates the effectiveness of dynamic vibration absorbers in reducing vibrations in both a lumped system and a beam with various cross sections and boundary conditions. The study included in two parts. In the first part, a mathematical model of the lumped system is developed, incorporating two principles: negative stiffness and negative mass. Effect of several parameters on the dynamic response were investigated. A simple but effective direct research method is used to determine optimal damping ratios and frequency ratios for six mass ratio scenarios. The theoretical results show that the amplitude response of the primary response decreases dramatically as the damping ratio increases. The dynamic response of the main system is not quite sensitive to the variations of the damping ratio of the absorber compared to that of the main system. The variations of frequency and mass ratio have no effect on amplitude response when frequency ratio is less than 0.25. In addition, the difference in frequency response of the main system is smaller at smaller values of the frequency ratios and increases dramatically as this ratio increases to 1.5. The frequency ranges of the optimal designs increase as the mass ratio increases, and the maximum frequency range of 0.510 to 1.022 is attained at a mass ratio and damping ratio of 0.6 and 0.321, respectively.

In the second part, experimental studies were conducted to analyze the dynamic behavior of a beam with and without dynamic vibration absorber for different boundary conditions. (pinned-free, cantilever, and fixed-fixed). The beam is subjected to the dynamic input, and the response of the beam was measured at various locations using accelerometers. The experimental results show that both mass and stiffness have a significant effect on reducing the dynamic response up to 97%. The minimal requirements of the DVA

parameters can achieve better reduction in the dynamic response if the DVA is located at the point of maximum displacement.

Contents

List of Figures	VIII
List of Tables	XIV
Nomenclature	XV
Abstract	II
Chapter ONE (INTRODUCTION).....	
Introduction.....	1
1.2 Definition of Metamaterials	2
1.3 Types of Metamaterials.....	3
1.3.1 Electromagnetic Metamaterials	3
1.3.2 Terahertz Metamaterials	3
1.3.3 Photonic Metamaterials	4
1.3.4 Tunable Metamaterials	5
1.3.5. Elastic Metamaterial	5
1.3.5.1 Dynamic Vibration Absorber (DVA)	6
1.3.5.2 Applications of DVA	8
1.4 Present Work Objective	10
1.5 Thesis Layout	11
CHAPTER TWO (LITERATURE REVIEW)	
2.1 Introduction	13
2.2 Concluding Remarks	26
CHAPTER THREE (TEORITICAL CONSIDERATION).....	
3.1 Introduction	29

3.2 Dynamic Vibration Absorber	29
3.2.1 Metamaterials Negative Properties	29
3.2.1.1 Negative Effective Mass	29
3.2.1.2 Negative Effective Stiffness	32
3.3 Design a spring-mass absorber for vibration attenuation.	35
CHAPTER FOURE (EXPERIMANTAL SETUP)	
4.1 Introduction	42
4.2 The Main Components of the Rig	45
4.2.1 Supporting frame	45
4.2.2 D.C Motor	45
4.2.3 Mass and spring	47
4.2.4 Accelerometer Sensors	48
4.2.5 Data Acquisition (DAQ- NI 9234)	50
4.2.6 Speed control Unit and Exciter Motor	52
4.3 Experimental procedure	53
CHAPTER FIVE (RESULTS AND DISCUSSION)	
5.1 Introduction	57
5.2 Theoretical Results for the discrete system.	57
5.2.1 Negative mass	57
5.2.2 Negative stiffness	58
5.3 Application of DVA for vibration absorber	59
5.3.1 General comments	59

5.3.1.1 Effect of the damping factor ζ_1 on the dynamic response	60
5.3.1.2 Effect of the damping factor ζ_2 on the dynamic response...	62
5.3.1.3 Effect of mass ratio on the dynamic response	63
5.3.1.4 Effect of frequency ratio on the dynamic response	64
5.4 Optimal design of DVA	65
5.5 Comparison with other works	69
5.6 Experimental work	70
5.6.1 Dynamic response of Beam	71
5.6.1.1 Pinned-free boundary condition.....	71
5.6.1.1.1 Effect of stiffness	71
5.6.1.1.2 Effect of mass	78
5.6.2 Dynamic response of Beam 2	84
5.6.2.1 Pin free for the second Beam2	84
5.6.2.1.1 Effect of Stiffness	84
5.6.2.1.2 Effect of mass	90
5.6.2.2 Cantilever Boundary	95
5.6.2.2.1 Effect of Stiffness	95
5.6.2.2.2 Effect of Mass	98
5.6.2.3 Fixed-Fixed Boundary Condition	100
5.6.2.3.1 Effect of stiffness	100
5.6.2.3.2 Effect of Mass	101

CHAPTER SIX (CONCLUSIONS AND RECOMMENDATIONS).....	
6.1 Conclusions	104
6.2 Recommendations.....	105
Reference.....	106

List of Figures

Figure (1-1) Electromagnetic Metamaterials [9]	3
Figure (1-2) Terahertz (THz) metamaterials [10].....	4
Figure (1-3) Illustration of the three-dimensional carpet cloak [11]	4
Figure (1-4) Tunable metamaterial [12]	5
Figure (1-5) Elements of the single degree of freedom DVA attached to a main system	6
Figure (1-6) schematic diagram of the rolling & vibration rig [25]	8
Figure (1-7) Schematic for using DVA for reduce vibration of a wing [26].....	9
Figure (1-8) Continuous dynamic vibration absorber for oil refinery pipe applications [27]	9
Figure (3-1) mass-in-mass 2-DOF system	32
Figure (3-2) Spring-mass system with effective stiffness	33
Figure (3-3) Damped 2-DOF vibratory system	36
Figure (4-1) Experimental Test-Rig	43
Figure (4-2) Schematic diagram of experimental setup	44
Figure (4-3) Supporting frame	45
Figure (4-4) Electric motor (exciter)	46
Figure (4-5) mass and spring of suspension	47
Figure (4-6) Schematic shows sensors connection	49
Figure (4-7) Certification of the accelerometers calibration	49
Figure (4-8) DAQ system and a sample of measurements	51
Figure (4-9) Speed controller.....	52
Figure (5-1) Variations of effective mass due to variation of the frequency ratio (Ω / ω_2), $m_1 = 1kg, m_2 = (0.1 - 0.7)m_1$	58
Figure (5-2) Variations of effective spring due to variation of the frequency ratio (ω_2 / Ω), $k_1 = 100N/m, k_2 = (0.1-0.7)k_1N/m$	59

Figure (5-3) Amplitude response when $\zeta_2 = 0.2, m_r = 0.1$ for different values of damping ratio and frequency ratio, a) $\omega_r = 0.5$, b) $\omega_r = 1$, c) $\omega_r = 1.5$	61
Figure (5-4) Amplitude response when $\zeta_1 = 0.2, m_r = 0.1$ for different values of damping ratio and frequency ratio, a) $\omega_r = 0.5$, b) $\omega_r = 1$, c) $\omega_r = 1.5$	62
Figure (5-5) Amplitude response when $\zeta_1 = \zeta_1 = 0.2$, for different values mas ratio and frequency ratio, a) $\omega_r = 0.5$, b) $\omega_r = 1$, c) $\omega_r = 1.5$	63
Figure (5-6) Amplitude response when $\zeta_1 = \zeta_1 = 0.2$, for different values of frequency ratio and mass ratio, a) $m_r = 0.05$, b) $m_r = 0.1$, c) $m_r = 0.5$	64
Figure (5-7) Nonlinear effect of damping at $\zeta_1 = 0.1, m_r = 0.1, w_r = 1$	66
Figure (5-8) Effect of arbitrary damping ratio on the amplitude response when $\zeta_1 = 0.1, m_r = 0.1$ for several values of ω_r	67
Figure (5-9) Optimal values for absorber parameters for different values of mass ratio m_r	68
Figure (5-10) Optimum values for the parameters of a vibration absorber and the resulting amplitude response of $m_r=0.1$ and $\zeta_1=0.1$	69
Figure (5-11) Effect of stiffness at beam ($t=0.12m$) pin free with and without DVA at $\omega = 6.75 \pi$ rad/sec $.x/l = 1$	72
Figure (5-12) Effect of stiffness at beam ($t=0.12m$) pin free with and without DVA at $\omega = 6.75\pi$ rad/sec , $x/l = 1$	72
Figure (5-13) Effect of stiffness at beam ($t=0.12m$) pin free with and without DVA at $\omega = 6.75\pi$ rad/sec $.x/l = 1$	73
Figure (5-14) effect of stiffness at beam ($t=0.12m$) of pin free with and without DVA at $\omega = 6.75\pi$ rad/sec , $x/l = 0.5$	74
Figure (5-15) Amplitude response beam ($t=0.12$) of pin free with and without DVA at $\omega = 6.75\pi$ rad/sec, $x/l = 0.5$	74
Figure (5-16)) Amplitude response of pin free with and without DVA at $\omega = 6.75\pi$ rad/sec , $x/l = 0.5$	75

Figure (5-17) Amplitude response of pin free with and without DVA at $\omega = 6.75\pi$ rad/sec, $x/l = 0.337$.	75
Figure (5-18) Amplitude response of pin free with and without DVA at $\omega = 6.75\pi$ rad/sec, $x/l = 0.337$.	76
Figure (5-19) Amplitude response of pin free with and without DVA at $\omega = 6.75\pi$ rad/sec, $x/l = 0.337$.	76
Figure (5-20) effect of mass at beam of pin free with and without DVA at $\omega = 6.75\pi$ rad/sec, $x/l = 1$.	78
Figure (5-21) effect of mass at beam of pin free with and without DVA at $\omega = 6.75\pi$, $x/l = 1$.	79
Figure (5-22) effect of mass at beam of pin free with and without DVA at $\omega = 6.75\pi$ rad/sec, $x/l = 1$.	79
Figure (5-23) Fig (5.23) effect of mass at beam of pin free with and without DVA at $\omega = 6.75\pi$ rad/sec, $x/l = 0.5$.	80
Figure (5-24) effect of mass at beam ($t=0.12m$) of pin free with and without DVA at $\omega = 6.75\pi$ rad/sec, $x/l = 0.5$.	81
Figure (5-25)) effect of mass at beam ($t=0.12m$) of pin free with and without DVA at $\omega = 6.75\pi$ rad/sec, $x/l = 0.5$.	81
Figure (5-26) Amplitude response of pin free with and without DVA at $\omega = 6.75\pi$ rad/sec, $x/l = 0.337$.	82
Figure (5-27) Amplitude response of pin free with and without DVA at $\omega = 6.75\pi$ rad/sec, $x/l = 0.337$.	82
Figure (5-28) Amplitude response of pin free with and without DVA at $\omega = 6.75\pi$ rad/sec, $x/l = 0.337$.	83
Figure (5-29) effect of stiffness at pin free with and without DVA at $\omega = 8.1\pi$ rad/sec, $x/l = 1$.	85
Figure (5-30) effect of stiffness at pin free with and without DVA at $\omega = 8.1$ rad/sec, $x/l = 1$.	85

Figure (5-31) effect of stiffness at pin free with and without DVA at $\omega = 8.1\pi \text{ rad/sec}$, $x/l = 1$	86
Figure (5-32) effect of stiffness at pin free with and without DVA at $\omega = 8.1\pi \text{ rad/sec}$, $x / l = 0.5$	86
Figure (5-33) effect of stiffness at pin free with and without DVA at $\omega = 8.1\pi \text{ rad/sec}$, $x / l = 0.5$	87
Figure (5-34) the effect of stiffness at pin free with and without DVA at $\omega = 8.1\pi \text{ rad/sec}$, $k = 140.2, 377.3 \text{ N/m}$, $m = 500 \text{ g}$, $x / l = 0.5$	87
Figure (5-35) effect of mass of pin free with and without DVA at $\omega = 8.1\pi \text{ rad/sec}$, $x / l = 0.337$	88
Figure (5-36) effect of mass of pin free with and without DVA at $\omega = 8.1\pi \text{ rad/sec}$, $x / l = 0.337$	88
Figure (5-37) effect of mass of pin free with and without DVA at $\omega = 8.1\pi \text{ rad/sec}$, $x / l = 0.337$	89
Figure (5-38) the effect of mass at pin free with and without DVA at $\omega = 8.1\pi \text{ rad/sec}$, $x/l = 1$	90
Figure (5-39) the effect of mass at pin free with and without DVA at $\omega = 8.1\pi \text{ rad/sec}$, $x/l = 1$	90
Figure (5-40) the effect of mass at pin free with and without DVA at $\omega = 8.1 \text{ rad/sec}$, $x = 1$	91
Figure (5-41) the effect of mass at pin free with and without DVA at $\omega = 8.1\pi \text{ rad/sec}$, $x / l = 0.5$	92
Figure (5-42) the effect mass at pin free with and without DVA at $\omega = 8.1 \pi \text{ rad/sec}$, $x / l = 0.5$	92
Figure (5-43) the effect mass at pin free with and without DVA at $\omega = 8.1\pi \text{ rad/sec}$, $x / l = 0.5$	93
Figure (5-44) the effect of mass at pin free with and without DVA at $\omega = 8.1\pi \text{ rad/sec}$, $x / l = 0.377$	93

Figure (5-45) the effect mass at pin free with and without DVA at $\omega = 8.1\pi$ rad/sec, $x / l = 0.337$ 94

Figure (5-46) the effect of mass at pin free with and without DVA at $\omega = 8.1\pi$ rad/sec , $x / l = 0.337$ 94

List of Tables

Table (4-1) Specifications of the accelerometer	48
Table (4-2) NI Cdaq-9234 technical info	50
Table (5.1) Optimal values of absorber parameters for six cases of mass ratio (m_r) and at $\zeta_1=0.1$	64
Table (5.2) effect of stiffness at cantilever beam with and without DVA at $\omega = 16.5 \pi$ rad/sec , $x/l = 1$	96
Table (5.3) effect of stiffness at cantilever beam with and without DVA at $\omega = 16.5 \pi$ rad/sec , $x/l = 0.5$	97
Table (5.4) effect of mass at cantilever beam with and without DVA at $\omega = 16.5 \pi$ rad/sec , $x/l = 1$	99
Table(5.5) the effect of Stiffness at Fixed-fixed beam with and without DVA at $\omega = 30$ rad/sec , $x/l = 0.5$	101
Table(5.6) the effect of mass at Fixed-fixed beam with and without DVA at $\omega = 30$ rad/sec , $x/l = 0.5$	102

Nomenclature

Symbol	Definition
$u(t)$	Unit step function
F	excitation harmonic forces
$F(s)$	Laplace transform of forcing
a	acceleration
$F(t)$	External force
i, j	Unit vector
k	Stiffness
m	Mass
$H(\Omega)$	Frequency response function
$H_{ij}(\Omega)$	Amplitude response function of inertial element i to force applied to inertial element j
$\dot{u}(t)$	Velocity
$\ddot{u}(t)$	acceleration
$[m]$	Mass matrix
$[k]$	Stiffness matrix
c	Damper vector
$[C]$	Damper matrix
m_r	Mass ratio , m_2 / m_1
ω_r	Frequency ratio , ω_2 / ω_1
ω	Excitation frequency , rad / s
Ω	Excitation frequency
k_{32}	Stiffness ratio , k_3 / k_2
c_{32}	Damping ratio , c_3 / c_2

CHAPTER ONE

INTRODUCTION

CHAPTER ONE

INTRODUCTION

1.1 Background

Vibration is a pervasive phenomenon in human activities. Light waves vibrate to enable vision, while eardrums vibrate to facilitate hearing. In engineering, the effects of vibration are considered in the design of machines, buildings, turbines, and engines. Vibration, or oscillation, refers to any repeated motion over time. A vibration system typically comprises a mechanism to store potential energy, such as a spring or elastic property, a means to store kinetic energy, such as mass or inertia, and a way to gradually release energy, such as a damper. The vibration system transforms potential energy into kinetic energy and vice versa in a cyclical fashion. However, if the system is damped, energy dissipates during each cycle of vibration, requiring an external source to maintain the system's continuous vibration.

Most vibrations are considered undesirable due to their negative consequences such as elevated stress levels, energy loss, fatigue, reduced efficiency, and others. Excessive vibration in a system often leads to disruption, discomfort, damage, or even destruction. To prevent such outcomes in machinery or structures, it is necessary to control unwanted vibrations. One effective solution is to use what they called by Metamaterials for vibration attenuation [1-3]. A brief introduction about metamaterials will be introduced in the next section.

1.2 Definition of Metamaterials

Metamaterials are engineered materials with unique properties not found in nature, derived from specially designed microstructures rather than the inherent properties of the constituent materials. They are often composed of single or multiphase conventional materials arranged in low-dimensional repetitive patterns, and the term "meta" in "metamaterial" comes from the Greek word meaning "beyond" or "advanced" [4, 7].

In 1968, metamaterials were first introduced in the study of materials exhibiting negative electromagnetic properties such as negative electric permittivity and magnetic permeability. While such properties are absent in natural materials, no natural materials with negative dynamic acoustic properties have been found [5]. The term "metamaterial" was coined by Rodger M. Walser of the University of Texas at Austin in 1999, initially defined as "Macroscopic composites having a synthetic, three-dimensional, periodic cellular architecture designed to produce an optimized combination, not available in nature, of two or more responses to specific excitation" [6]. Not all aspects of metamaterials are captured by previous definitions. Metamaterials are composites made up of periodic or non-periodic structures whose properties arise from both their cellular architecture and chemical composition. For a metamaterial to be considered an effective medium, its cellular size must be sub-wavelength or smaller. Effective medium theory describes metamaterials that have a sub-wavelength unit cell [7]. There are several types of metamaterials in the real world applications, a brief introduction about these materials and applications is illustrated in the next section.

1.3 Types of Metamaterials

Based on the usage and applications, metamaterials can be divided into several types, they are:

1.3.1 Electromagnetic Metamaterials

Metamaterials have emerged as a new subfield in physics and electromagnetism, with particular applications in optics and photonics [8]. They are utilized for optical and microwave purposes, including beam steering, modulation, filtering, lensing, microwave coupling, and antenna. By possessing structural elements smaller than the wavelength of the electromagnetic waves they interact with, metamaterials impact electromagnetic radiation as shown in Fig. 1.1 [9].

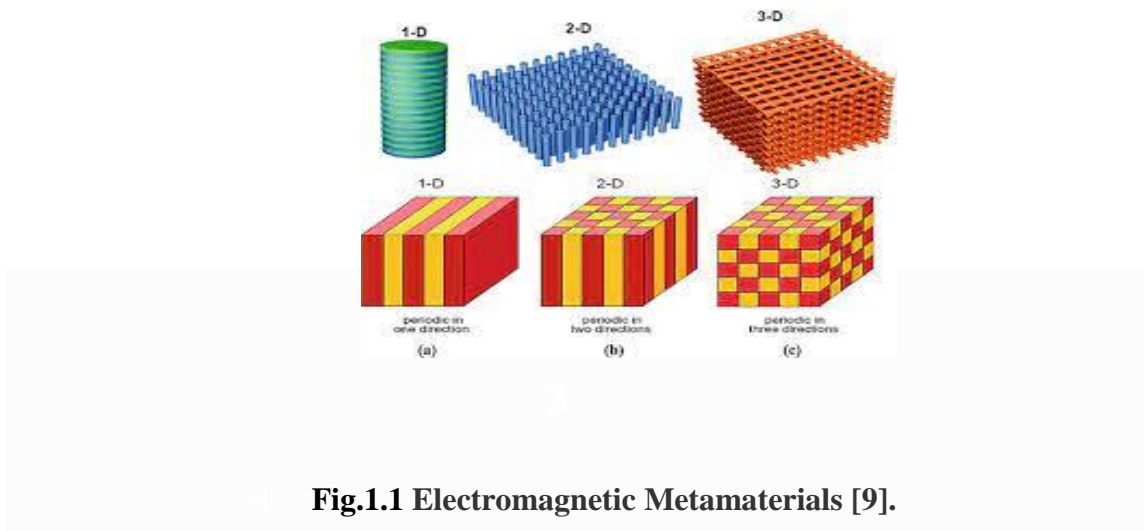


Fig.1.1 Electromagnetic Metamaterials [9].

1.3.2 Terahertz Metamaterials

Terahertz metamaterials interact with electromagnetic waves at frequencies between 0.1 to 10 THz, corresponding to wavelengths between 3 mm (EHF band) and 0.03 mm (long-wavelength edge of far-infrared light). These materials are studied and applied in fields such as optics and photonics. THz-TDS is commonly used to measure and analyze the frequency characteristics of THz metamaterials. A simple design of this type is presented in Fig. 1.2 [10]

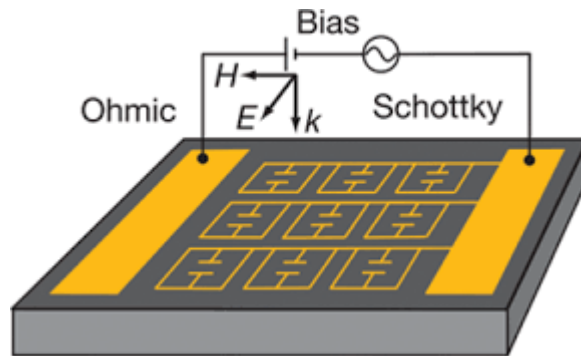


Fig.1.2 Terahertz (THz) metamaterials [10]

1.3.3 Photonic Metamaterials

A photonic metamaterial is a man-made periodic structure, as shown in Fig. 1.3, that interacts with optical frequencies and has a subwavelength period, distinguishing it from a photonic band gap structure [11].

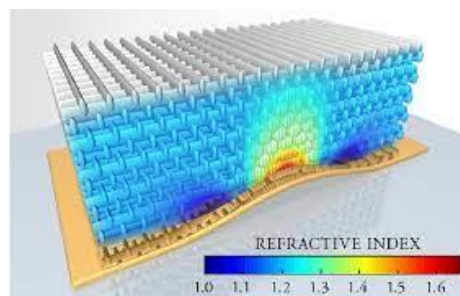


Fig.1.3 Illustration of the three-dimensional carpet cloak [11]

1.3.4 Tunable Metamaterials

A tunable metamaterial is a type of metamaterial that allows for arbitrary adjustments in the refractive index at different frequencies. Such materials typically use individual resonators, such as split-ring resonators, that are strongly coupled to transmission lines or antennas. These metamaterial-inspired devices can serve as proof of concept or final applications for the design [12]. An example about this type is presented in Fig. 1.4.

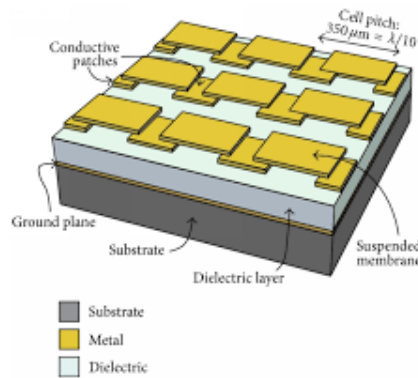


Fig.1.4 Tunable metamaterial [12].

1.3.5. Elastic Metamaterial

Only recently did scientists begin to study metamaterials in-depth due to the discovery of negative permittivity and permeability in some artificial materials, which are not found in nature. This discovery has inspired engineers to design new materials that surpass the performance limitations of conventional materials [13]. Elastic metamaterials (EMMs) have gained attention in recent decades due to their unique properties [14, 15]. EMMs manage elastic waves in deformable solids, while acoustic metamaterials manage acoustic waves in fluids. Due to the fact that both manage elastic

waves within the audible frequency range (20 Hz to 20 kHz), some researchers refer to EMMs as acoustic metamaterials [16].

EMMs are man-made materials designed to manipulate elastic waves by utilizing a locally resonant mechanism between propagating acoustic/elastic waves and the microstructure of the material. These materials exhibit unique properties, such as negative effective stiffness and negative effective mass density, similar to the way EMs exhibit negative permittivity and permeability. These properties have been explored for various applications, including seismic waveguides, sound absorption, and vibration suppression [17, 18].

While EMs exhibit their properties by having much smaller distances between atoms/molecules than the wavelength of electromagnetic waves, EMMs exhibit their properties by having much smaller distances between atoms/molecules than the wavelength of elastic waves. EMMs are typically fabricated by assembling periodic mechanical subunits into a naturally occurring material to introduce a locally resonant response to propagating waves, which can alter the wave's speed, direction, and wavelength. The geometry of EMM subunits is often constrained since these models are only valid for wavelengths longer than their overall size. Popular research topics related to EMMs include acoustic absorbers, elastic wave absorption [19], and structural vibration mitigation by using dynamic vibration absorber (DVA) [20]. Definition and applications of the dynamic vibration absorber will be given next.

1.3.5.1 Dynamic Vibration Absorber (DVA)

DVAs are mechanical devices used to reduce or control the amount of vibration or oscillation of a system. The main purpose of a DVA is to reduce the amplitude of the vibrations of a structure, by absorbing and

dissipating energy, and altering the natural frequency of the structure. DVAs consist of a mass-spring-damper system that is attached to the main structure. The absorber is designed to vibrate in opposition to the vibration of the main system, thereby reducing or eliminating the vibrations. [21-23]. A simple design for the DVA is presented in Fig. 1.5 below. The mass (m_1) represents the mass of the main system need to be controlled under effect of the external forced vibration excitation defined by the force $F = F_0 e^{i\Omega t}$, while the mass (m_2) and the spring (k_2) are the mass and the elastic elements of the DVA, respectively. In general, DVAs can be designed not only in single degrees of freedom, but also by two or higher degrees of freedom based on the requirements and complexity of structures.

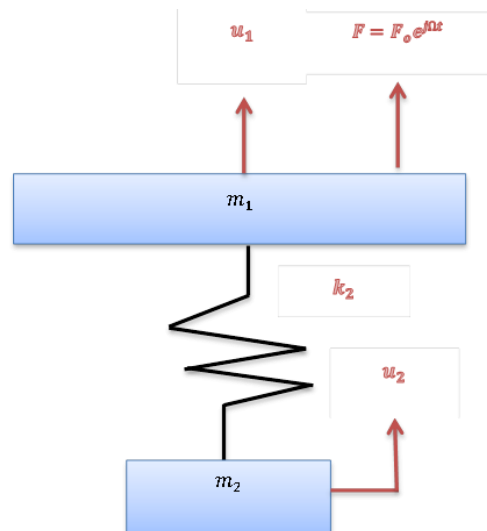


Fig. 1.5 Elements of the single degree of freedom DVA attached to a main system

The design of the DVA depends on the type of structure being controlled and the frequency of the vibration. A well-designed DVA can effectively control the vibration of a structure, even under varying loading conditions. The mass of the absorber is an important factor in the design of the DVA. It is usually chosen to be a fraction of the mass of the structure

being controlled. The stiffness of the spring and the damping ratio of the damper (damping is considered) are also critical factors in the design of the DVA [24].

In addition to reducing the amplitude of vibrations, DVAs can also help to increase the lifespan of a structure. Vibrations can cause fatigue and damage to the structure, leading to reduced lifespan. By reducing the vibrations, the DVA can help to prevent damage and extend the life of the structure.

1.3.5.2 Applications of DVA

DVAs are commonly used in engineering and industrial applications, such as in the automotive and aerospace industries. For example, in the automotive industry, DVAs are used to reduce the vibration of engine components by attaching a relatively small mass at a specific locations, thereby reducing noise and improving the durability of the components.

To reduce body vibration in high-speed electric multiple units (EMUs), a dynamic vibration absorber (DVA) was employed. The suspension characteristics, including suspension frequency, damping ratio, mounting location, and mass, had a significant effect on the vibration of both the car body and equipment. A small DVA is attached at the man body of the car to control its response as shown in Fig. 1.6 [25].

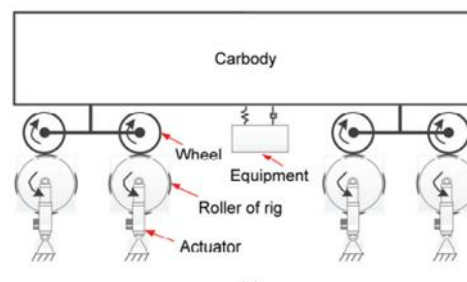


Fig.1.6 schematic diagram of the rolling & vibration rig [25].

In the aerospace industry, DVAs are used to reduce the vibration of aircraft components, such as wings as shown in Fig. 1.7 [26].

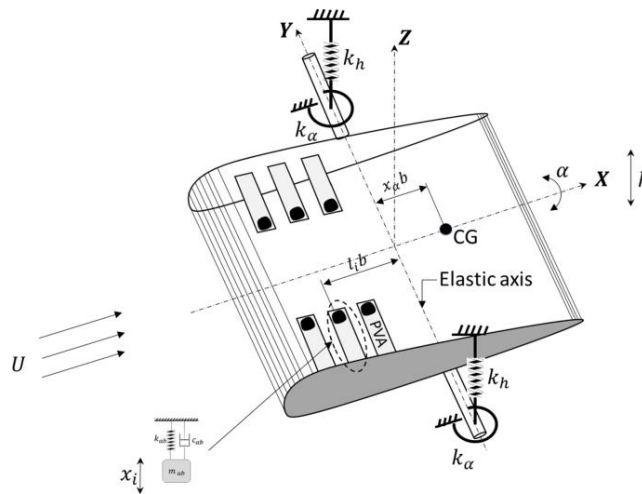


Fig. 1.7 Schematic for using DVA for reduce vibration of a wing [26].

Dynamic vibration absorber was also introduced by a continuous stiffness rather than a discrete spring. For example, a concentric mass attached at a specific location on a cantilever beam was used for vibration attenuation of a large pipe system as shown in Fig. 1.8 below [27].



Fig.1.8: Continuous dynamic vibration absorber for oil refinery pipe applications [27]

In summary, dynamic vibration absorbers are mechanical devices that are used to reduce the amount of vibration or oscillation of a structure. They work by absorbing and dissipating energy, altering the natural frequency of the structure, and vibrating in opposition to the vibration of the main system. DVAs are an effective tool for reducing the amplitude of vibrations, increasing the lifespan of a structure, and improving the performance of mechanical systems.

1.4 Present Work Objective

- 1- To understand the principles of dynamic vibration absorbers, including their design, operation, and effectiveness in reducing vibration levels.
- 2- To learn how to analyze and model the behavior of dynamic vibration absorbers, including the impact of factors such as mass, stiffness, and damping.
- 3- To gain knowledge of related topics, such as vibration analysis, modal analysis, and finite element analysis, which are relevant to the design and implementation of dynamic vibration absorbers.
- 4- To explore the impact of various factors on the performance of dynamic vibration absorbers, such as the amplitude and frequency of vibrations, the properties of the absorber (e.g., mass and stiffness), and the location of the absorber.
- 5- To run experimental work to understand the real behavior of a dynamic vibration absorber attached to a beam with three boundary conditions and several cross sectional area.

1.5. Thesis Layout

This thesis is organized in six chapters:

Chapter One: presents some of the basic definitions concerned with the dynamic vibration absorbers, their importance, and applications. The objectives and the aim of the current work are also presented.

Chapter Two: contains a brief review of previous studies on the subject under consideration.

Chapter Three: presents the details of the theoretical consideration of the discrete dynamic vibration absorber in details and how to be executed to obtain the optimum design, in addition to structural consideration analyses concerned with the free vibration, and dynamic analyses.

Chapter Four: presents the experimental work of the dynamic vibration absorber attached to a beam for different boundary conditions and cross sections. Complete description for the tools and measurement used in the experiment is presented.

Chapter Five: presents the results of the analytical and experimental works based on the effective parameters studied accordingly.

Chapter six: gives a summary of conclusions which can be drawn from this work and the suggestions for future.

CHAPTER TWO
LITERATURE REVIEWS

CHAPTER TWO

LITERATURE REVIEW

2.1 Introduction

Dynamic vibration absorbers (DVAs) have been extensively studied in recent years as a highly effective solution for controlling vibrations in various engineering applications. DVAs are passive devices that are attached to a vibrating structure to reduce its amplitude and improve its stability. Dynamic vibration absorber (DVA) have continuous increasing usage in primary and secondary applications for vibration attenuation of real life applications owing to their superior functions, easy to install, and low unit cost, as mentioned previously

Based on this, numerous studies have investigated the effectiveness and performance of DVAs in various applications, including mechanical and civil engineering, aerospace, and automotive industries. Based on this, DVA has attracted many research workers and has been considerably improved to achieve realistic results.

Despite the significant progress made in DVA research, there are still some challenges that need to be addressed. For instance, the optimal design of DVAs is still an active area of research, with many studies focusing on finding the optimal mass and stiffness of the device [28]. In addition, the effectiveness of DVAs in real-world applications is affected by various factors, such as the level of damping in the system, the type of excitation, and the mounting location of the DVA [29]. The study of literature on DVA is essential for engineers and researchers who want to design and implement effective vibration control systems. It helps them to

understand the concept, optimize the design, evaluate the performance, and choose the best parameters for a given application. It also allows them to stay up-to-date with the latest advancements in the field and to consider the environmental and safety impacts of their designs. Some of these literatures will be introduced in the next section.

P. FRANK PAI.(2010)[30] investigated longitudinal metamaterial bars as elastic wave absorbers for controlling the vibration wave frequencies. A cantilever bar of length 1 m with different boundary conditions was studied. The elastic bar was modeled by several unit cells of spring and mass attached together to maintain the bar. The time response due to the external excitation was determined theoretically. The results revealed that discrete unit cell models based on integration and finite difference can only be employed for elastic waves with wavelengths substantially greater than the length of the unit cell. A metamaterial-based elastic absorber was revealed to be based on the concept of traditional mechanical vibration absorbers. Negative effective mass and negative effective stiffness principles were discussed as well.

G.L.Huang et al.(2010)[31] explored a multi-resonator mass-in-mass lattice system's dispersion curves. The lattice system's unit cell is made up of three distinct masses connected by linear springs. The findings showed that by altering the spring constant and the magnitude of the internal masses, the frequency and dynamic responses can be adjusted. The effective mass was discovered to become negative for frequencies in the band gaps when utilizing the traditional single mass lattice model as an analogous system. Stiffness and masses of the lattice affected the response and energy dissipation.

M.H. Zainulabidin and N. Jaini.(2012)[32] performed an experimental analysis to determine the transverse vibration of a fixed-fixed

end beam attached with dynamic vibration absorbers (DVA). The DVA is made out of a flexible beam with two masses positioned symmetrically on either side of it. The DVAs were then joined to the fixed end beam after it had been secured to a static frame structure. An electric shaker transversely excites the harmonic excitation of the beam's one side. The beam amplitudes prior to and following the connection of the absorbers were compared and discussed. The experimental findings showed that the DVA greatly reduced the beam structure's vibration amplitude by absorbing the beam vibration.

G. Gantzounis et al.(2013)[33] investigated analytically the response of a one-dimensional metamaterial for vibration dissipation that utilized local resonances to filter the excitation of the low frequency. In order to check the validity of the analytical modeling, an experimental investigation was illustrated as well. Resonance nonlinear behavior was investigated by means of addition nonlinear spring. To match the experimental system's driving amplitude, the theoretical results have been scaled by a constant factor. The results showed that employing numerous frequencies of the same structure to block vibrations at different frequencies could be a viable vibration mitigation strategy.

Hao Peng et al. (2014)[34], presented a modified metamaterial beam for broadband vibration absorption by using multi-frequency vibration absorbers. Finite element method was used for the analytical modeling of the beam. The terms "negative effective mass" and "effective stiffness" were used interchangeably. The presented concept was supported by numerical examples. The results showed that the used boundary conditions (B.Cs) showed insignificant effect on the absorption of high-frequency response. However, they showed a critical impact in case of the low frequency vibration.

SHI HuaiLong et al. (2014)[35] used the dynamic vibration absorber (DVA) theory to reduce vibration in the car body. The electronics mounted on the chassis was thought of as a DVA, and the car body was treated as an Euler-Bernoulli beam. Based on the modal analysis of the beam and parameter optimization of the DVA, suspension parameters of the apparatus were optimized. To investigate the impact of the suspension parameters on the vibration of the car body, vertical motion equations of the car body and equipment were developed. The governing equations included the suspension frequency, damping ratio, and mounting position. The findings demonstrate that the apparatus installed on the car body chassis may be viewed as a DVA to lessen the flexible vibration of the car body, and that the ideal suspension frequency can be theoretically estimated taking into account the first-order vertical bending mode of the car body. Light equipment has a very small impact on vibration reduction, however heavy equipment should be installed as near to the car body center as possible.

SHUYI JIANG. (2015)[36] presented modeling and analysis strategies for designing metamaterial beam as elastic wave absorbers. Tiny subsystems are attached to an isotropic beam at different spots to create an acoustic metamaterial beam. To determine the stopband of a metamaterial beam, dispersion analysis and frequency response analysis were used. The concept of negative effective mass was discussed. This idea was also applied to the creation of a multi-stopband metamaterial beam capable of absorbing broadband elastic waves. The findings revealed that the amplitude response of the beam significantly affected by selecting a suitable values of the beam as a dynamic vibration absorber. Elastic waves can be controlled by controlling choosing a suitable values of metamaterial beam parameter.

Hao Peng et al. (2015)[37] designed acoustic multi-stopband metamaterial plates for broadband elastic wave absorption and vibration suppression. They integrated two-degree of freedom (DOF) mass–spring subsystems with an isotropic plate to act as vibration absorbers to create the metamaterial plate. A working unit was modeled using the extended Hamilton's principle for an infinite metamaterial plate without damping, and two stopbands were observed by dispersion analysis on the averaged three-DOF model. Frequency response analysis and transient analysis were used to study stopbands. The effects of absorber resonant frequencies and damping ratios, plate boundary conditions and dimensions, and effective plate-absorber vibration modes were all explored exhaustively. The metamaterial plate was largely based on the concept of conventional vibration absorbers. According to the findings, altering the absorber mass and/or reduce the average mass of the isotropic plate in each working unit increased the bandwidth of each stop band. A sensitivity analysis of absorber resonant frequencies was carried out, and the two stopband regions showed reasonably high sensitivity.

Livia Cveticanin et al. (2016)[38] studied theoretically metamaterials and their applications in vibration absorption. The acoustic metamaterials must have negative effective (dynamic) mass in order to enable vibration elimination at a specific frequency due to the analogy with these materials. The motion of an externally excited mass-in-mass system, where the mass-spring unit is responsible for the vibration elimination at a specific frequency, were used to explain the idea of negative effective mass. These vibration absorber modules were used to create the acoustic metamaterial beams. The manner in which the units were fastened to the beam determined Beams formed of acoustic metamaterial to be vibration absorber units. The structure may absorb waves in one direction (for

example, longitudinal waves) or waves in two directions (for example, transversal and longitudinal waves), depending on how the units were linked to the beam. Also, based on the frequency the characteristics of the absorber units One, two, or many frequency gaps could be produced by the acoustic metamaterial beams.

Yongquan Liu et al. (2016) [39] utilized the monoatomic lattice system with linear on-site potential to design elastic metamaterials with a low frequency passband. The theoretical and numerical results of the transmittance of the system with finite unit cells were achieved. Waves can only propagate in the tunable passband, it was demonstrated. There were two types of elastic metamaterials with twin passbands that developed. For locally resonant type metamaterial, great wave attenuation performance can be produced at frequencies between the two passbands. In practice, when designing band-pass filters, a structure with the same mass at both ends was recommended. It demonstrated how to design two-dimensional (2D) metamaterials. COMSOL MULTIPHYSICS was used to create the dispersion curves.

M. H. Zainulabidin et al. (2016)[40] examined theoretically the idea of tuned vibration absorbers applied to a beam structure using finite element analysis. Depending on where they were attached, the tuned vibration absorbers had four different conditions for being attached to the fixed-fixed end beam. Prior to that, modal analysis has been done to obtain the natural frequency and mode shape. Then, using harmonic analysis, the impact of tuned absorber positions on beam vibration characteristics was investigated. When the absorbers were placed close to the fixed end, the amplitudes of the beam's first and second modes of vibration were reduced by 99.9% and 99.8%, respectively.

Muhammad Mohamed Salleh et al. (2016)[41] investigated the effectiveness of a lightweight dynamic vibration absorber (LDVA) in reducing vibration in thin-walled structures. The study involved performing free and forced vibration response analyses using the finite element method. Ansys workbench 14.5 was then used to conduct a detailed analysis of the effects of single and dual LDVAs on the plate. The results showed that a single LDVA attached at the center of the plate successfully attenuated vibration over a frequency range of 0-600 Hz. On the other hand, dual LDVAs only suppressed the resonance of the first, second, and fourth modes, but not the third and fifth modes of the thin-walled structure. Additionally, the study found that simply increasing the mass of the LDVA did not improve vibration absorption across the entire frequency range. Based on the findings, the study concluded that single LDVAs were more effective than dual LDVAs for reducing vibration in thin-walled structures across the entire frequency range.

T. WANG et al. (2017)[42] presented an acoustic metamaterial that comprised a damped plate with resonators (DVAs) attached in parallel. The problem was studied analytically and the free and forced vibration analyses were considered. The fixed plate was fixed in all sides. The results showed that the metamaterial plate can produce multiple resonant-type band gaps, where the lower-bound frequency of each gap coincides with the resonance frequencies of the resonators. In addition, it was noteworthy that damping significantly affected the system frequencies, particularly the damping of the resonators. Specifically, in practical engineering applications, damping cannot be neglected. The damping of the host plate smoothed and lowered the responses in the entire frequency range, especially in the higher frequency range.

Antoniadis I.A et al. (2017)[43] proposed K-Damping concept which replaces the internally resonating masses with negative stiffness elements. This concept exploited the negative stiffness damping phenomenon and eliminated the need for heavy locally added masses. Classical modal analysis to the one-dimensional mass-in-mass lattice was analyzed, and corresponding dispersion relations were derived. The preliminary results showed significant advantages over the conventional mass-in-mass lattice, such as broader band-gaps and increased damping ratio. The presented concept showed a significant potential in seismic meta-structures and low-frequency acoustic isolation-damping.

Ying Li et al. (2017)[44] demonstrated an experimental study for design mechanical metamaterials for simultaneous mechanical vibration attenuation and energy harvesting using finite element analysis and a 3D printing. The mechanical metamaterials consisted of a square array of free-standing cantilevers with piezoelectric properties attached to a primary vibrated frame. The strong coupling of the bulk elastic wave propagating along the structural frame and the distributed local resonance associated with the square array of piezoelectrically active cantilevers created a complete bandgap. External vibration energy was trapped and transferred into the kinetic energy of the cantilevers, which was further converted into electric energy through mechano-electrical conversion of its integrated piezoelectric elements, operating within the stop-band. The designed mechanical metamaterials achieved two distinct functions, vibration isolation, and energy harvesting, simultaneously. The results showed that metamaterials achieved a good reduction in vibration response of the vibrated structure.

Sheng Sang et al. (2018) [45] presented comprehensive study of a two-dimensional acoustic metamaterial based on mass-in-mass lattice

model with both one resonator and multi-resonators. The dynamic property of a two-dimensional lattice system and the existence of multiple stop bands of mass-in-mass lattice systems with more than one resonator were demonstrated analytically. A two-dimensional stable lattice structure, composed of unit mass-in-mass cells, was proposed and studied by adapting both an exact model and a continuum model. The dispersion surfaces and stop band obtained by the exact model showed that the stop band of this metamaterial existed. In contrast, the dispersion surface obtained through the continuum model described the acoustic mode well, but was only accurate at low frequencies response. By attaching a secondary resonator to the primary resonator, an additional stop band was achieved.

Arnaldo Casalotti et al. (2018)[46] Examined the capacity of a nonlinear metamaterial beam to absorb multi-mode vibration. The frequency response of the metamaterial beam was obtained to study a multi-frequency stop band system by adding an array of embedded nonlinear local resonators. The dynamic behavior of the metamaterial beam was first investigated via the classical approach used for periodic structures, which determined the frequency stop bands of a single cell. The best frequency-response curves of the metamaterial beam in the nonlinear regime were obtained using a route following technique combined with a differential evolutionary optimization algorithm.

Sheng Sang et al. (2018)[47] focused on a single-phase elastic metamaterial featuring for vibration and elastic wave suppression. The resonator was made up of a cylindrical central core, surrounded by evenly distributed ligaments, and embedded in a matrix arranged in a square lattice. The study achieved both theoretically and experimentally. The findings showed that the translational resonance of the unit cell produced

negative effective mass, while the rotational resonance created negative effective modulus. When these resonances worked together, they generated double-negative effective material properties. This elastic metamaterial also exhibited wave attenuation due to its negative effective mass. The findings established a theoretical foundation for the design of single-phase elastic metamaterials.

William R et al. (2018)[48] analyzed several resonance-based metamaterial concepts using analytical models and finite element analysis as potential retrofits or replacements for elastic supports in heavy machinery, specifically large generators. One such concept involved using grounded resonators to create a mechanical high pass filter that reduces vibration at the frequency of interest. The resonators consisted of mass and spring systems work like a DVAs. Another concept targeted a significant contributing rotational mode of the generator to reduce longitudinal vibration of the supports indirectly. These concepts successfully reduced off-resonance operating frequencies of the generator at the low frequency range of heavy machinery. The simulations demonstrated that resonance-based metamaterial concepts effectively reduced vibration transmission at operating frequencies of heavy machinery.

Guangxu Dong et al. (2018)[49] presented the development of a nonlinear dynamic vibration absorber (NDVA) with negative stiffness to broaden the bandwidth and suppress resonance in vibration absorption. The NDVA was equipped with a magnetic negative stiffness spring (MNSS), which composed of three magnet rings arranged in attraction and connected in parallel with a mechanical spring. The magnetic force and stiffness of the MNSS were studied, and the dynamic equations of the coupled system were established by attaching the NDVA to the main mass. The averaging method was used to analyze the dynamic responses. To achieve optimal

vibration absorption performance of the NDVA, an iterative algorithm was proposed for parameter optimization to reduce time consumption. The results showed that the optimization algorithm significantly improved the efficiency of parameter selection, resulted in a remarkable vibration attenuation for the primary system and a broader bandwidth for vibration absorption.

W. S. Ong et al.(2019)[50] analyzed the vibration characteristics of a fixed-end beam using dynamic vibration absorbers (DVAs) attached to the beam using finite element method. The DVAs were attached to the fixed-end beam at vibrational nodes and antinodes for three vibration modes. Modal and harmonic analysis were performed to determine the beam's natural frequency and frequency response, respectively. The simulation results showed a reduction in vibration response of the beam, particularly when the DVA was attached at the optimal locations. The DVA amplitude increased as the beam amplitude decreases. The study confirmed that increasing the number of DVAs did not affect the percentage reduction of vibration amplitude as long as they were placed at the optimum location.

Winner Anigbogu et al. (2020)[51] presented a magnetomechanical metamaterial construction capable of both vibration attenuation and energy harvesting. The metamaterial dual-function structure prototype was built. The proposed structure consisted of local resonators (DVAs) arranged periodically combining cantilever beams and permanent magnetcoil systems. The results revealed that the model simulation and the experiment were in good agreement. The metamaterial structure's vibration attenuation and energy harvesting properties were linked, according to the findings. In addition, the metamaterial structure shown here improved the electric power generation significantly by vibration energy harvesting.

Yubao Song et al.(2020)[52] investigated the vibration and sound properties of a type of metamaterial sandwich panels. The panels consisted of a host sandwich panel and periodically attached resonant units, and both panels with and without damping were considered. The effects of the periodic design on vibration, sound radiation, and sound transmission properties were analyzed numerically by comparing metamaterial and bare panels. The study showed that the periodic design significantly reduces vibration and sound over a wide frequency range, which was larger than the reduction obtained by increasing the mass. Experimental specimens of bare and metamaterial sandwich panels were designed and tested, and the reduction was observed in a wide frequency range. Additionally, the effects of structural parameters of sandwich panels on the reduction of vibration and sound properties from periodic design were investigated. The study revealed that the periodic design generated a nice reduction of vibration for panels with various parameter settings, and the reduction characteristics were changed accordingly.

Yubao Song et al. (2020)[53] investigated the vibration and acoustic properties of a type of metamaterial sandwich panel. These panels consisted of a standard sandwich panel combined with resonant components at regular intervals (DVAs). The study focused on the effects of a periodic design on wave propagation, vibration, sound radiation, and sound transmission properties. Numerical analysis was used to compare the performance of the metamaterial sandwich panels with standard sandwich panels, with a particular emphasis on the reduction of vibration and sound. The results indicated significant reductions in vibration, sound radiation, and sound transmission across a wide frequency range. Experimental specimens of both standard and metamaterial sandwich panels were designed, evaluated, and compared. The experimental results confirmed the

numerical findings, and the impacts of different structural parameters on vibration and sound reduction were examined in detail. The study also investigated the underlying reasons for the observed reductions in vibration and sound qualities, as well as other potential consequences of using a periodic design.

Huihuang Bao et al.(2021)[54] explored the use of metamaterials as a means of mitigating structural vibrations that can negatively impact a structure's performance and safety. This work proposed an enhanced dual-resonator metamaterial beam (DRMB), which utilized a series dual-resonator with a spring-connected rigid body at the free end. The mass and frequency response of the DRMB and were derived and the theoretical dispersion relation was derives analytically using a transfer matrix method. The study analyzed the impact of the number of cells, mass ratio, and spring stiffness ratio on the DRMB's bandgap and transmissibility performance. The experimental results confirmed the theoretical model and showed that the DRMB's bandgap and vibration suppression performance significantly enhanced in the low-frequency range with an increase in the number of cells, mass ratio, and spring stiffness ratio. The dual-resonator with three springs was effective in suppressing beam vibration.

Rupesh Tatte and Vishal Dhende.(2022)[55] investigated the use of a DVA to reduce the overall vibrations of a fixed-fixed Euler-Bernoulli beam subjected to forced excitation. The theoretical solution used to determine the optimal resonance frequency of the DVA to reduce vibration to a large extent. An experimental test was conducted to validate the theoretical results, which showed that a single DVA can reduce amplitude by around 80-85% theoretically and 75-80% experimentally. It was noted that the DVA locations is a critical factor in vibration response of the beam.

In addition, vibration reduction was maximum when the DVA located close to the point of maximum displacement.

2.2 Concluding Remarks

Based on the deep studying of the literature above, important conclusions can be drawn when studying dynamic vibration absorbers (DVA). Some of these conclusions must be taken into consideration, including:

- 1- Characteristics of the primary structure: The characteristics of the primary structure, such as its mass, stiffness, and damping, can affect the design and performance of the DVA. Therefore, it is essential to consider the primary structure's characteristics when designing and optimizing the DVA. The optimal values of these parameters will be determined for both analytical and experimental analysis in this work.
- 2- Frequency range of vibration: The frequency range of vibration that the DVA is designed to reduce is a critical consideration. It is important to choose the correct design parameters, such as the mass ratio, damping ratio, and frequency ratio, to ensure that the DVA effectively reduces vibrations in the desired frequency range. The above parameters will be determined in this work.
- 3- Performance evaluation: It is important to evaluate the performance of the DVA to ensure that it is effective in reducing vibrations in the desired frequency range. Performance evaluation can be done through analytical, numerical, or experimental methods.
- 4- Operating conditions: The operating conditions of the primary structure or equipment can affect the performance of the DVA. For instance, if the primary structure experiences varying loads or forces,

the DVA must be designed to accommodate these changes. Therefore, harmonic analysis will be studied in this work.

- 5- System complexity: The complexity of the DVA system can affect its performance and cost. A more complex DVA system may be more effective in reducing vibrations, but it may also be more costly to design and implement. Simple but efficient DVA will be adopted in the present work for both analytical and experimental work.
- 6- The principles of negative stiffness and negative mass were used and verified by several works. Based on that, these principles will be adopted in the presented work.

Overall, the design and implementation of a DVA system require careful consideration of the primary structure's characteristics, frequency range of vibration, environmental factors, cost, performance evaluation, and safety. By taking these factors into consideration, engineers can design and implement effective and efficient DVA system.

Chapter Three

Theoretical consideration

CHAPTER TREE

THEORETICAL CONSIDERATION

3.1 Introduction

In this section, an introduction about the dynamic vibration absorbers is introduced. The conventional two degrees of freedom system and beam with several dynamic vibration absorbers are studied. The conventional dynamic vibration absorber is studied and the mathematical model along with their differential equations from scratch for fully understand the principle of vibration reduction of the main mass or main system (beam structure). The next step is to use finite element method and its formulations to formulate element stiffness and mass matrices for the beam structure with the dynamic vibration absorbers. Description about element that used in this work, its nodes, degrees of freedom, and element mass and stiffness matrix are presented as well.

3.2 Dynamic Vibration Absorber

3.2.1 Metamaterials Negative Properties

A brief introduction about negative mass and negative spring is presented in this section in order to explain effect of these properties on the vibration characteristics of the system.

3.2.1.1 Negative Effective Mass

Consider the two degree-of-freedom (2-DOF) mass-in-mass system represented in Fig. (3.1) exposed to harmonic excitation.

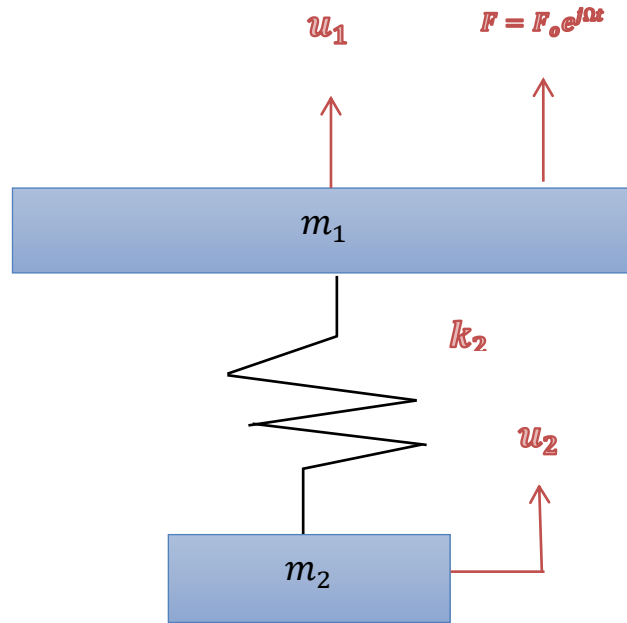


Figure (3.1) mass-in-mass 2-DOF system

The equations of motion, frequency response functions (FRFs) H_{11} and H_{22} between the response $u_1(t)$ and $u_2(t)$ and the input harmonic force $F(t)$, are given by:

$$+\uparrow \sum F = m_1 \ddot{u}_1 \quad \dots(3.1)$$

$$m_1 \ddot{u}_1 + k_2(u_1 - u_2) = F(t) \quad \dots(3.2)$$

$$+\uparrow \sum F = m_2 \ddot{u}_2 \quad \dots(3.3)$$

$$m_2 \ddot{u}_2 - k_2(u_1 - u_2) = 0 \quad \dots(3.4)$$

$$\begin{bmatrix} m_1 & 0 \\ 0 & m_2 \end{bmatrix} \begin{Bmatrix} \ddot{u}_1 \\ \ddot{u}_2 \end{Bmatrix} + \begin{bmatrix} k_2 & -k_2 \\ -k_2 & k_2 \end{bmatrix} \begin{Bmatrix} u_1 \\ u_2 \end{Bmatrix} = \begin{Bmatrix} F(t) \\ 0 \end{Bmatrix}, \quad \dots(3.5)$$

Take L.T for Eq (3.2) and Eq (3.4) will produce

$$m_1 s^2 u_1(s) + k_2(u_1(s) - u_2(s)) = F(s) \quad \dots(3.6)$$

$$m_2 s^2 u_2(s) - k_2(u_1(s) - u_2(s)) = 0 \quad \dots(3.7)$$

From Eq (3.7)

$$u_2(s) = \frac{k_2}{(m_2s^2+k_2)} u_1(s) \quad \dots(3.8)$$

Sub eq (3.8) in to Eq (3.6)

$$(m_1s^2 + k_2)u_1(s) - k_2 \frac{k_2}{(m_2s^2+k_2)} u_1(s) = F(s) \quad \dots(3.9)$$

$$u_1(s) = \frac{(m_2s^2+k_2)}{(m_1s^2+k_2)(m_2s^2+k_2)-k_2^2} F(s) \quad \dots(3.10)$$

Sub Eq (3.10) to Eq (3.8)

$$u_2(s) = \frac{k_2}{(m_1s^2+k_2)(m_2s^2+k_2)-k_2^2} F(s) \quad \dots(3.11)$$

$$F \equiv F_0 e^{j\Omega t}, \begin{Bmatrix} u_1 \\ u_2 \end{Bmatrix} \equiv \begin{Bmatrix} a_1 \\ a_2 \end{Bmatrix} e^{j\Omega t} \quad \dots(3.12)$$

$$u_1(j\Omega) = \frac{(m_2(j\Omega)^2+k_2)}{(m_1(j\Omega)^2+k_2)(m_2(j\Omega)^2+k_2)-k_2^2} F_0 e^{j\Omega t} \quad \dots(3.13)$$

$$u_1 = \frac{(k_2 - m_2\Omega^2)}{(k_2 - m_1\Omega^2)(k_2 - m_2\Omega^2) - k_2^2} F_0 e^{j\Omega t}$$

$$u_2(j\Omega) = \frac{k_2}{(m_1(j\Omega)^2+k_2)(m_2(j\Omega)^2+k_2)-k_2^2} F_0 e^{j\Omega t}$$

$$u_2 = \frac{k_2}{(k_2 - m_1\Omega^2)(k_2 - m_2\Omega^2) - k_2^2} F_0 e^{j\Omega t} \quad \dots(3.14)$$

$$\begin{Bmatrix} u_1 \\ u_2 \end{Bmatrix} \equiv \begin{Bmatrix} a_1 \\ a_2 \end{Bmatrix} e^{j\Omega t}$$

$$\text{if } n = 1, H_{11} \equiv \frac{a_1}{F_0} = \frac{k_2 - m_2\Omega^2}{(k_2 - m_1\Omega^2)(k_2 - m_2\Omega^2) - k_2^2} \quad \dots (3.15)$$

$$\text{if } n = 2, H_{21} \equiv \frac{a_2}{F_0} = \frac{k_2}{(k_2 - m_1\Omega^2)(k_2 - m_2\Omega^2) - k_2^2}$$

For more convenience, the following terms are simplified as:

$$\tilde{m}_1 \equiv \frac{F}{\ddot{u}_1} = \frac{F_0}{-\Omega^2 a_1} = m_1 + \frac{m_2}{1 - \frac{\Omega^2}{\omega_2^2}}, \omega_2 \equiv \sqrt{\frac{k_2}{m_2}} \quad \dots(3.16)$$

Where m_1 and m_2 are the principal and absorber masses, respectively. F is the excitation harmonic forces applied at the principal mass. u_1 and u_2 are the degrees of freedom of principal and absorber mass, respectively. Ω is the excitation frequency, $j \equiv \sqrt{-1}$, $\dot{u}_1 \equiv du_1/dt$, t is time, and ω_2 is the resonance frequency of the added absorber representing by the stiffness k_2 and mass m_2 . The effective mass \tilde{m}_1 is calculating by considering the presented system in Fig. 1 as a single degree of freedom instead of two degrees of freedom. If $\Omega = \omega_2$, Eqn. (3.16) shows that $|\tilde{m}_1|$ is ∞ , and

$$H_{11} = u_1(t) = 0, F_0 = -k_2 a_2 \quad \dots(3.17)$$

$$F(t) = -k_2 u_2(t) = m_2 \ddot{u}_2(t) \quad \dots(3.18)$$

That simplification means the inertia force of the mass of absorber ($-m_2 \ddot{u}_2$) has cancelled the effect of the external force by the presence of the spring k_2 , which considers as a good point to start to imply that the time response of the principal mass is $u_1(t) = 0$. The zero response of this mass is the main key of vibration reduction concept by using the vibration absorber. In addition, the presented explanation discloses that for a specific characteristics of the harmonic excitation as noticed in Eqn. (3.17), the term a_2 increases as absorber mass m_2 decreases.

3.2.1.2 Negative Effective Stiffness

Similar analogy to the negative effective mass can be used to demonstrate the negative effective spring. To do that, consider the 2-DOF system illustrated in Fig.(3.2)

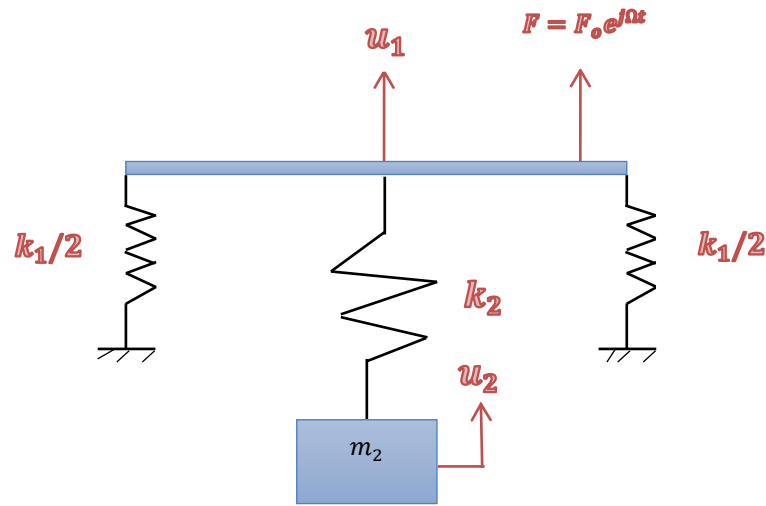


Figure (3.2) Spring-mass system with effective stiffness

This system is similar to the figure presented in Fig. (3.1). However, another spring k_2 is added as two sub springs at the left and right ends of the principal mass. The equations of motion and the corresponding magnification factors $H_{n1}(\Omega)(n = 1,2)$ are given by:

$$+\uparrow \sum F = m_1 \ddot{u}_1 \quad \dots(3.19)$$

$$-\frac{k_1}{2}u_1 - \frac{k_1}{2}u_1 - k_2(u_1 - u_2) + F = 0 \quad \dots(3.20)$$

$$(k_1 + k_2)u_1 - k_2u_2 = F \quad \dots(3.21)$$

$$+\uparrow \sum F = m_2 \ddot{u}_2 \quad \dots(3.22)$$

$$k_2(u_1 - u_2) = m_2 \ddot{u}_2 \quad \dots(3.23)$$

$$m_2 \ddot{u}_2 - k_2(u_1 - u_2) = 0 \quad \dots(3.24)$$

$$\begin{bmatrix} 0 & 0 \\ 0 & m_2 \end{bmatrix} \begin{Bmatrix} \ddot{u}_1 \\ \ddot{u}_2 \end{Bmatrix} + \begin{bmatrix} k_1 + k_2 & -k_2 \\ -k_2 & k_2 \end{bmatrix} \begin{Bmatrix} u_1 \\ u_2 \end{Bmatrix} = \begin{Bmatrix} F \\ 0 \end{Bmatrix} \quad \dots(3.25)$$

Take L.T for Eq. (3.21) and Eq. (3.24) will produce

$$(k_1 + k_2)u_1(s) - k_2u_2(s) = F(s) \quad \dots(3.26)$$

$$m_2 s^2 u_2(s) - k_2 u_1(s) + k_2 u_2(s) = 0 \quad \dots(3.27)$$

$$u_2(s) = \frac{k_2}{(m_2s^2+k_2)} u_1(s) \quad \dots(3.28)$$

Sub Eq. (3.28) to Eq. (3.26)

$$(k_1 + k_2)u_1(s) - k_2 \frac{k_2}{(m_2s^2+k_2)} u_1(s) = F(s)$$

...(3.29)

$$u_1(s) = \frac{(m_2s^2+k_2)}{(k_1+k_2)(m_2s^2+k_2)-k_2^2} F(s) \quad \dots(3.30)$$

Sub Eq. (3.30) to Eq. (3.28)

$$u_2(s) = \frac{k_2}{(k_1+k_2)(m_2s^2+k_2)-k_2^2} \quad \dots(3.31)$$

$$F \equiv F_0 e^{j\Omega t}, \begin{Bmatrix} u_1 \\ u_2 \end{Bmatrix} \equiv \begin{Bmatrix} a_1 \\ a_2 \end{Bmatrix} e^{j\Omega t} \quad \dots(3.32)$$

$$u_1(j\Omega) = \frac{(m_2(j\Omega)^2+k_2)}{(k_1+k_2)(m_2(j\Omega)^2+k_2)-k_2^2} F_0 e^{j\Omega t}$$

$$u_1 = \frac{k_2 - m_2\Omega^2}{(k_1+k_2)(k_2 - m_2\Omega^2) - k_2^2} F_0 e^{j\Omega t} \quad \dots(3.33)$$

$$u_2(j\Omega) = \frac{k_2}{(k_1+k_2)(m_2(j\Omega)^2+k_2)-k_2^2} F_0 e^{j\Omega t}$$

$$u_2 = \frac{k_2}{(k_1+k_2)(k_2 - m_2\Omega^2) - k_2^2} F_0 e^{j\Omega t} \quad \dots(3.34)$$

$$\begin{Bmatrix} u_1 \\ u_2 \end{Bmatrix} \equiv \begin{Bmatrix} a_1 \\ a_2 \end{Bmatrix} e^{j\Omega t} \quad \dots(3.35)$$

$$\text{if } n = 1, H_{n1} = \frac{a_1}{F_0} = \frac{k_2 - m_2\Omega^2}{(k_1+k_2)(k_2 - m_2\Omega^2) - k_2^2} = \frac{1}{\tilde{k}_1}$$

$$\text{if } n = 2, H_{n1} = \frac{a_2}{F_0} = \frac{k_2}{(k_1+k_2)(k_2 - m_2\Omega^2) - k_2^2} \quad \dots(3.36)$$

For more convenience, the following terms are simplified as:

$$\tilde{k}_1 \equiv \frac{F}{u_1} = \frac{F_0}{a_1} = k_1 + \frac{k_2}{1 - \omega_2^2/\Omega^2}, \omega_2 \equiv \sqrt{\frac{k_2}{m_2}} \quad \dots(3.37)$$

Where, \tilde{k}_1 is the effective spring when the presented system is considered as a single degree of freedom instead of two degrees of freedom. Similar condition of the negative mass concept can be used here for qualifying the effect of added spring. That means, if $\Omega = \omega_2$, Eqn. (3.37) shows that $|\tilde{k}_1| \rightarrow \infty$, and,

$$H_{11} = u_1 = 0 \quad \dots(3.38)$$

$$F(t) = -k_2 u_2(t) = m_2 \ddot{u}_2(t) \quad \dots(3.39)$$

This simplification means that the mass of absorber ($-m_2 \ddot{u}_2$) has cancelled the effect of the external force by the presence of the spring k_2 , and hence, $u_1(t) = 0$. This also reveals that for a specific harmonic excitation with $\Omega = \omega_2$, $a_2 (= -F_0/k_2 = -F_0/(m_2 \Omega^2))$ increases when m_2 decreases. More importantly is that when the $k_2/(\omega_2^2/\Omega^2 - 1) > k_1$ for $\Omega < \omega_2$, the effective value of the stiffness \tilde{k}_1 becomes negative (negative stiffness). It is important to explain that when $\tilde{k}_1 < 0$ and $\Omega < \omega_2$, a developed downward force built up in the spring pulled against $F(t)$ is presented and can be given by:

$$k_2(a_1 - a_2) = F_0(\tilde{k}_1 - k_1)/\tilde{k}_1 \quad \dots(3.40)$$

This force is greater than the force F_0 according to Eqn. (3.40). This conclusion explains the negative value of the stiffness.

3.3 Design a spring-mass absorber for vibration attenuation.

The responses of vibratory systems characterized by linear multi-degree-of-freedom systems can be determined in the same way as the responses of vibratory systems defined by linear single-degree-of-freedom systems can. As a result, the information offered here serves as a foundation for the subsequent discussions of vibration absorbers to explain

the main design parameters that can be used to design an efficient spring-mass absorber.

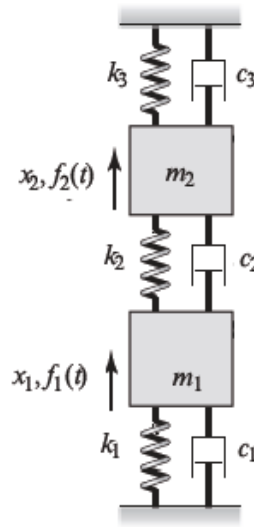


Fig. (3.3) Damped 2-DOF vibratory system

Dynamic response

The governing differential equations of the physical system described by fig.(3.3) can be determined using Newton’s second law as follow:

$$+\uparrow \sum F = m_1 \ddot{x}_1$$

...(3.41)

$$-k_1 x_1 + k_2(x_2 - x_1) - c_1 \dot{x}_1 + c_2(\dot{x}_2 - \dot{x}_1) + f_1(t) = m_1 \ddot{x}_1$$

$$-k_1 x_1 + k_2 x_2 - k_2 x_1 - c_1 \dot{x}_1 + c_2 \dot{x}_2 - c_2 \dot{x}_1 + f_1(t) = m_1 \ddot{x}_1 \quad \dots(3.42)$$

$$m_1 \ddot{x}_1 + (c_1 + c_2) \dot{x}_1 - c_2 \dot{x}_2 + (k_1 + k_2)x_1 - k_2 x_2 = f_1(t)$$

$$+\uparrow \sum F = m_2 \ddot{x}_2 \quad \dots(3.43)$$

$$-k_2(x_2 - x_1) - k_3 x_2 - c_2(\dot{x}_2 - \dot{x}_1) - c_3 \dot{x}_2 + f_2(t) = m_2 \ddot{x}_2$$

$$-k_2 x_2 + k_2 x_1 - k_3 x_2 - c_2 \dot{x}_2 + c_2 \dot{x}_1 - c_3 \dot{x}_2 + f_2(t) = m_2 \ddot{x}_2 \quad \dots(3.44)$$

$$m_2 \ddot{x}_2 + (c_2 + c_3) \dot{x}_2 - c_2 \dot{x}_1 + (k_2 + k_3)x_2 - k_2 x_1 = f_2(t)$$

where $m_1, m_2, m_3, c_1, c_2, c_3, k_1, k_2, k_3$ are the system masses, dampers, and stiffness, respectively. $f_1(t)$ And $f_2(t)$ are the loads applied on the first and second masses, respectively. For more convenient, the above equations can be expressed in general matrix form as;

$$\begin{bmatrix} m_1 & 0 \\ 0 & m_2 \end{bmatrix} \begin{Bmatrix} \ddot{x}_1 \\ \ddot{x}_2 \end{Bmatrix} + \begin{bmatrix} c_1 + c_2 & -c_2 \\ -c_2 & c_2 + c_3 \end{bmatrix} \begin{Bmatrix} \dot{x}_1 \\ \dot{x}_2 \end{Bmatrix} + \begin{bmatrix} k_1 + k_2 & -k_2 \\ -k_2 & k_2 + k_3 \end{bmatrix} \begin{Bmatrix} x_1 \\ x_2 \end{Bmatrix} = \begin{Bmatrix} f_1 \\ f_2 \end{Bmatrix} \quad \dots(3.45)$$

The force vector on the right hand side of the Eqn. 3.45 represents two harmonic excitation, so that, system is considered to be subject to harmonic excitation of the kind

$$\begin{aligned} f_1(t) &= F_1 e^{j\omega t} \\ f_2(t) &= F_2 e^{j\omega t} \end{aligned} \quad \dots(3.46)$$

where ω is the excitation frequency. The general solution of Eq. 3.45 can be presumed as,

$$x_i(t) = X_i(j\omega) e^{j\omega t} \quad \dots(3.47)$$

where $i=1$ and 2 refer to the first and second coordinates of the system.

Substituting Eqs. (3.46) and (3.47) into Eq. (3.45), the results are

$$\begin{bmatrix} a_{11}(j\omega) & a_{12}(j\omega) \\ a_{21}(j\omega) & a_{22}(j\omega) \end{bmatrix} \begin{Bmatrix} X_1(j\omega) \\ X_2(j\omega) \end{Bmatrix} = \begin{Bmatrix} F_1 \\ F_2 \end{Bmatrix} \quad \dots(3.48)$$

Where $a_{ik}(j\omega)$ Frequency response functions

$$a_{ik}(j\omega) = -m_{ik}\omega^2 + jc_{ik}\omega + k_{ik} \quad i, k = 1, 2 \text{ N/m} \quad \dots(3.49)$$

Equation 3.48 can be solved for obtaining the amplitude of the presumed time response as follows,

$$X_1(j\omega) = \frac{a_{22}(j\omega)F_1 - a_{12}(j\omega)F_2}{D_o(j\omega)} \quad \dots(3.50)$$

$$X_2(j\omega) = \frac{a_{11}(j\omega)F_2 - a_{21}(j\omega)F_1}{D_o(j\omega)}$$

$$D_o(j\omega) = a_{11}(j\omega)a_{22}(j\omega) - a_{12}(j\omega)a_{21}(j\omega), \quad \text{N}^2/\text{m}^2 \quad \dots(3.51)$$

Definition of frequency response functions.

First of all, the force F_2 is set to be zero ($F_2=0$). So that Eq. 3.50 can be solved at this case, so that,

$$\begin{aligned} \lambda M_{11}(j\omega) &= \lambda \frac{X_1(j\omega)}{F_1} = \lambda \frac{a_{22}(j\omega)}{D_o(j\omega)} \\ \lambda M_{21}(j\omega) &= \lambda \frac{X_2(j\omega)}{F_1} = -\lambda \frac{a_{21}(j\omega)}{D_o(j\omega)} \end{aligned} \quad \dots(3.52)$$

where $\lambda H_{11}(j\omega)$ and $\lambda H_{21}(j\omega)$ are frequency-response functions due to effect of F_1 only. The parameter λ measured by (N/m) is a dimensional parameter introduced to make Eq. 3.52 as a nondimensional parameter.

To obtain the other second frequency response functions due to effect of F_2 only. The force F_1 is then set to zero ($F_1 = 0$). Eq. 3.50 can be solved at this case, so that,

$$\begin{aligned} \lambda M_{12}(j\omega) &= \lambda \frac{X_1(j\omega)}{F_2} = -\lambda \frac{a_{12}(j\omega)}{D_o(j\omega)} \\ \lambda M_{22}(j\omega) &= \lambda \frac{X_2(j\omega)}{F_2} = \lambda \frac{a_{11}(j\omega)}{D_o(j\omega)} \end{aligned} \quad \dots(3.53)$$

Then, the frequency response functions finally can be given by:

$$H_{ij}(\omega) = \beta |M_{ij}(j\omega)| \quad i, j = 1, 2 \quad \dots(3.54)$$

and the phase responses that go with them are given by

$$\varphi_{ij}(j\omega) = \tan^{-1} \frac{\text{Im}[M_{ij}(j\omega)]}{\text{Re}[M_{ij}(j\omega)]} \quad i, j = 1, 2 \quad \dots(3.55)$$

Back to the system presented in Fig. (3.3) above, the matrix $a_{ij}(j\omega)$ given in Eq. 3.50 can be determined by,

$$\begin{aligned} a_{11}(j\omega) &= -m_1\omega^2 + j(c_1 + c_2)\omega + k_1 + k_2 \\ a_{12}(j\omega) &= -jc_2\omega - k_2 \\ a_{21}(j\omega) &= -jc_2\omega - k_2 \\ a_{22}(j\omega) &= -m_2\omega^2 + j(c_2 + c_3)\omega + k_2 + k_3 \end{aligned} \quad \dots(3.56)$$

Some of non-dimensional parameters can be introduced to make Eq. 3.56 more general, these parameters are,

$$\Omega = \frac{\omega}{\omega_{n1}} \quad , \quad \omega_r = \frac{\omega_{n2}}{\omega_{n1}} \quad , \quad 2\zeta_i = \frac{c_i}{m_i\omega_{ni}} \quad (i = 1,2) \quad , \quad c_{32} = \frac{c_3}{c_2} \quad \dots(3.57)$$

Substitution of Eqn. 3.56 into Eqn. 3.57 yields to,

$$\begin{aligned} a_{11}(j\omega) &= A(j\Omega)k_1, \\ a_{12}(j\omega) &= -B(j\Omega)B(j\Omega)k_1m_r \\ a_{21}(j\omega) &= -k_1m_r \\ a_{22}(j\omega) &= D(j\Omega)k_1m_r \end{aligned} \quad \dots(3.58)$$

Where

$$\begin{aligned} A(j\Omega) &= -\Omega^2 + 2(\zeta_1 + \zeta_2m_r\omega_r)j\Omega + 1 + m_r\omega_r^2 \\ B(j\Omega) &= 2\zeta_2\omega_rj\Omega + \omega_r^2 \\ D(j\Omega) &= -\Omega^2 + 2\zeta_2\omega_r(1 + c_{32})j\Omega + \omega_r^2(1 + k_{32}) \end{aligned} \quad \dots(3.59)$$

Where $A(j\Omega), B(j\Omega), D(j\Omega)$ are the functions for simplification

Eq. 3.51 based on this simplification, can be expressed by $D_o(j\omega) = k_1^2 m_r R(j\Omega)$, where $R(j\Omega)$ can be expressed by,

$$\begin{aligned} R(j\Omega) &= \Omega^4 - 2j\Omega^3(\zeta_2\omega_r(c_{32} + m_r + 1) + \zeta_1) - \Omega^2(c_{32}(4\zeta_2^2m_r\omega_r^2 + \\ & 4\zeta_1\zeta_2\omega_r) + k_{32}\omega_r^2 + m_r\omega_r^2 + 4\zeta_1\zeta_2\omega_r + \omega_r^2 + 1) + 2j\Omega\omega_r(c_{32}(\zeta_2 + \\ & \zeta_2m_r\omega_r^2) + \zeta_2 + k_{32}(\zeta_2m_r\omega_r^2 + \zeta_1\omega_r) + \zeta_1\omega_r) + k_{32}m_r\omega_r^4k_{32}\omega_r^2 + \omega_r^2 \\ & \dots \quad (3.60) \end{aligned}$$

Where

$$k_{32} = \frac{k_3}{k_2}. \quad \dots(3.61)$$

Finally, the frequency response functions, described by Eqn. 3.54, can be given as,

$$H_{11}(\omega) = k_1 \left| \frac{k_1 m_r D(j\Omega)}{k_1^2 m_r R(j\Omega)} \right| = \left| \frac{D(j\Omega)}{R(j\Omega)} \right|$$

$$H_{21}(\omega) = k_1 \left| \frac{-k_1 m_r B(j\Omega)}{k_1^2 m_r R(j\Omega)} \right| = \left| \frac{B(j\Omega)}{R(j\Omega)} \right| \quad \dots(3.62)$$

$$H_{12}(\omega) = k_1 \left| \frac{-k_1 m_r B(j\Omega)}{k_1^2 m_r R(j\Omega)} \right| = \left| \frac{B(j\Omega)}{R(j\Omega)} \right|$$

$$H_{22}(\omega) = k_1 \left| \frac{k_1 A(j\Omega)}{k_1^2 m_r R(j\Omega)} \right| = \left| \frac{A(j\Omega)}{m_r R(j\Omega)} \right|$$

Where $H_{ij}(\omega)$ are the frequency response functions

Chapter Four

Experimental set-up

CHAPTER FOUR

EXPERIMENTAL AND SETUP

4.1 Introduction

An experimental setup for a dynamic vibration absorber (DVA) attached to a beam involves a physical system designed to study the effectiveness of a DVA in reducing the vibration and displacement of the beam. The setup typically consisted of a beam, a DVA, and a means to excite the beam with a harmonic force or other dynamic input, measurement system for obtaining the dynamic response. The DVA was attached to the beam at a specific location that is determined based on the properties of the beam and the DVA.

During the experiment, the beam was subjected to the dynamic input, and the response of the beam was measured at various locations using sensors such as accelerometers. The response of the beam was then compared to the response of the beam with the DVA attached, and the effectiveness of the DVA in reducing the vibration and displacement of the beam was evaluated.

The experimental setup was used to study the effect of different parameters on the performance of the DVA, such as the location of the attachment point, the stiffness and damping of the DVA, and the amplitude of the beam. Overall, an experimental setup for a DVA attached to a beam provides a valuable tool for understanding and improving the performance

of vibration control systems in various engineering applications, such as aerospace, automotive, and civil engineering.

The experimental test rig, in this work, was designed and developed in the laboratory of mechanical vibration of the university of Babylon I belonged to the college of engineering. The experimental setup is presented in Fig. 4-1 below and a schematic diagram is presented in Fig. 4-2.

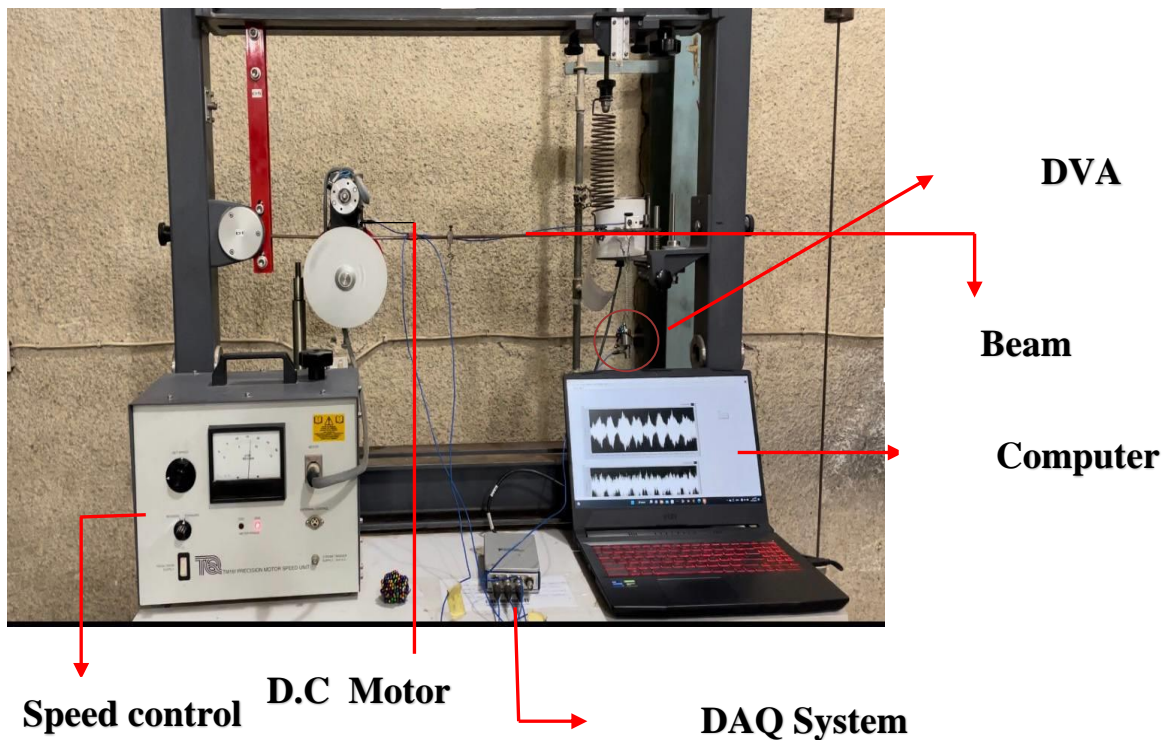


Fig (4-1) Experimental Test-Rig



Beam

Beam

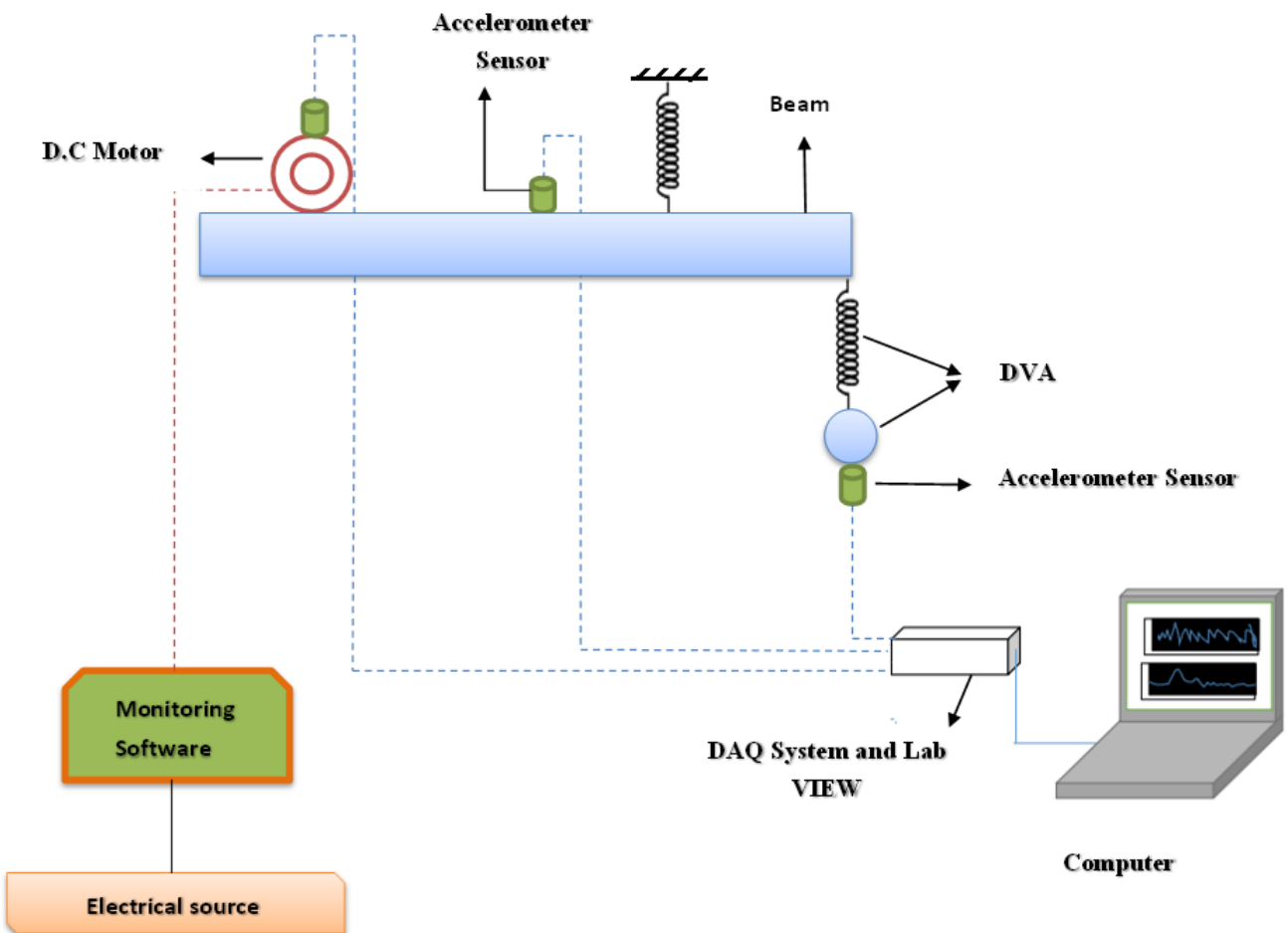


Fig (4- 2) Schematic diagram of experimental setup

4.2 The Main Components of the Rig

4.2.1 Supporting frame

The steel frame is intended to support every component of the experiment. It used for supporting the pinned beam by inserting a spring at a specific location of the beam and the frame.

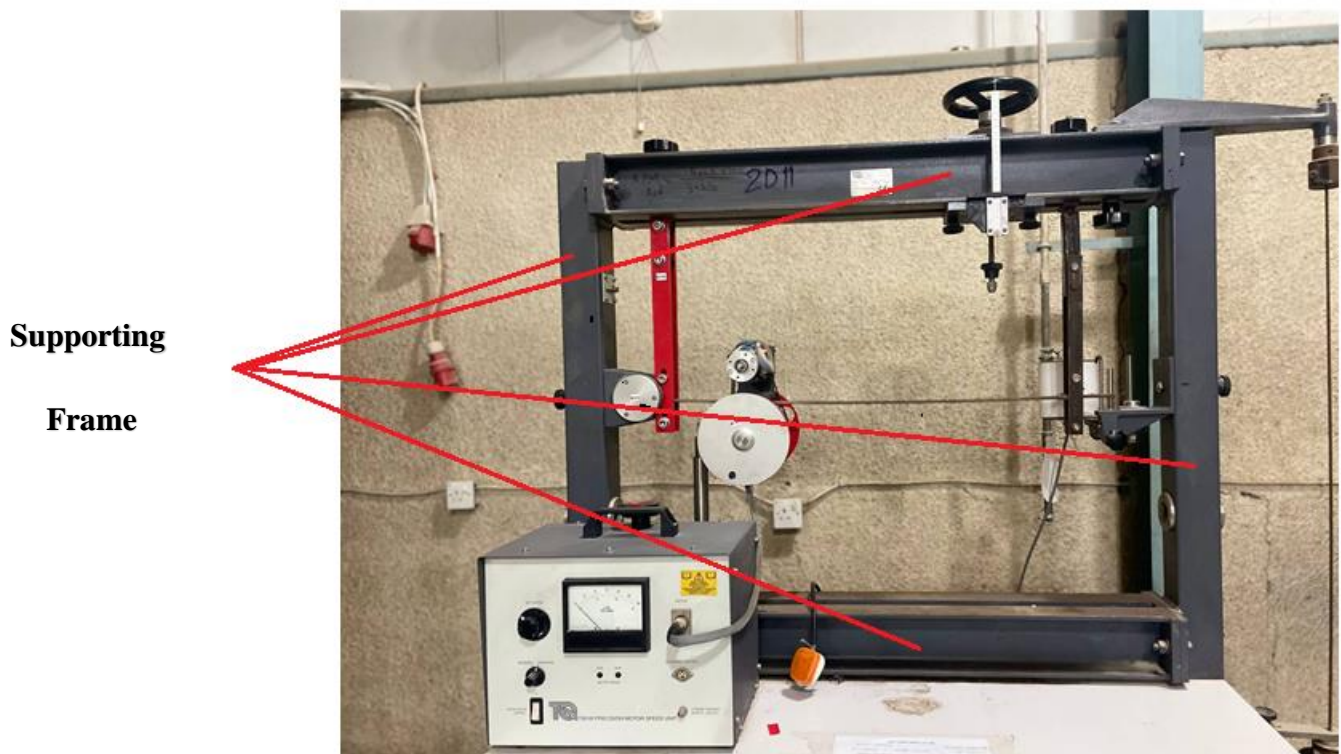


Fig (4- 3) Supporting frame

4.2.2 D.C Motor

A DC motor with a hollow disc can be used as a harmonic force exciter to generate mechanical vibrations at a desired frequency and amplitude. The hollow disc serves as a rotor, which is mounted on the shaft of the DC motor, and is driven by an electrical current supplied to the motor. The excitation force is applied to the test structure through an

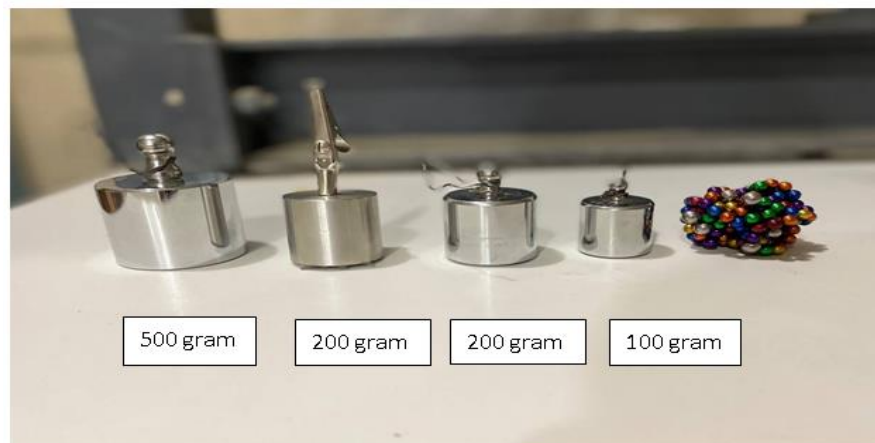
attachment mechanism that connects the hollow disc to the structure. The excitation force generated by the DC motor with a hollow disc is a harmonic force, which means it has a sinusoidal waveform with a fixed frequency and amplitude. The frequency of the excitation force can be adjusted by changing the speed of the motor. The hollow disc is designed to provide a relatively constant excitation force over a broad range of frequencies, which makes it suitable for generating mechanical vibrations in many different applications. Overall, the use of a DC motor with a hollow disc as a harmonic force exciter provides a flexible and reliable means of generating mechanical vibrations in experimental setups for various applications. The ability to control the frequency and amplitude of the excitation force, as well as the ability to generate a relatively constant force over a broad range of frequencies, makes it a versatile tool for researchers and engineers in the fields of mechanical, civil, and aerospace engineering. Fig (4-4) shows a schematic diagram of the motor. The dimensions of the rotating disc and the removed volume (hollow), and the calculations for obtaining the unbalance force as the amplitude of the harmonic excitation can be reviewed in Appendix A.



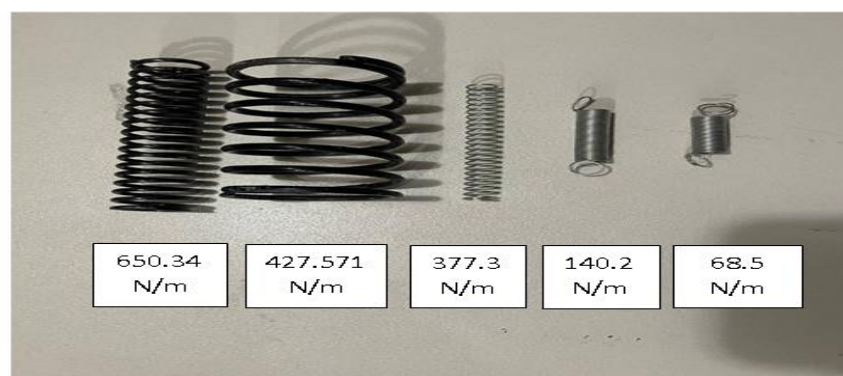
Fig (4- 4) Electric motor (exciter)

4.2.3 Mass and Spring

Mass-spring systems have been used extensively in experimental work to study the behavior of DVAs attached to beams. In such experiments, the mass and spring constants were varied, and the resulting vibration responses are measured. Several springs and masses were used in this work as shown in Fig (4-5). The colored small balls are magnetic balls of 1 gram each. These small magnetic balls were used to achieve the required values of the mass if the four standard available mass were not work well. The constants of the springs presented in Fig. (4-5) are calculated in appendix A.



a) Mass used in the present work



b) Springs used in the present work

Fig (4- 5) mass and spring of suspension

4.2.4 Accelerometer Sensors

Piezoelectric accelerometers are a commonly used type of sensor in vibration measurement systems. These sensors are designed to convert mechanical motion, such as vibration or acceleration, into an electrical signal that can be measured and analyzed. Piezoelectric accelerometers offer several advantages over other types of vibration sensors, including their high sensitivity, broad frequency range, and low noise levels. These sensors are also durable and reliable, making them suitable for use in a wide range of applications, from structural health monitoring and machinery condition monitoring to aerospace and automotive testing [56]. A quartz piezoelectric crystal is enclosed in this device's small body. The crystal produces a voltage that is in relation to the accelerating force of a piezoelectric quartz crystal because of the unique self-creating feature. The piezoelectric crystals' cyclic deformation is what causes the device's voltage output. Table (4-1) shows the accelerometer's specification. Figure illustrates the certification's calibration (4-8).

Table (4-1) Specifications of the accelerometer

Frequency	1 – 1000 Hz
Sensitivity	9.93 mV/g , 1.013 mv / m / s ²
Weight	30 gram
Mounting	Stud
Resonance Frequency	57.5 Hz

Figure 4-6 illustrates a schematic that demonstrates the manner in which the sensors are connected to the beam at varying positions. Fig. (4-7) shows the certification of accuracy and calibration of the sensors.



Fig. 4-6: Schematic shows sensors connection

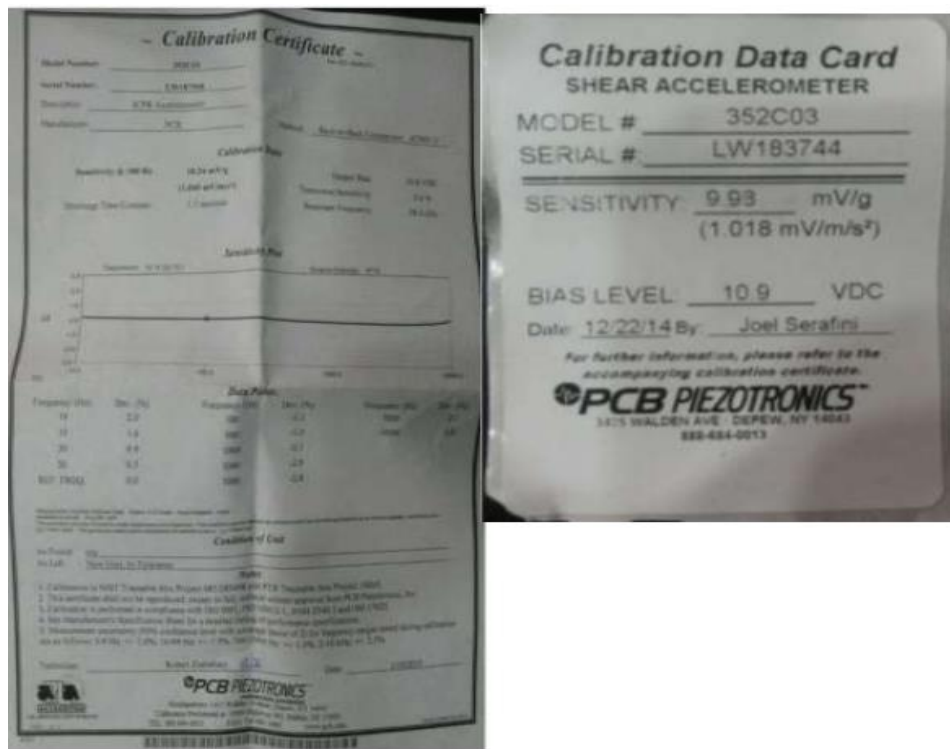


Fig (4- 7) Certification of the accelerometers calibration

4.2.5 Data Acquisition (DAQ- NI 9234)

For software acquisition and data logging, DAQ-multifunction information acquisition (DAQ) systems provide access to connect to a variety of desktop and mobile applications via USB devices. Nova gadgets with straight forward and inexpensive direct connection for interface sensors are offered via screw terminals or BNC connectors. The device has multiple signal communication choices for the signal (-10v-+10v) and -bit, kS/s, analog outputs for reliable output signals. SLOT USB Frame offers a simplified LabVIEW user interface with DAQ functionality and a universal programming interface. The DAQ system parameters are illustrated in Table 4-2.

Table (4- 2) NI cDAQ-9234 technical info.

Bus	USB
Analog Input	16 SE/8 DI
Input Resolution	16 bits
Sampling Rate	250 KS/s
Input Range	± 0.05 to ± 10 V
Analog Outputs	4
Output Resolution	16 bits
Output Rate	300 S/s
Output Range	± 10 V
Digital I/O	32
Counter /Timers	2

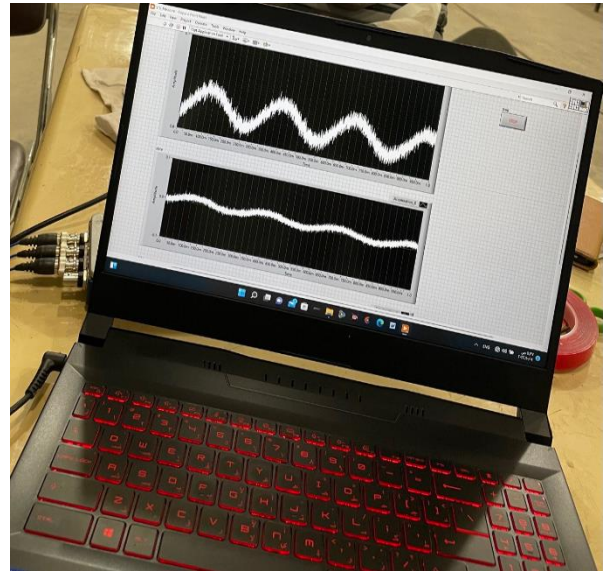
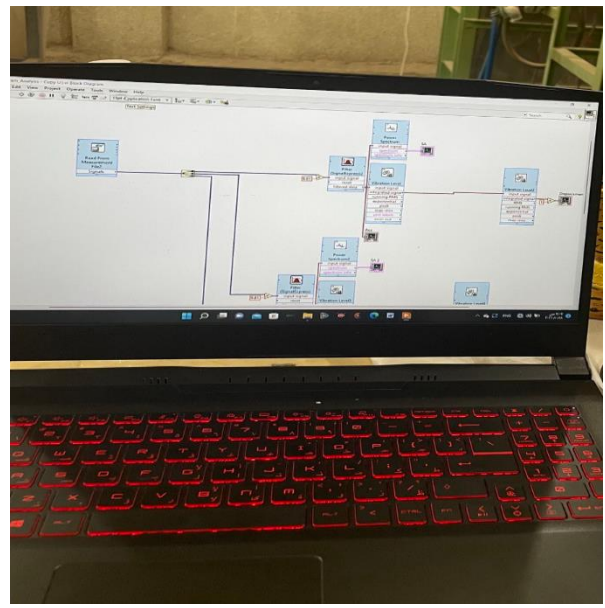


Fig (4- 8) DAQ system and a sample of measurements

4.2.6 Speed control Unit and Exciter Motor

The speed control unit utilized in this study allows for complete bidirectional motor drive and precise speed control under normal conditions. As previously explained, an amplifier detects any deviation between the motor speed and the voltage input from the "Set Speed" control on the front panel. The amplifier then drives the motor until the deviation is nearly zero. The unit is designed to handle high currents during acceleration and deceleration automatically. The speed meter has two ranges, 0 - 1500 rev/min and 0 - 3000 rev/min, and switches automatically as the motor speed exceeds or falls below 1500 rev/min. The range of the meter is indicated by the lamps beneath it. Fig. (4-11) shows the speed control

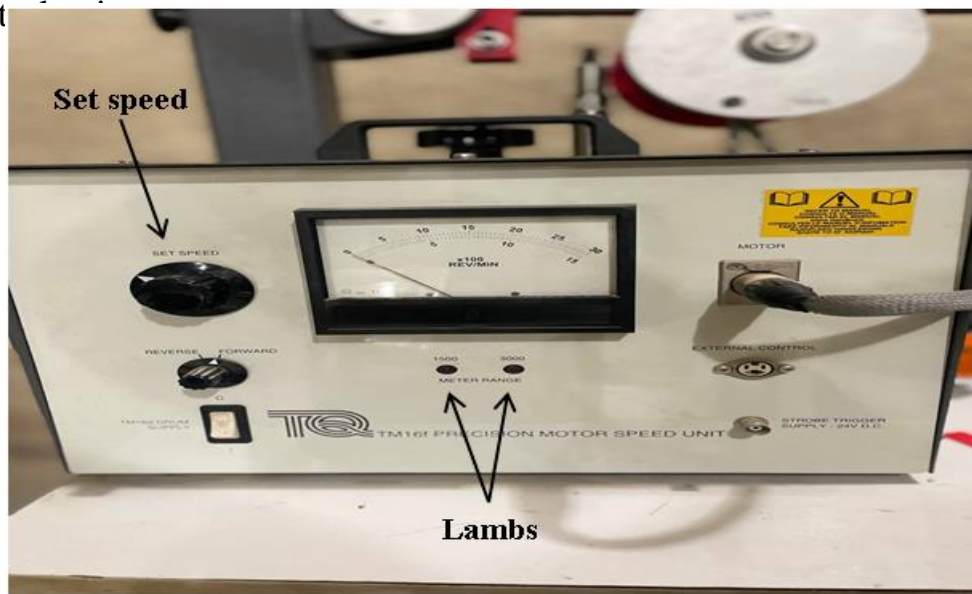


Fig (4- 9) Speed controller

4.3 Experimental procedure

The experimental procedure for the harmonic analysis of the dynamic vibration absorber (DVA) attached to a beam typically involves the following steps:

- 1- Mount the beam: The beam was mounted on a vibration isolation table or a shaker system that can provide the desired dynamic input to the beam.
- 2- Install the DVA: The DVA was attached to the beam at a specific location that is determined based on the properties of the beam and the DVA.
- 3- Install sensors: Sensors such as accelerometers were installed at various points along the desired locations of the beam to measure its response.
- 4- Calibrate the sensors: The sensors were calibrated to ensure accurate measurement of the response of the beam.
- 5- Excite the beam: The beam was excited with a harmonic force delivered by the mass eccentricities and the response of the beam was measured using the installed sensors.
- 6- Record the response: The response of the beam with the DVA attached was recorded and compared to the response of the beam without the DVA attached.
- 7- Analyze the data: The data collected from the experiment was analyzed to evaluate the effectiveness of the DVA in reducing the vibration and displacement of the beam.
- 8- Adjust the DVA parameters: The parameters of the DVA such as mass, spring stiffness, and location can be adjusted to optimize the performance of the DVA for the specific application.

- 9- Repeat the experiment: The experiment is repeated with different parameters to study the effect of different variables on the performance of the DVA.

Overall, the experimental procedure for a DVA attached to a beam involves careful measurement of the response of the beam under dynamic loading conditions, and the use of this data to optimize the design of the DVA for specific applications.

Chapter Five

Results and Discussion

CHAPTER FIVE

RESULTS AND DISCUSSION

5.1 Introduction

The main objective of this work is to investigate effect of the more sensitive parameters of a spring-mass absorber and obtain the optimal values of a unit cell absorber (optimal spring and optimal mass for the absorber) to enhance absorption capacity and vibration attenuation. Introducing the principles of negative mass and negative stiffness is discussed in details. In this chapter, the results will be discussed for both discrete system (spring-mass) and continuous system (beam).

5.2. Theoretical Results for the discrete system.

5.2.1 Negative mass

Fig. 5-1 shows the variations of effective mass with frequency ratio (Ω/ω_2) for different values of mass absorber $m_2 = (0.1 - 0.7)m_1$. In general, effective mass varies with the excitation frequency Ω and absorber mass m_2 . When $\Omega > \omega_2$, the effective mass denoted by Eqn. (3.16) becomes negative (negative mass). This character is the key point of using metamaterials for vibration attenuation that corresponds to $u_1(t) = 0$, as shown by Eqn. 3.17. However, when $\Omega < \omega_2$, the effective mass is positive and hence the two terms $\frac{F_0}{a_1} = -\tilde{m}_1\Omega^2$ and $\frac{F_0}{a_2}$ are both negative values which means that no one of $u_1(t)$ and $u_2(t)$ equals to zero and also means that both of the masses in the system vibrate in same phase. Hence, vibration of the main mass cannot be attenuated. In the other hand, Figure (3.1) shows that the absolute value of the

effective mass increase with increasing absorber mass. However, this increment become less sensitive at higher values of the absorber mass.

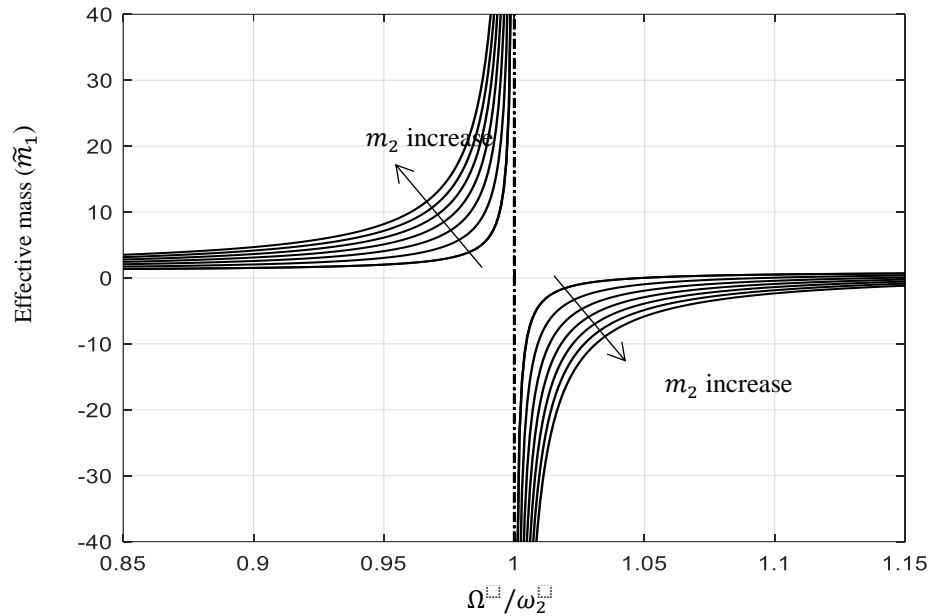


Fig. 5.1 Variations of effective mass due to variation of the frequency ratio (Ω^2 / ω_2^2), $m_1 = 1kg$, $m_2 = (0.1 - 0.7)m_1$.

5.2.2 Negative stiffness

Figure (5.2) shows the variations of effective spring with frequency ratio (ω_2 / Ω) for different values of absorber spring $k_2 = (0.1-0.7)k_1$. The variation of the effective spring due variations of the excitation frequency is similar to that corresponding of the effective mass. However, the frequency ratio is represented by ω_2 / Ω in Fig. 5.2 instead of the Ω / ω_2 for the negative mass represented by Fig. (5.1). In other words, $\omega_2 > \Omega$, the effective spring denoted by Eqn. (3.37) is negative. A developed downward force built up in the spring pulled against the applied force $F(t)$. The developed force is generally greater than F_0 according to Eqn. 3.40. This behavior explains the importance of the negative stiffness value for vibration attenuation.

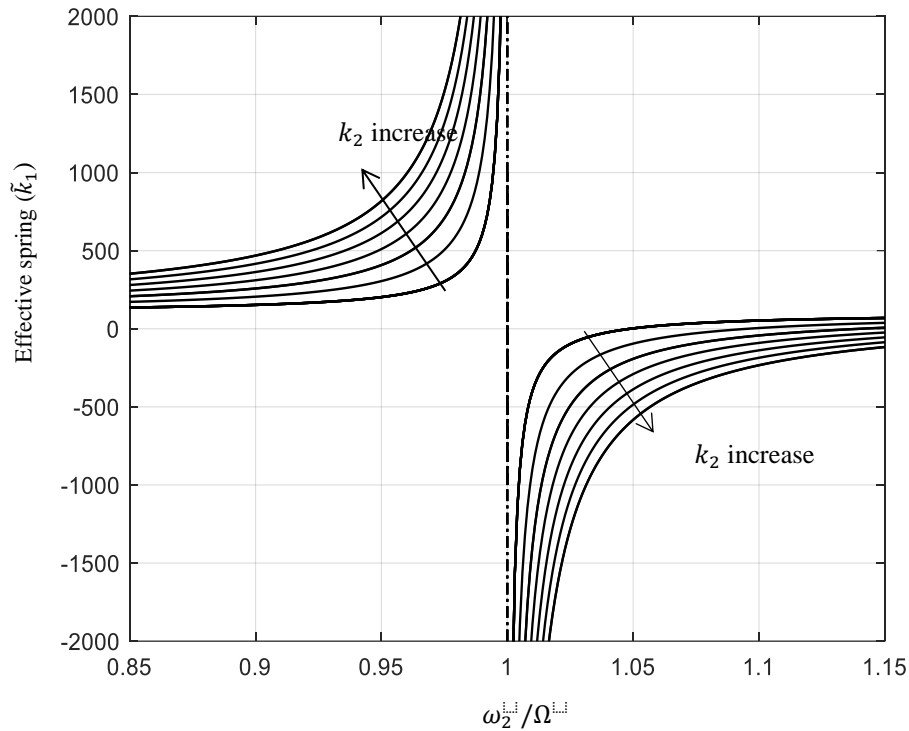


Fig. 5.2 Variations of effective spring due to variation of the frequency ratio (ω_2^T/Ω^T), $k_1 = 100N/m$, $k_2 = (0.1-0.7)k_1N/m$.

5.3 Application of DVA for vibration absorber

In this section, two designs of absorbers are investigated to study effect of design parameters, such as frequency ratio, mass ratio, and damping factors on the amplitude response of 2-DOF absorber system. This section shows the sensitivity of the absorber performance to the variations of the design parameters as well.

5.3.1 General comments

The primary and secondary systems are assumed to be damped by introducing ζ_1 and ζ_2 for both systems, respectively. However, to reduce design requirements, let us first assume $\zeta_2 = 0$. Back to Fig. 3.3, where $c_2 = c_3 = k_3 = 0$ and the primary system is the only excited system. The key point of designing a good vibration absorber is the selection proper values of m_2 and k_2 to reduce response of the main vibratory system (primary mass). The only way

to get zero response for the primary mass, based on Eqn.(3.55), is by making the parameter $a_{22}(j\omega) = 0$ or $a_{22}(j\omega)$ or $D(j\Omega) = 0$ when $\Omega=\omega_r$. The above condition can be easily applied for designing an absorber.

5.3.1.1 Effect of the damping factor ζ_1 on the dynamic response

Effect of first damping ratio is presented by Fig. (5.3) for three values of the frequency ratio, while the mass ratio is held constant. In general, no infinite amplitude response is presented because both of the introduced damping ratios are not zero, and this is the major role of the damping additions to a vibratory system. It is also noted that the amplitude response decrease dramatically as damping ratio increase. The difference in response decreased as well. The responses are very close at the excitation frequency smaller and greater than the first and second resonance frequencies, respectively. However, the behavior is different as frequency ratio increase (this will be explained in the next sections). Increasing damping ratio from (0.1 to 0.4) reduced the amplitude response by 400%.

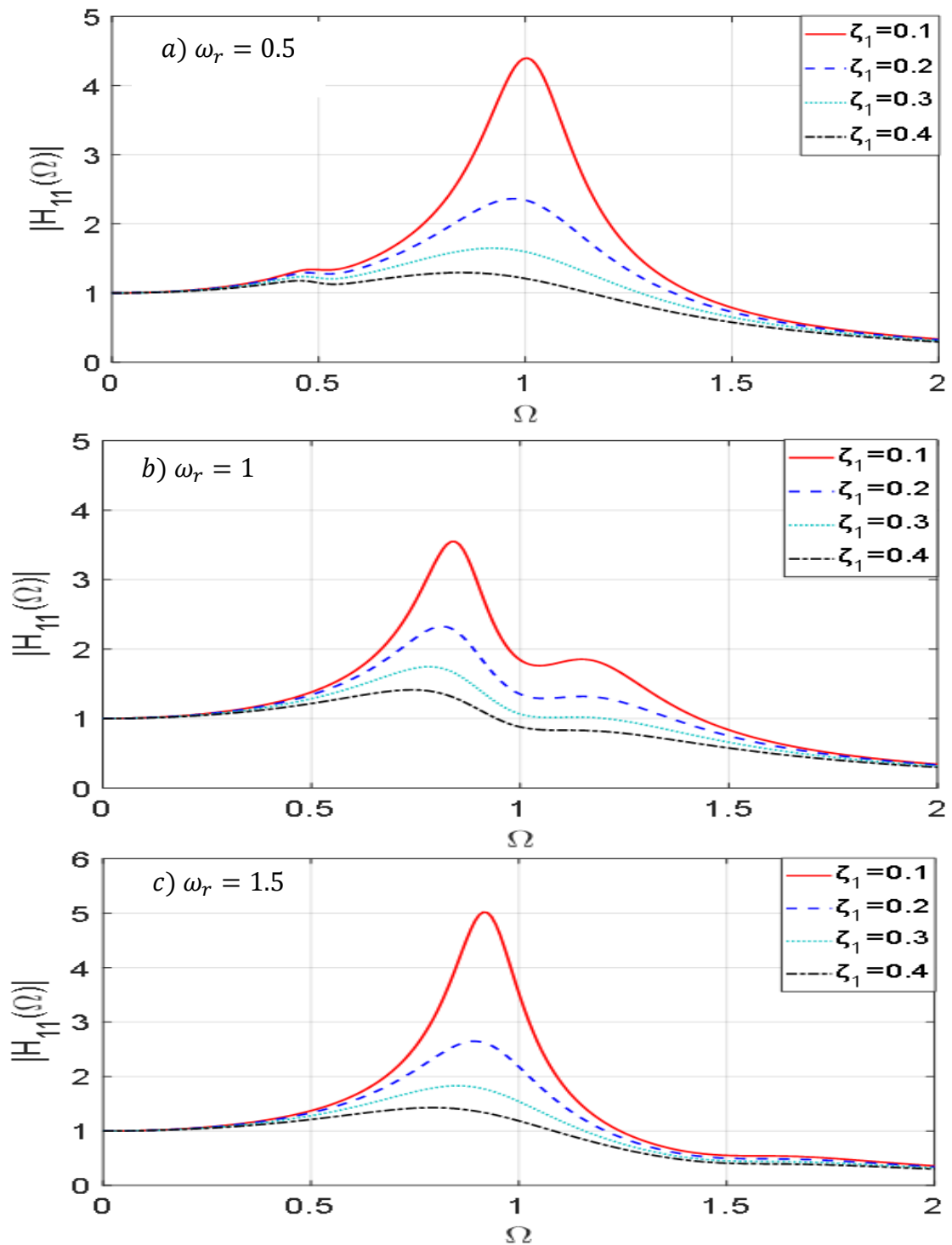


Fig 5.3: Amplitude response when $\zeta_2 = 0.2$, $m_r = 0.1$ for different values of damping ratio and frequency ratio, a) $\omega_r = 0.5$, b) $\omega_r = 1$, c) $\omega_r = 1.5$.

5.3.1.2 Effect of the damping factor ζ_2 on the dynamic response.

Fig. (5.4) shows variation of amplitude response due to variation of ζ_2 for three values of frequency ratios. It is noticed that the peaks disappear as damping ratio increase. Even peaks locations change as frequency ratio increase. The greater effect of ζ_2 is noticed at its maximum value and $\Omega = 1$. Fig. (5.3) and Fig.(5.4) show that ζ_1 is more dominant on the amplitude response than ζ_2 . However, the response of the primary mass can be controlled by choosing a suitable values of ζ_2 .

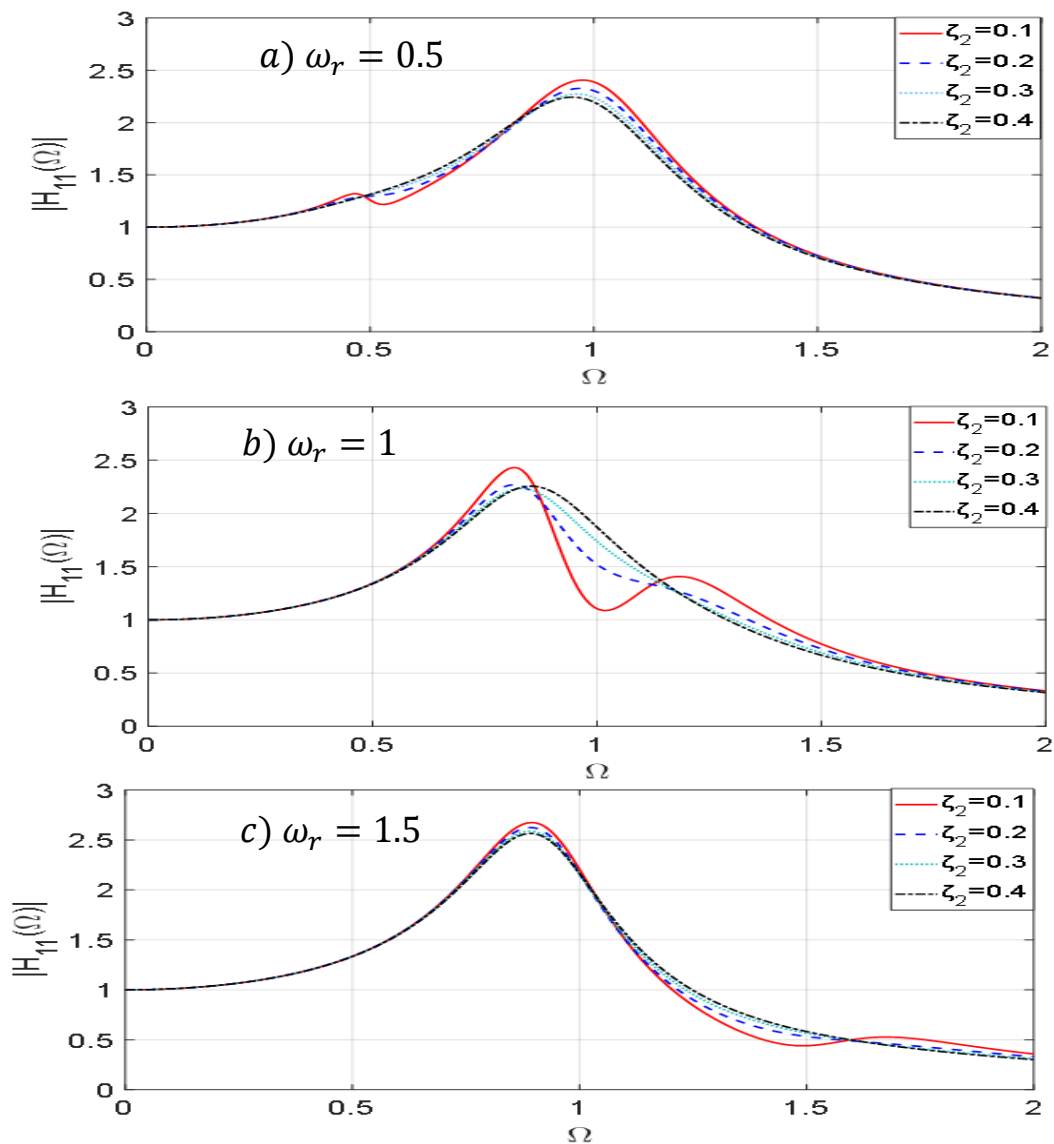


Fig 5.4: Amplitude response when $\zeta_1 = 0.2$, $m_r = 0.1$ for different values of damping ratio and frequency ratio, a) $\omega_r = 0.5$, b) $\omega_r = 1$, c) $\omega_r = 1.5$.

5.3.1.3 Effect of mass ratio on the dynamic response.

Effect of mass ratio is presented by Fig.(5.5). At a small value of the mass ratio altered the amplitude response to be smoother and the peaks gradually disappeared. However, at high values of the mass ratio peaks become more obvious and higher amplitude specifically when the frequency ratio equal or more than 1. It worthy to mention that variation of frequency and mass ratio show no effect on amplitude response when ($\Omega < 0.25$).

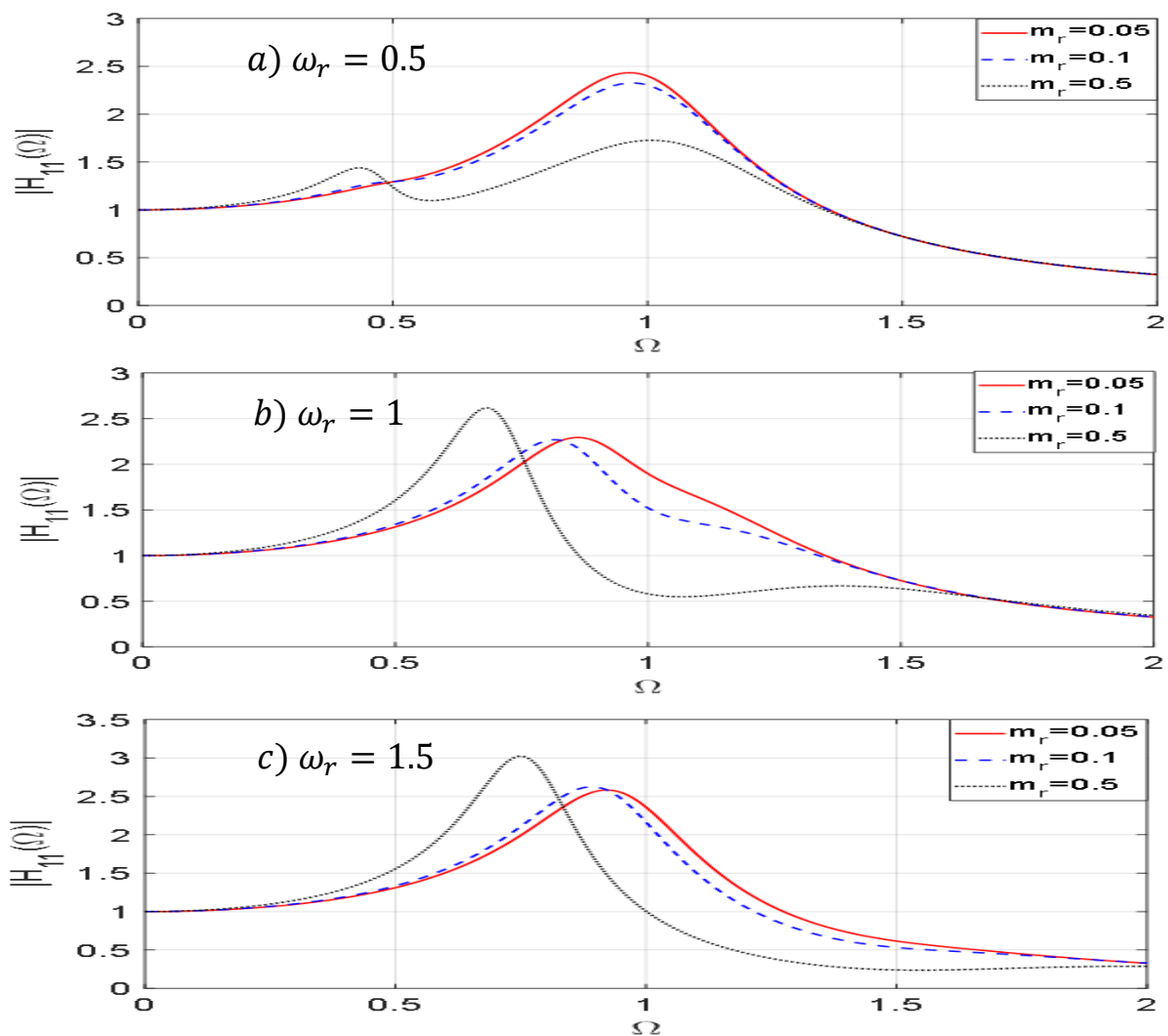


Fig 5.5 : Amplitude response when $\zeta_1 = \zeta_2 = 0.2$, for different values mas ratio and frequency ratio, a) $\omega_r = 0.5$, b) $\omega_r = 1$, c) $\omega_r = 1.5$.

5.3.1.4 Effect of frequency ratio on the dynamic response.

Fig. (5.6) shows the effect of frequency ratio on the amplitude response for different values of mass ratios. The range of the non-dimensional frequency (Ω) at which the amplitude response showed no change in between is ($0.5 < \Omega < 1.5$). The amplitude responses are invariant for the other values. In addition, the difference in behavior is smaller at the smaller values of the frequency ratios and increases dramatically as this ratio increases to 1.5.

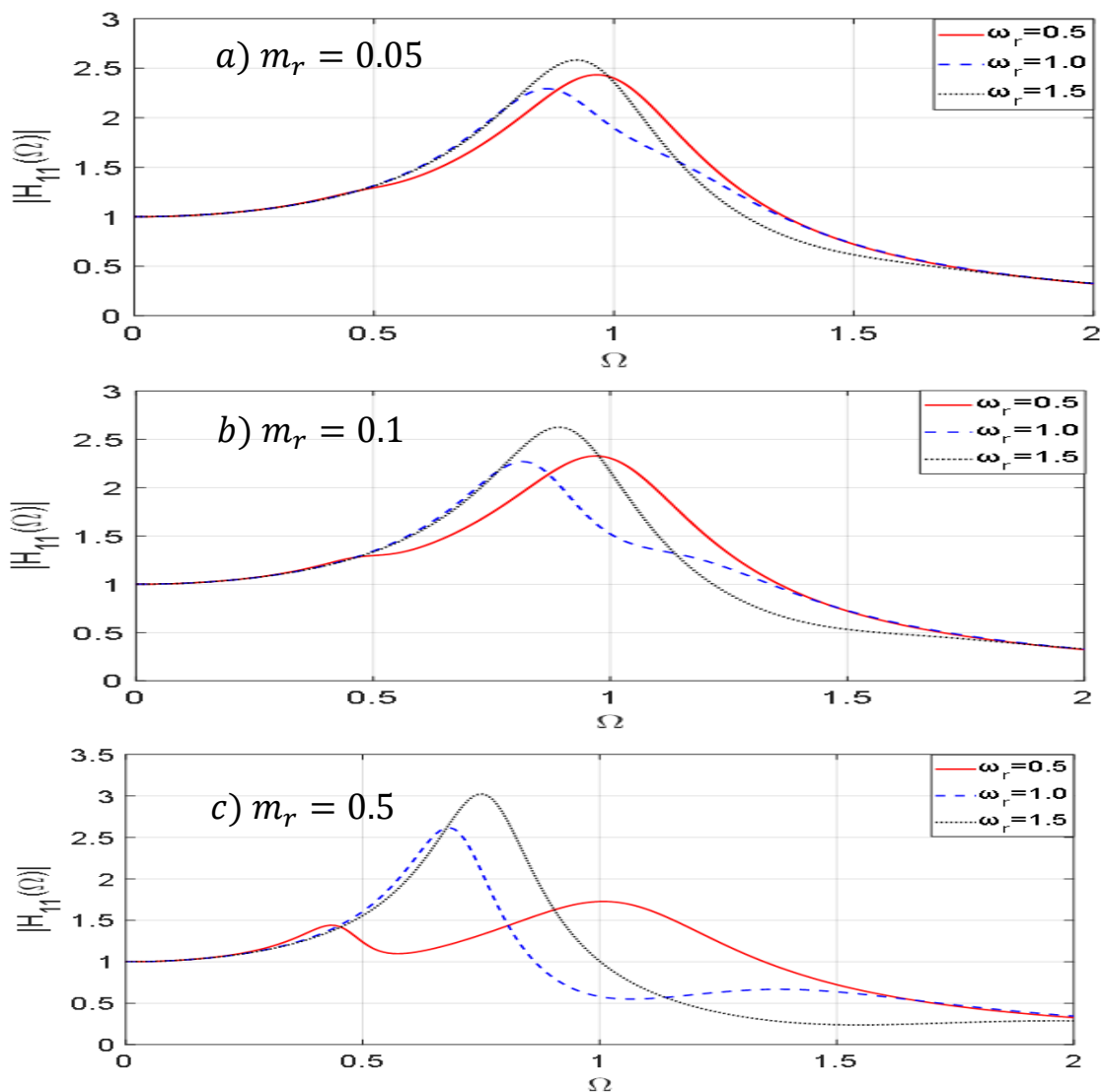


Fig 5.6: Amplitude response when $\zeta_1 = \zeta_2 = 0.2$, for different values of frequency ratio and mass ratio, a) $m_r = 0.05$, b) $m_r = 0.1$, c) $m_r = 0.5$.

5.4 Optimal design of DVA

The response of the primary mass can be attained to be zero when $\zeta_2=0$. However, this condition is ideal because of the existence of the structural and frictional damping. In this case, selection optimal combination of system parameters is not an easy task because of the nonlinear and fluctuated behavior of ζ_2 on the absorber mass (as will be discussed in the next section). Fig. (5.7) shows effect of ζ_2 , in details, on the amplitude response. Similar behavior as verified in previous sections, that the response is zero when $\Omega=\omega_r=1$ and $\zeta_2=0$. However, the behavior is different other than that. The amplitude response of the peaks goes smaller. But, both peaks ($\Omega\neq 0$) goes to infinite when $\zeta_2=0$ and $\zeta_2=\infty$. In other words, there is a critical value of ζ_2 in between these values at which the peaks are smaller or minimum. In addition, Fig 5.7 shows the three curves of response are intersected exactly at two points, O_1 and O_2 . This is simply means that amplitude responses for all cases in this figure are not sensitive to the variations of ζ_2 at these points. These points can be called invariant points. For optimization purposes, the best behavior for these curves are the curves which make the difference between these two points as smaller as possible for a wide range of non-dimensional frequency including $\Omega=1$ when $\zeta_2\neq 0$. It is important to mention that the optimal values of ζ_2 and ω_r vary with m_r . For more explanations about this, Fig 5.8 shows effect of arbitrary damping ratio ζ_2 on the amplitude response when $\zeta_1 = 0.1$, $m_r = 0.1$ for several values of ω_r . It is noticed that the amplitude response is quite sensitive to the variations of damping ratio and mass ratio and a mathematical tool is needed to obtain the optimal design of the dynamic vibration absorber that makes the differences between the invariant points introduced above as smaller as possible. Simple, but efficient, direct search method is used to obtain optimal values for several trials of the amplitude response as shown in Fig. (5.9) presenting how amplitude response vary when mass ratio increase or

decrease. The dashed curves are the closest response at which the difference between invariant points are minimal. These curves in Fig. (5.8) show that minimum amplitude for the primary system is attained at the higher value of frequency ratio. However, this corresponds a limitation in the frequency range. In other words, once the mass ratio get bigger, the frequency range, as shown in Table (5.1), frequency of the maximum peaks shifts to the left and also the frequency range varies and may not cover the resonance frequency as noticed when $m_r=0.4$ and $m_r=0.5$. This limits the performance of the absorber. The optimal values presented in Table (5.1) are calculated at $\zeta_1=0.1$ for now.

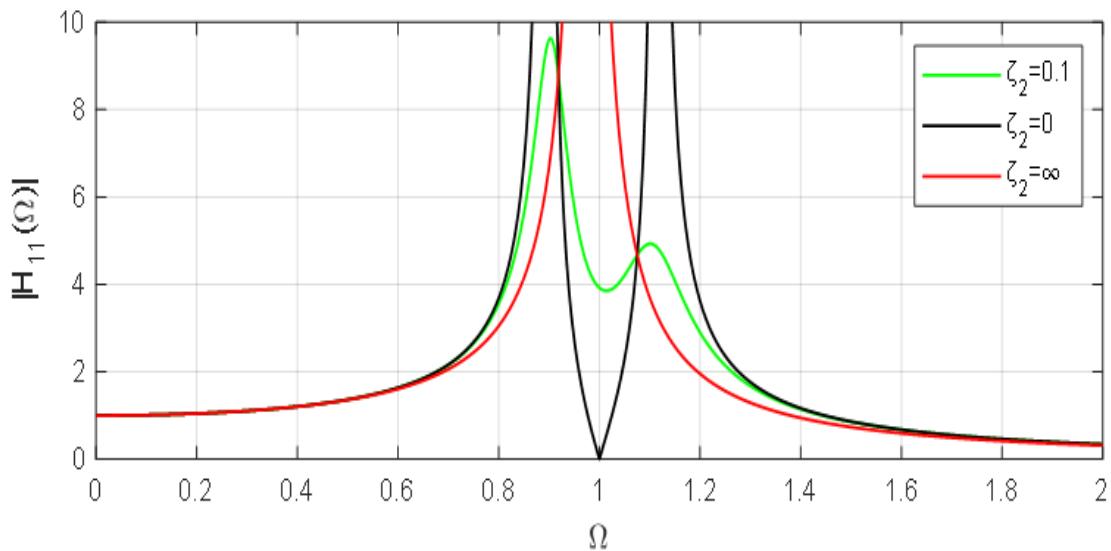


Fig 5.7: Nonlinear effect of damping at $\zeta_1 = 0.1, m_r = 0.1, w_r = 1$

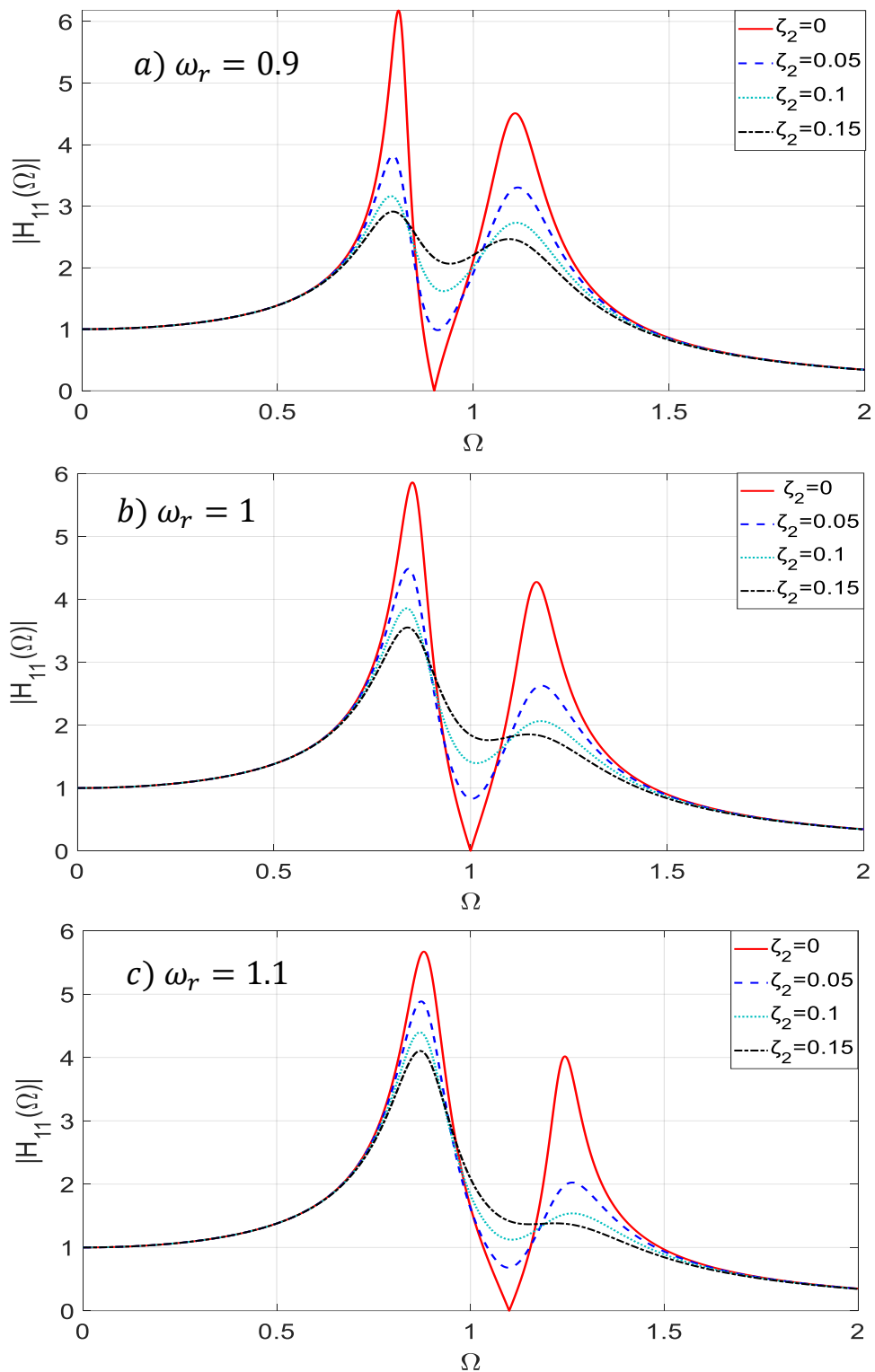


Fig 5.8 : Effect of arbitrary damping ratio on the amplitude response when $\zeta_1 = 0.1, m_r = 0.1$ for several values of ω_r .

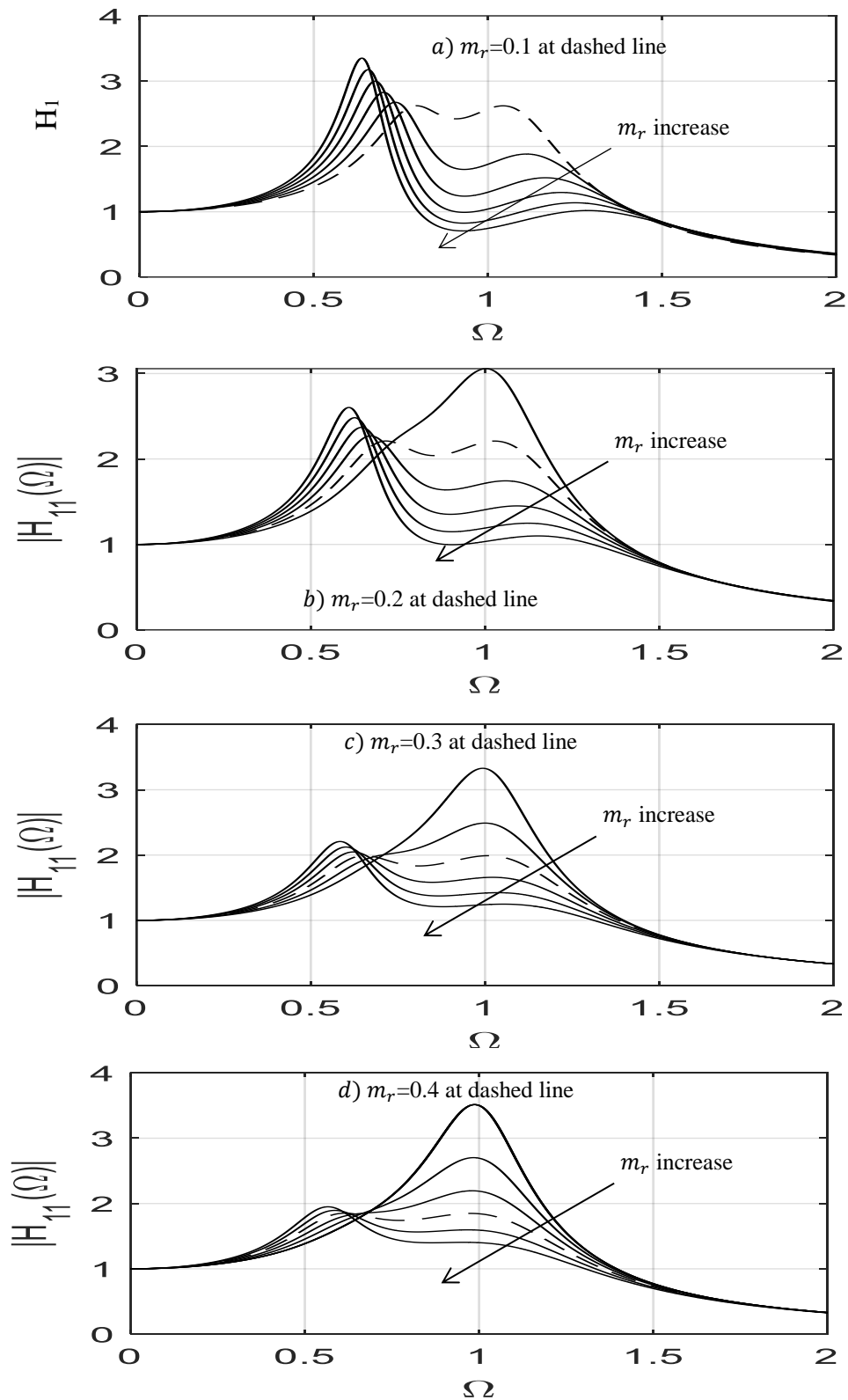


Fig 5.9 Optimal values for absorber parameters for different values of mass ratio m_r

Table (5.1): Optimal values of absorber parameters for six cases of mass ratio (m_r) and at $\zeta_1=0.1$.

m_r	ζ_2 (N.s/m)	ω_r	Peaks difference	Frequency range
0.1	0.195	0.859	$3.55 \cdot 10^{-3}$	0.789 to 1.051
0.2	0.259	0.771	$2.74 \cdot 10^{-3}$	0.716 to 1.031
0.3	0.301	0.696	$3.84 \cdot 10^{-3}$	0.647 to 1.015
0.4	0.351	0.649	$9.55 \cdot 10^{-3}$	0.303 to 0.965
0.5	0.407	0.603	$3.52 \cdot 10^{-3}$	0.586 to 0.920
0.6	0.321	0.574	$3.83 \cdot 10^{-3}$	0.510 to 1.022

5.5 Comparison with other works

In order to validate the results presented above, one comparison is presented with Ref [57] for one case of optimal values of the dynamic vibration absorber when the mass ratio ($m_r = 0.1$) and at ($\zeta_1=0.1$). The first row of Table 5.1 shows that the optimal values of the damping ratio $\zeta_2=0.195$ and the frequency ratio $\omega_r=0.859$. these values is very close to the results presented in Fig 5.10 of the same ref

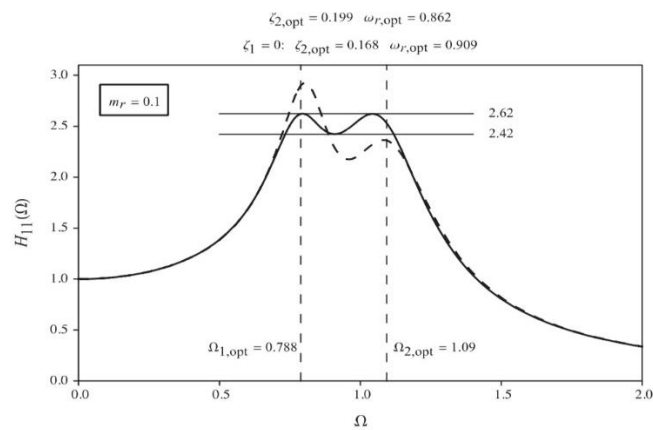


Fig 5.10 Optimum values for the parameters of a vibration absorber and the resulting amplitude response of $m_r = 0.1$ and $\zeta_1=0.1$.

5.6 Experimental work

The primary objective of the earlier sections was to enhance the understanding of the behavior of the main vibratory system when a dynamic vibration absorber is added and how the system responds to uncertainties in the design parameters of both the system and absorber. Based on this knowledge, the subsequent step involves the application of these findings to a new vibratory system, specifically a beam. Thus, the current section's main goal is to utilize a dynamic vibration absorber to minimize the beam's primary resonance vibrations due to periodic excitation, further building upon the insights gained from the previous sections.

To conduct the experimental run, the procedure outlined in Ch. 4 is followed. The study of the beam is carried out for three different cross-sectional area dimensions, while maintaining a constant beam length. Additionally, three boundary conditions (pinned-free, fixed-free (cantilever), fixed-fixed) are taken into account for the beams. The mass of the DVA may vary based on the values required in the parametric study. If the available masses are unsuitable for the experiment, small colored masses (each weighing 1 gram) are utilized to attain the required values.

In the following section, the impact of the mass, stiffness, and location of the dynamic vibration absorber will be elaborated upon for each case. The ultimate objective of the entire experimental setup is to attain a dynamic response of the main system at a specific location that yields a better and smaller system response.

5.6.1 Dynamic response of Beam 1

The dimensions of the rectangular beam are as follows: thickness of $t=0.012\text{m}$, width of $w=0.025\text{m}$, and length of $l=0.74\text{m}$. The boundary conditions are also described in the subsections.

5.6.1.1 Pinned-free boundary condition

The left-hand side of the beam is pinned, while the right-hand side is free.

5.6.1.1.1 Effect of stiffness

Figures (5.11 through 5.13) demonstrate how DVA stiffness affects the dynamic response of a beam for three different DVA masses. Both DVA stiffness and mass variations have a significant impact on the dynamic response of the beam, but to varying extents. Regardless of the stiffness and mass values of the DV, the dynamic response of the beam is reduced compared to its response without DVA. Specifically, in Fig. (5.11), reducing the stiffness with a DVA mass of 100 grams leads to a decrease in dynamic response, with the best reduction achieved at a stiffness of $k=68.5\text{ N/m}$. As previously mentioned in the theoretical part, the optimal reduction in the response of the primary system is achieved when the excitation frequency matches the natural frequency of the main system and the DVA. In other words, the DVA must be designed to match or come closer to the excitation frequency to achieve better reduction. The combination of $k=68.5\text{ N/m}$ and $m=100\text{ grams}$ satisfies this condition (the closer one among them).

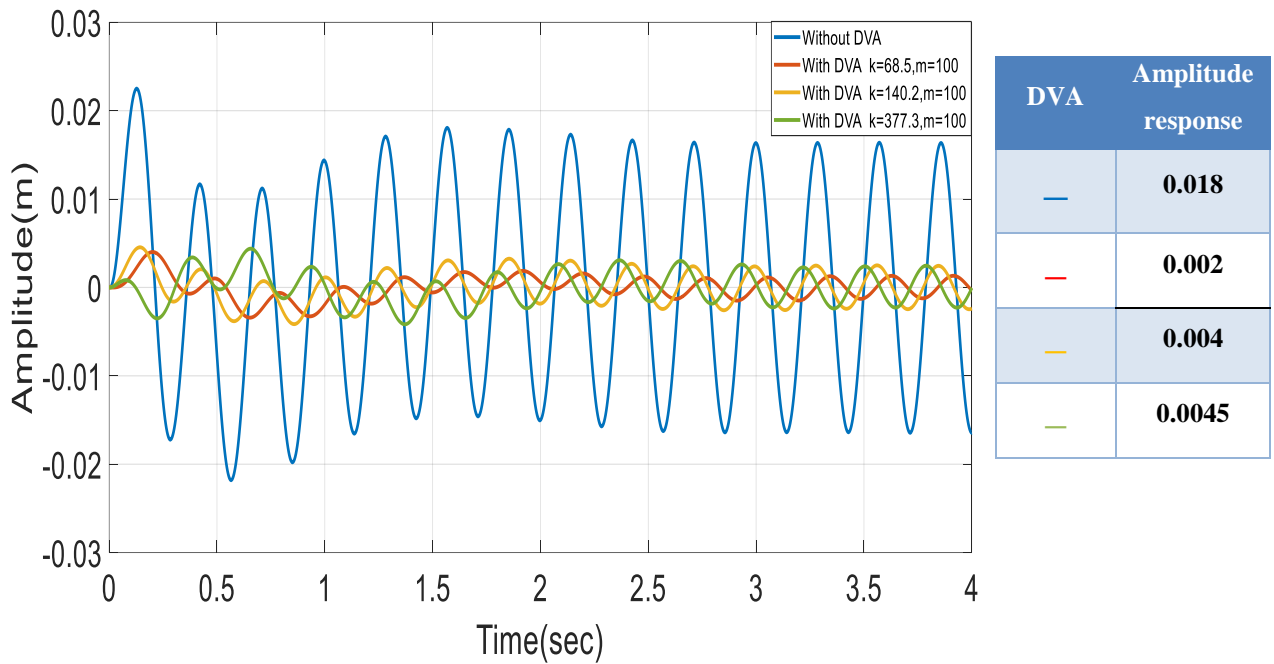


Fig. 5.11 Effect of stiffness at beam ($t=0.12m$) pin free with and without DVA at $\omega = 6.75 \pi$ rad/sec , $\alpha l=1$.

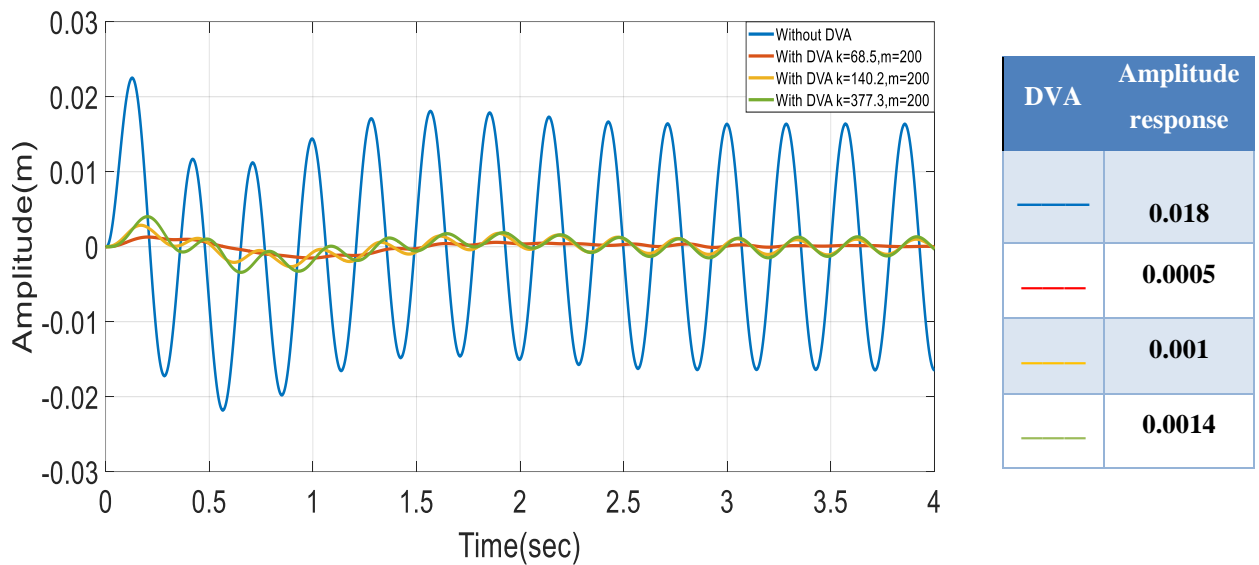


Fig (5.12) Effect of stiffness at beam ($t=0.12m$) pin free with and without DVA at $\omega = 6.75\pi$ rad/sec , $\alpha l=1$

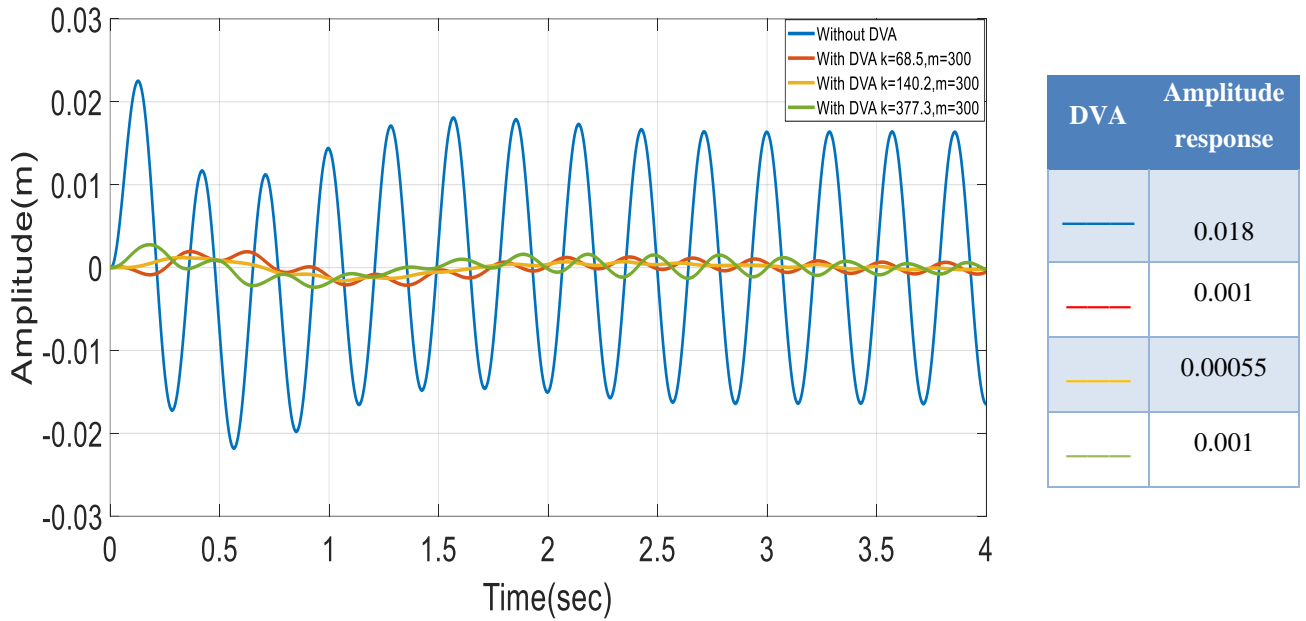


Fig (5.13) Effect of stiffness at beam ($t=0.12m$) pin free with and without DVA at $\omega = 6.75\pi\text{rad/sec}$ $x/l=1$.

Fig. (5.13), on the other hand, indicates a different locally optimal DVA design for the same reason mentioned earlier, with $k=140.2\text{N/m}$ and $m=300$ grams. Ultimately, the locally optimal DVA design (for Figures (5.11-5.13)) that results in the most significant reduction is achieved with $k=68.5\text{ N/m}$ and $m=200$ grams when the dynamic response is measured at $x/l=1$.

DVA location is another important factor need to be studied in details for each beam and the associated boundary conditions. The next section will discuss effect of DVA location with same stiffness and mass values studied above.

Figs. (5.14 through 5.16) show the dynamic response equivalent to Figs. (5.11-5.13) but when the DVA is located at the middle ($x/l=0.5$) instead of ($x/l=1$). In general, similar trend of the dynamic response is noticed when the DVA is attached at the middle of the beam as compared to the last three figures where the DVA is attached at the free end of the beam. The only difference is that the corresponding displacement response is bigger when the DVA attached

at the middle. However, the combination of $k=68.5$ N/m and $m=100$ grams satisfies this condition (the closer one among them) for Fig. (5.14) while the local optimal combination is achieved when $k=140.2$ N/m and $m=300$ grams.

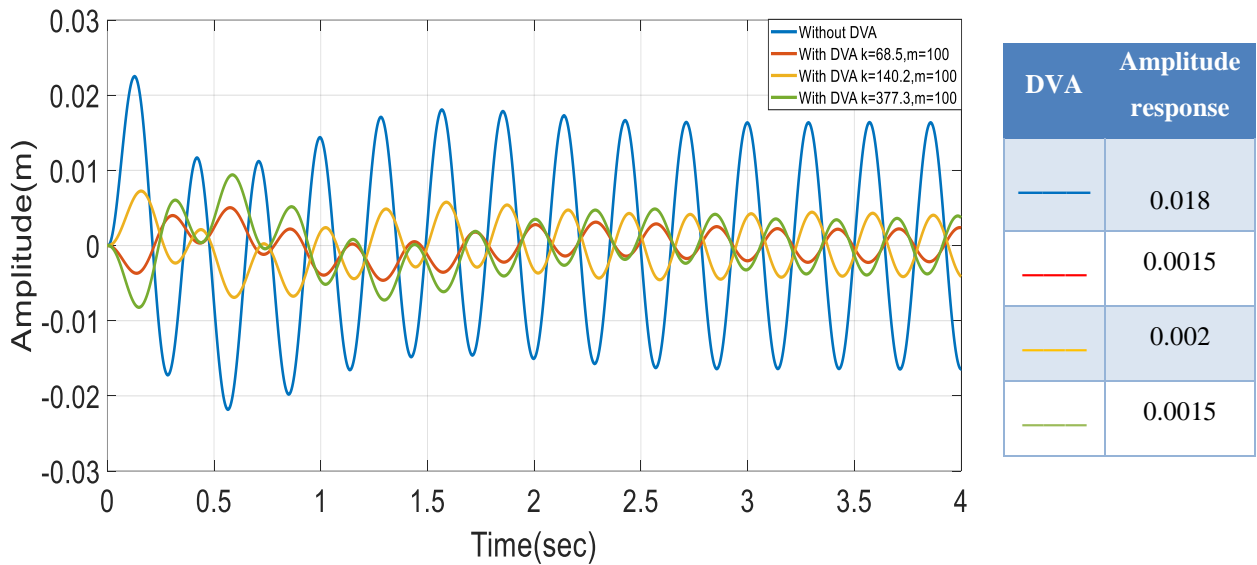


Fig (5.14) effect of stiffness at beam ($t=0.12$ m of pin free with and without DVA at $\omega = 6.75\pi$ rad/sec, $x/l = 0.5$.

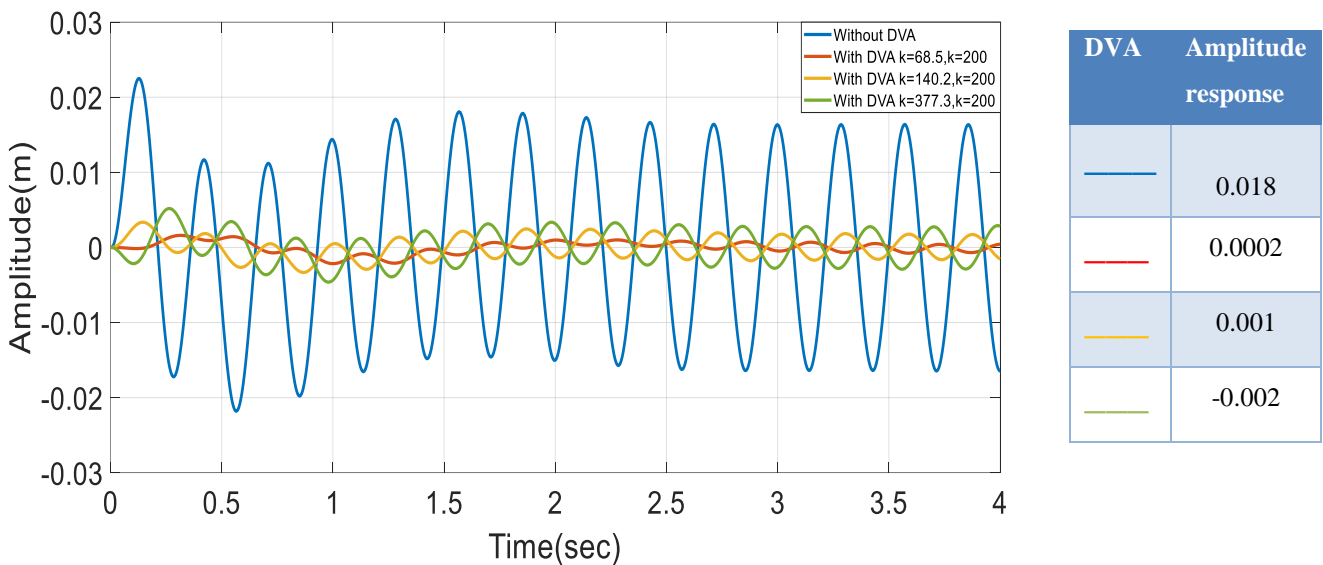


Fig. (5.15) Amplitude response beam ($t=0.12$) of pin free with and without DVA at $\omega = 6.75\pi$ rad/sec, $x/l = 0.5$.

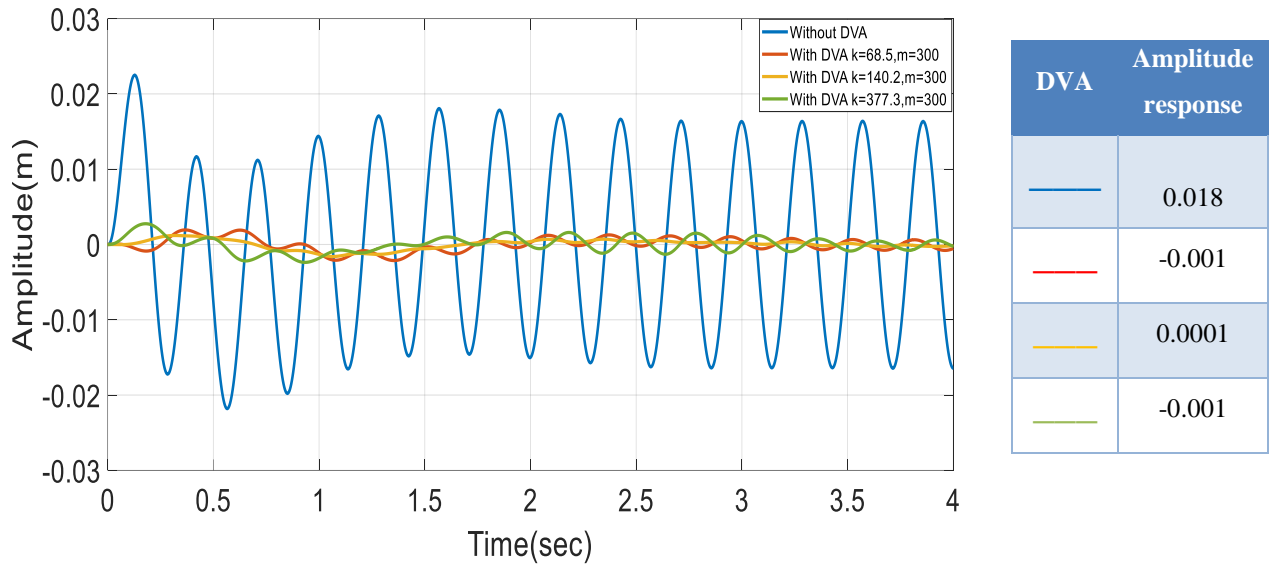


Fig. (5.16) Amplitude response of pin free with and without DVA at $\omega = 6.75\pi$ rad/sec, $x/l = 0.5$.

To quantify the effect of DVA location on the dynamic response of the beam, the DVA is located at one more location ($x/l=0.337$) and the results are presented in Figs. (5.17- 5.19).

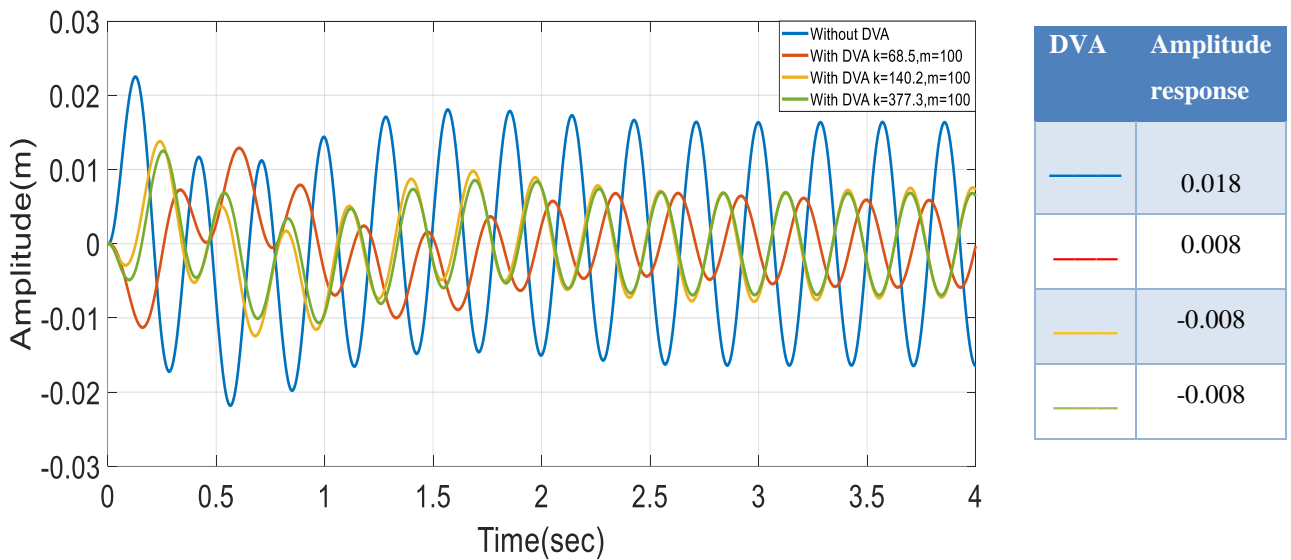


Fig. (5.17) Amplitude response of pin free with and without DVA at $\omega = 6.75\pi$ rad/sec, $x/l = 0.337$.

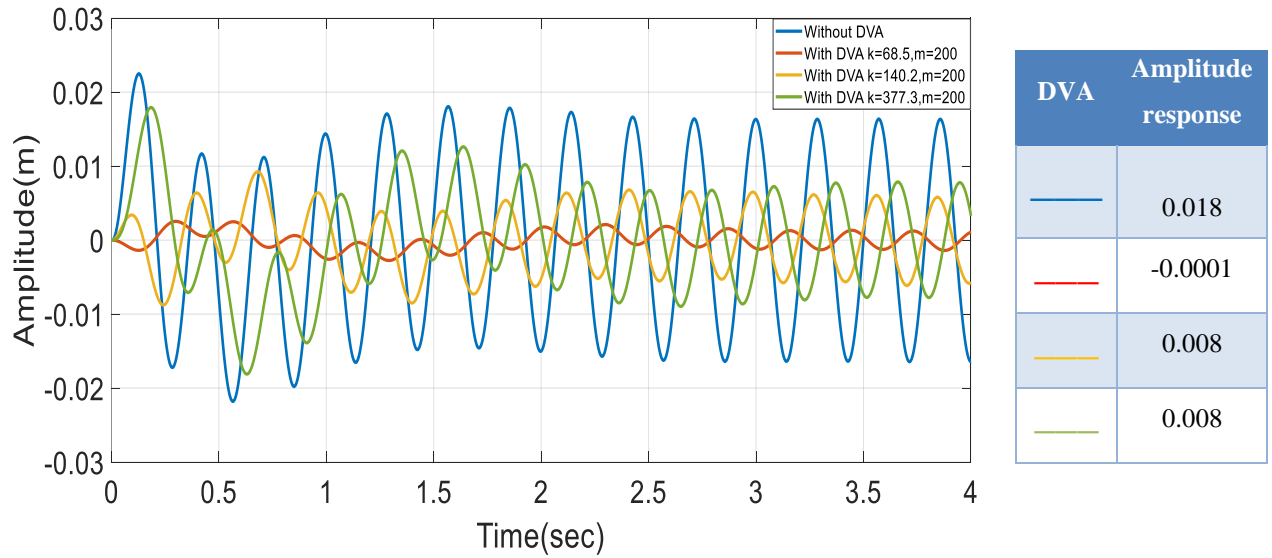


Fig. (5.18) Amplitude response of pin free with and without DVA at $\omega = 6.75\pi$ rad/sec, $x/l = 0.337$.

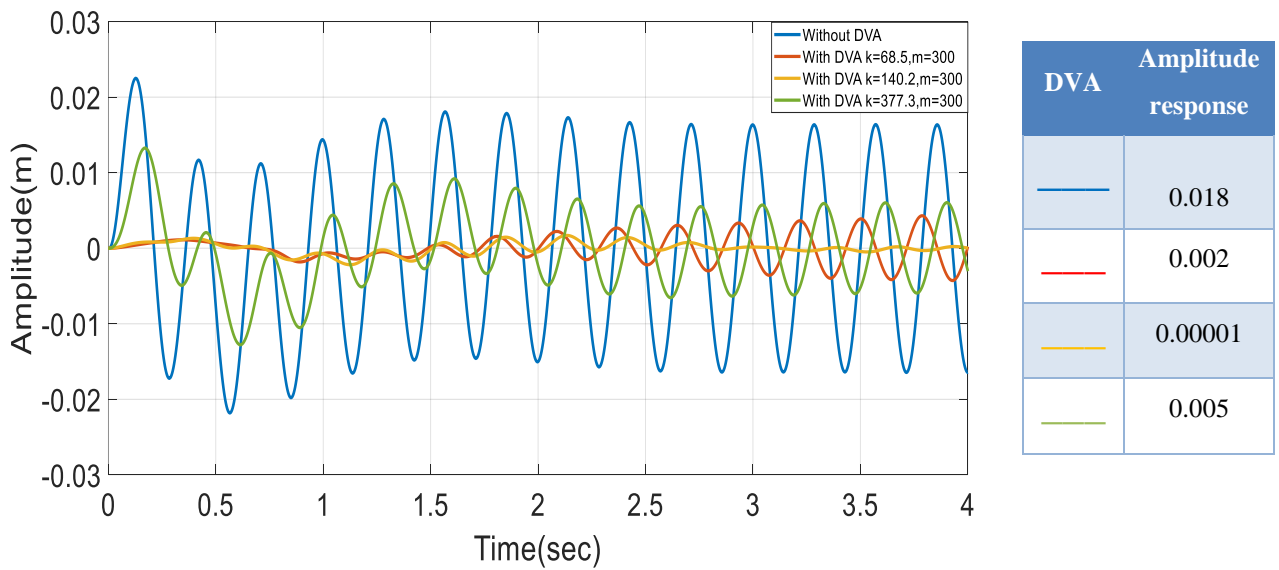


Fig. (5.19) Amplitude response of pin free with and without DVA at $\omega = 6.75\pi$ rad/sec, $x/l = 0.337$.

In general, the dynamic response of the structure is not an abnormal if compared to the response presented when DVA is attached at the free end or at the middle of the beam. However, the amplitude response is larger if the DVA is not designed at the suitable combinations of its mass and stiffness values. For example, the response is increases 400% for $k=68.5$ N/m and $m=100$ grams when the DVA is moved from the free end of the

beam to $x/l=0.337$. This behavior quantify the importance of using a suitable value for mass of DVA. In other words, the change in DVA locations must be adjusted by changing in DVA parameters in order to achieve an optimal DVA that is able to dissipate the kinetic energy of the main system at that specific location.

Next, last three figures reveal that the dynamic response of the main system decreases with increasing the mass of DVA for all values of the DVA stiffness as noticed when $k=140.5\text{N/m}$ and $m=300$ gram if compared with $k=140.5\text{N/m}$ and $m=100$ gram both at $x/l=0.337$. This behavior can attributed to the idea of kinetic energy of the main system and the location of DVA at which this energy is absorbed based on the DVA requirements. The kinetic energy of the main system at a specific location of the beam is a function of the effective mass of the beam and velocity at that location. For the pin-free beam, the nodal velocity (time derivative of the displacement) decreases as the nodes get closer to the pinned constraint of the beam and this reduction in the velocity of this point must be substituted by increasing the attached mass of the DVA in order to absorb higher energy of the main system. This explanation demonstrates the general behavior of the dynamic response at different locations of the DVA on the beam.

5.6.1.1.2 Effect of mass

This effect is implicitly studied in brief in the previous figures. However, detailed explanations are required to demonstrate effect of mass of DVA on the dynamic response of the beam. Figures (5.20 through 5.22) demonstrate how DVA mass affects the dynamic response of a beam for three different DVA stiffness. As noticed previously, both DVA mass and stiffness variations have a significant impact on the dynamic response of the beam, but to a limited extents. Regardless of the stiffness and mass values of the DVA, the dynamic response of the beam is reduced compared to its response without DVA.

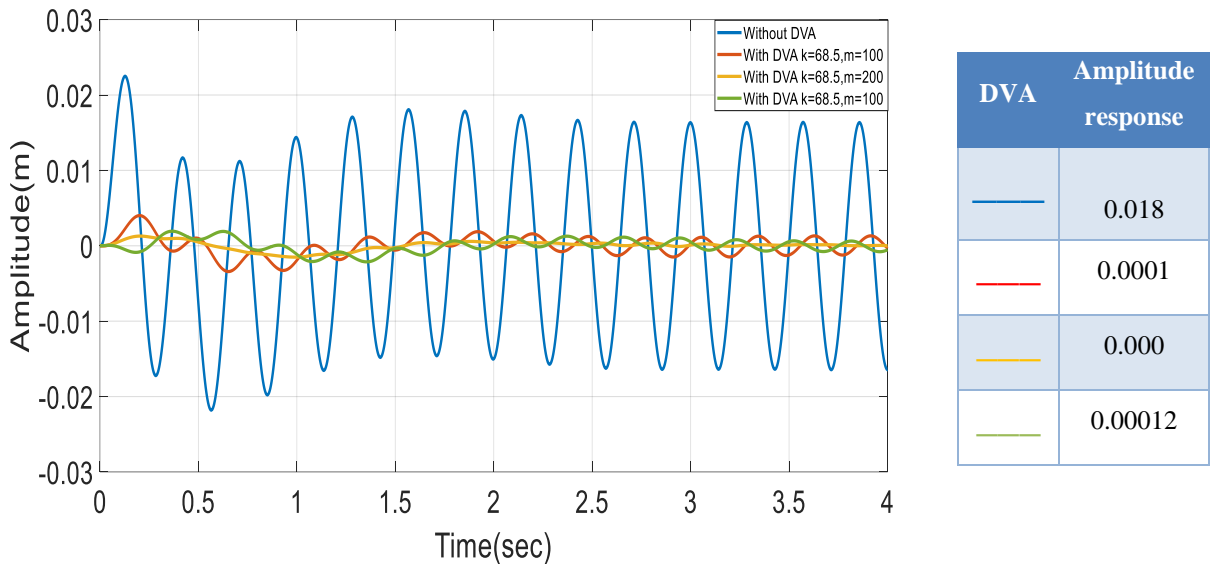


Fig. (5.20) effect of mass at beam ($t=0.12m$) of pin free with and without DVA at $\omega = 6.75\pi$ rad/sec, $x/l = 1$

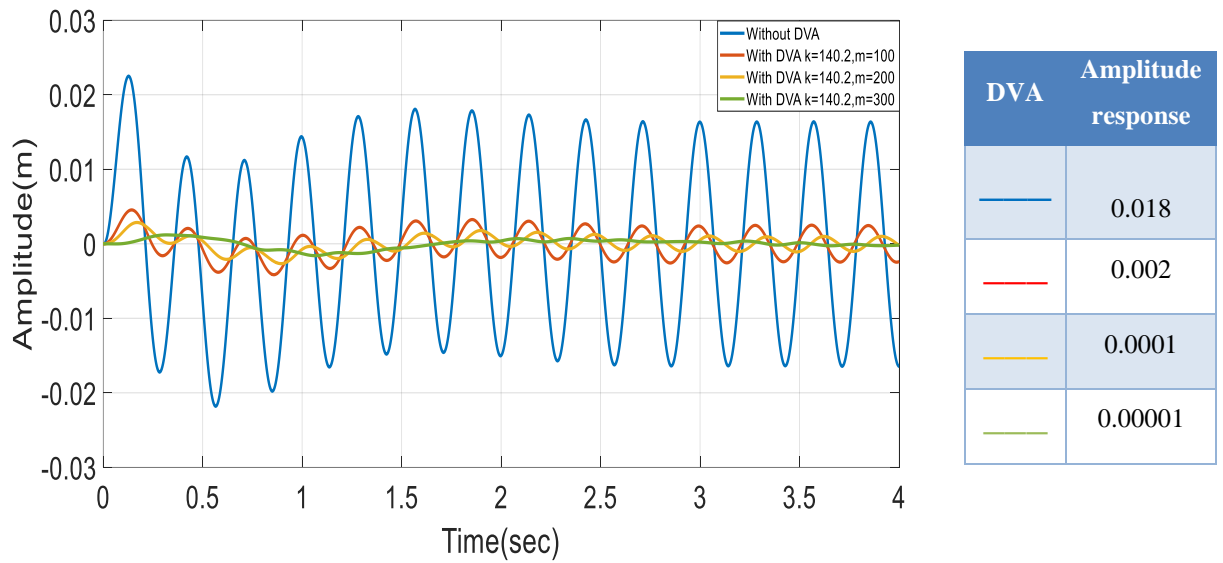


Fig. (5.21) effect of mass at beam ($t=0.12m$) of pin free with and without DVA at $\omega = 6.75\pi \text{rad/sec}$, $m = 100, 200, 300 \text{ gram}$, $k = 140.2 \text{ N/m}$, $x/l = 1$

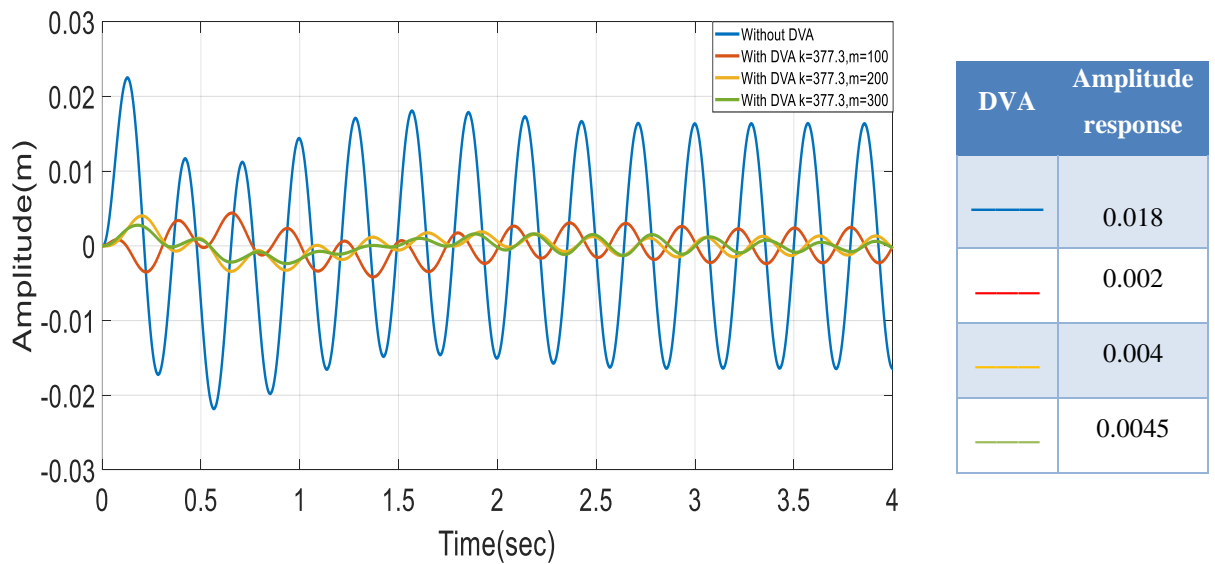


Fig. (5.22) effect of mass at beam ($t=0.12m$) of pin free with and without DVA at $\omega = 6.75 \pi \text{ rad/sec}$, $x/l = 1$

A simple comparison between these figures reveals that the minimum dynamic responses are achieved at the smaller values of the stiffness and increases with increasing the stiffness for all values of the DVA mass when the DVA is attached at the free end of the beam. The local optimal combination of the stiffness and mass occurs when $k=140.5$ N/m and $m=300$ gram.

As discussed earlier, DVA location is another important factor need to be studied in terms of effect of mass. The next section will discuss effect of DVA location. Figs. (5.23 through 5.25) and (5.26 through 5.28) show the dynamic response equivalent to Figs. (5.20-5.22) but when the DVA is located at the middle ($x/l=0.5$) and ($x/l=0.337$) instead of ($x/l=1$), respectively.

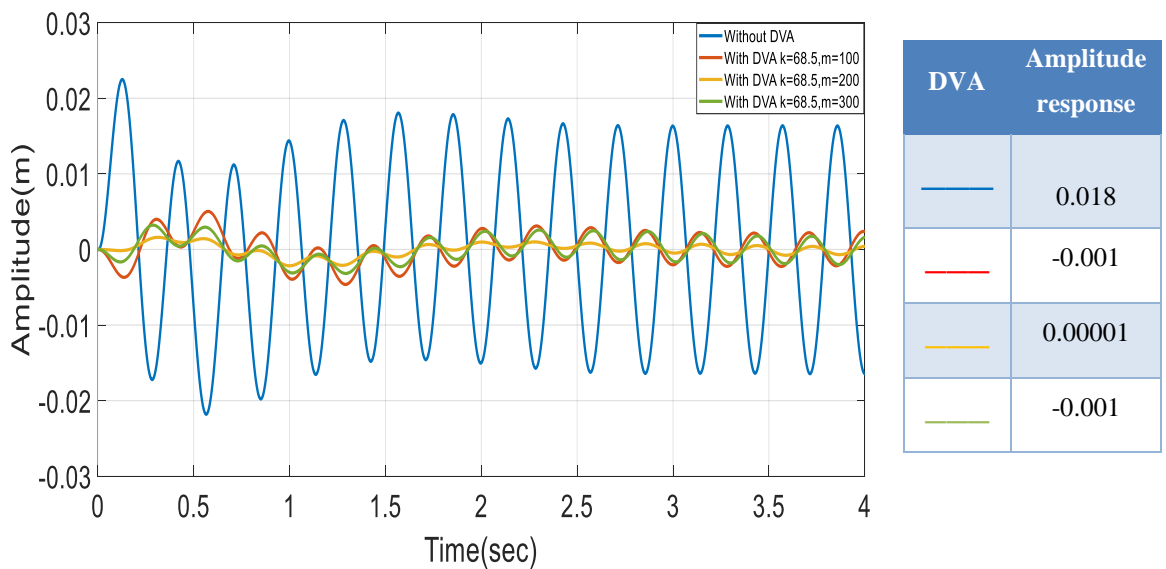


Fig (5.23) effect of mass at beam ($t=0.12m$) of pin free with and without DVA at $\omega = 6.75\pi$ rad/sec, $x/l = 0.5$

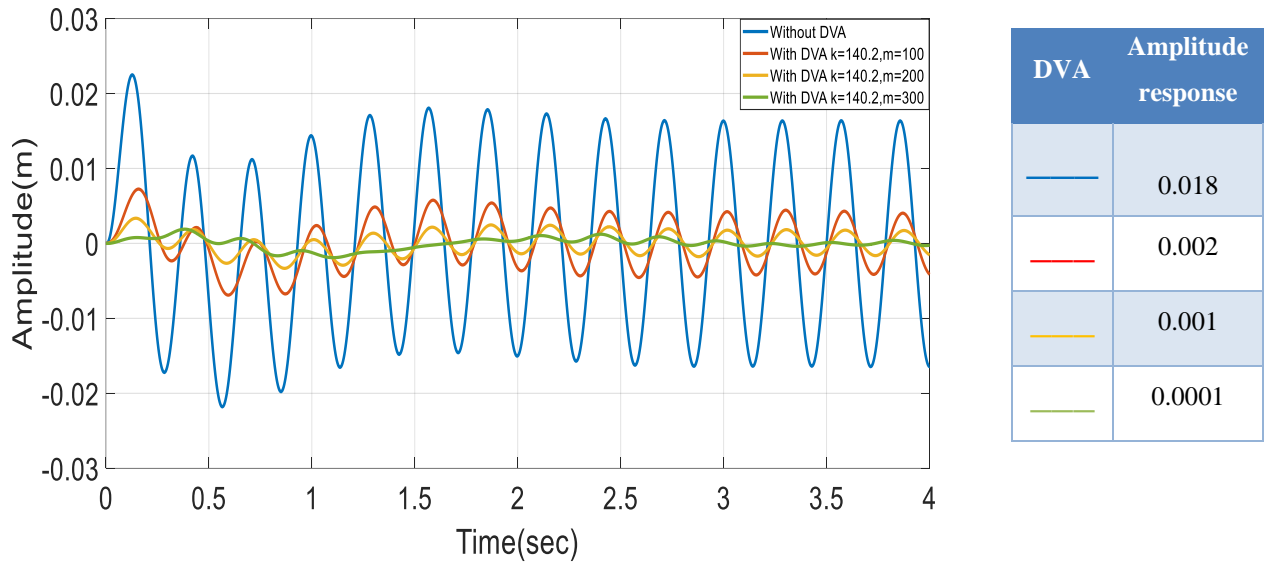


Fig (5.24) effect of mass at beam ($t=0.12m$) of pin free with and without DVA at $\omega = 6.75 \pi$ rad/sec, $x/l = 0.5$

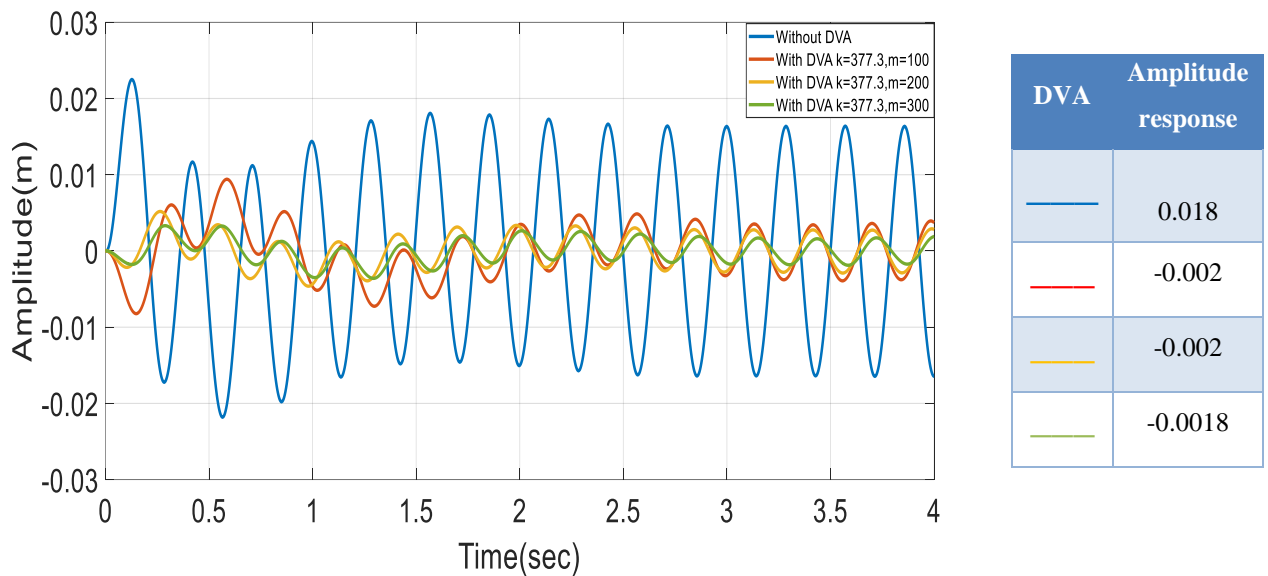


Fig (5.25) effect of mass at beam ($t=0.12m$) of pin free with and without DVA at $\omega = 6.75 \pi$ rad/sec, $x/l = 0.5$

Figs. (5.23-5.25) show a slightly change in the behavior if compared when DVA is located at the free end of the beam. However. The dynamic response has significantly reduced. Still the local combinations for the local optimal values are (68.5N/m, $m=200$ gram) and ($k=140.2$ N/m and $m=300$ gram),

respectively. The only difference that can be noticed is the amplitude of the dynamic response which is bigger when the DVA is not designed to be located at the free end of the beam (maximum deflection). Similar conclusions can be drawn when the DVA is located closer to the pinned point of the beam or farther relative to its free end as shown in Figs. (5.26-5.27) when the DVA is located at $x/l=0.337$. Higher dynamic response for the beam is noticed in these figures.

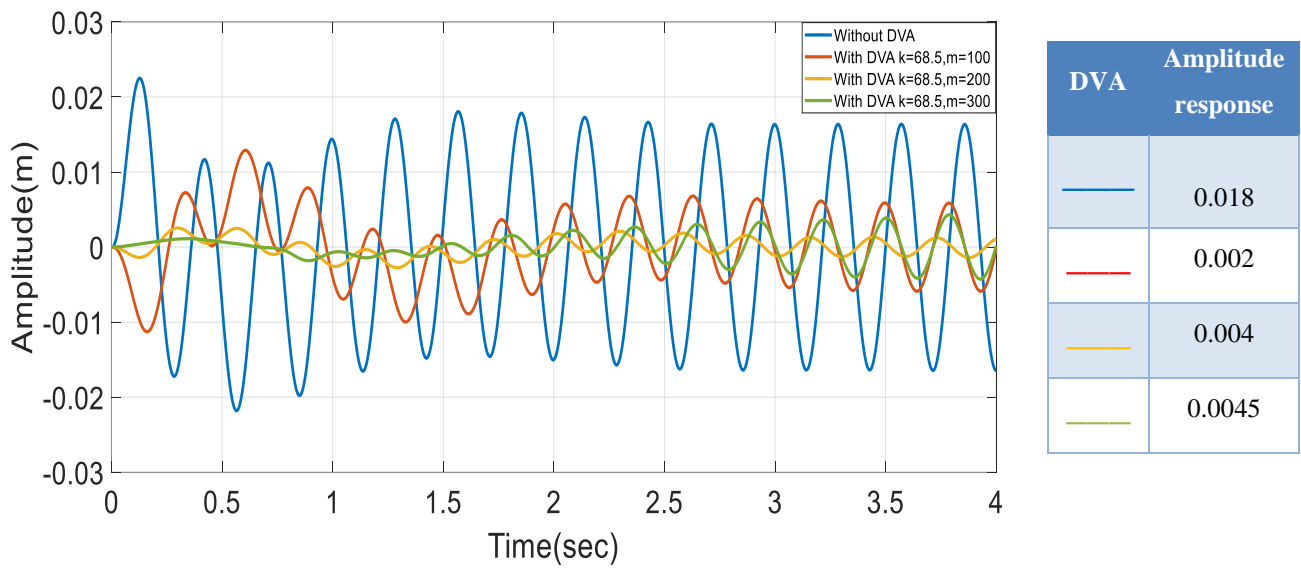


Fig (5.26) Amplitude response of pin free with and without DVA at $\omega = 6.75\pi$ rad/sec , $x/l = 0.337$

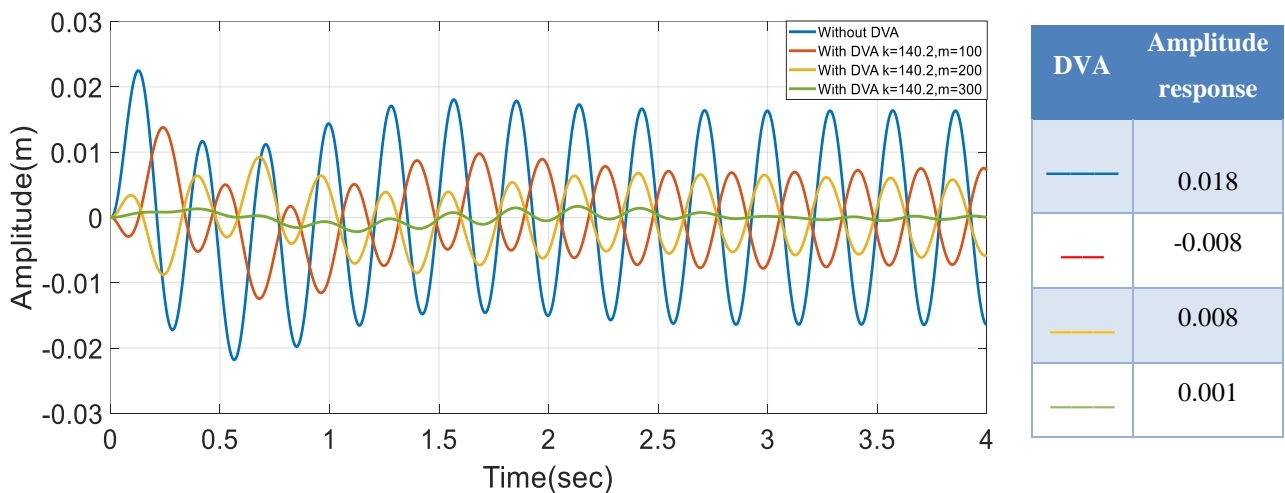


Fig (5.27) Amplitude response of pin free with and without DVA at $\omega = 6.75\pi$ rad/sec , $x/l = 0.337$

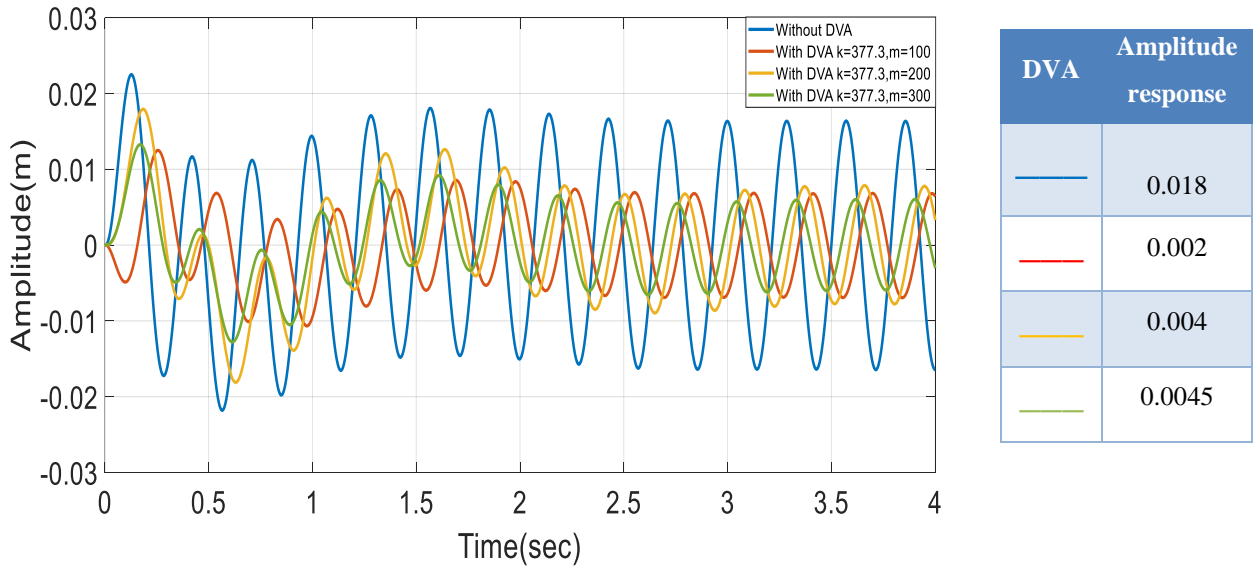


Fig (5.28) Amplitude response of pin free with and without DVA at $\omega = 6.75 \pi \text{ rad/sec}$, $x/l = 0.337$

At the higher values of the stiffness, when DVA is not located efficiently as shown in Fig. 5.28, increasing mass of DVA significantly increasing the amplitude of the time response while the DAV is considered as an inappropriate design, where no locally or globally optimal design is reached.

5.6.2 Dynamic response of Beam 2

The dimensions of the rectangular Beam 2 are as follows: thickness of $t=0.005\text{m}$, width of $w=0.025\text{m}$, and length of $l=0.84\text{m}$. The boundary conditions are also described in the following subsections.

5.6.2.1 Pin-free for the Beam2

5.6.2.1.1 Effect of stiffness

The dynamic response of the second beam (Beam2) is studied in light of changing the DVA stiffness for the pin-free boundary condition. Figs (5.29 through 5.31) presented the dynamic response for the beam under effect of three stiffness values. Generally speaking, both DVA stiffness and mass

variations have a noticeable effect on the dynamic response and the value of the reduction vary with DVA stiffness and mass variation. Specifically, in Fig. (5.47), the local minimal time response is noticed at the combination of $k=140.2\text{N/m}$ and $m=200$ gram. This combination is the closer to the excitation frequency of the DC motor. The other values of the reduction in the same figure are relatively higher because the mismatch in the frequencies.

Fig. (5.31), on the other hand, shows a different locally optimal DVA design for the same reason mentioned earlier, with $k=377.3$ N/m and $m=500$ gram. Ultimately, the locally optimal DVA design (for Figures (5.47-5.49)) that results in the most significant reduction is achieved with $k=140.2$ N/m and $m=200$ gram when the dynamic response is measured at $x/l=1$ and the DVA is located at the end of the beam.

The next section will discuss effect of DVA location with same stiffness and mass values studied above for the pin-free beam.

Figs. (5.32 through 5.34) show the dynamic response equivalent to Figs. (5.29-5.31) but when the DVA is located at the middle ($x/l=0.5$) instead of ($x/l=1$). In general, similar behavior of the dynamic response is noticed when the DVA is attached at the middle of the beam as compared to the last three figures where the DVA is attached at the free end of the beam. The only difference is that the corresponding displacement response is higher. However, the combination of $k=68.5$ N/m and $m=200$ gram still showing the smallest response among the other

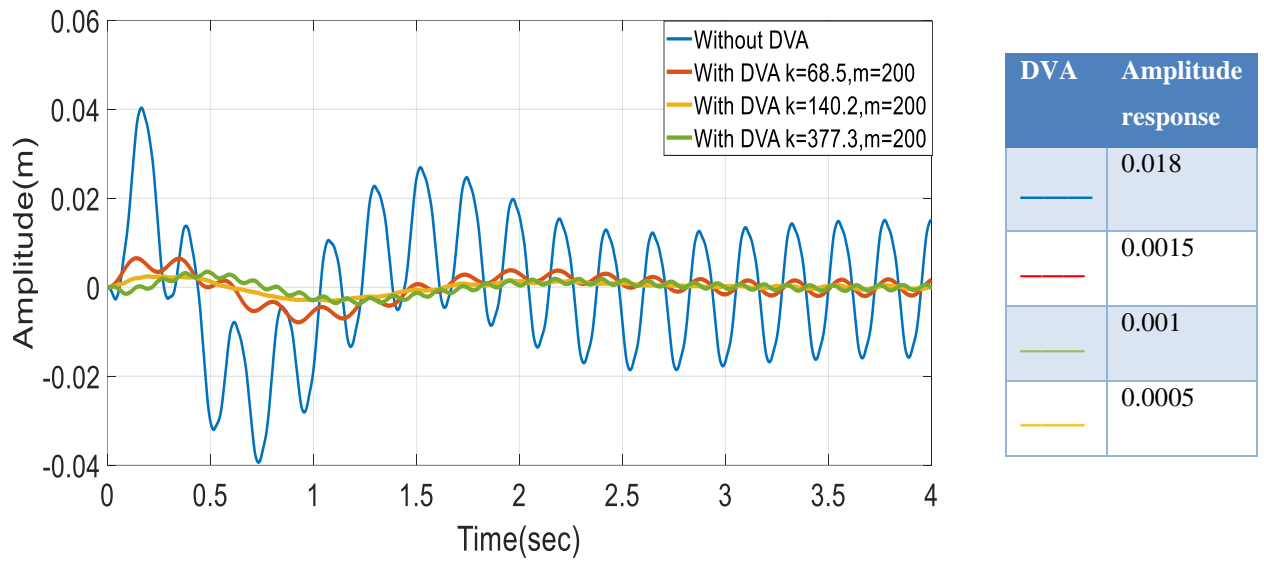


Fig (5.29) effect of stiffness at pin free with and without DVA at $\omega = 8.1\pi$ rad/sec, $x/l = 1$.

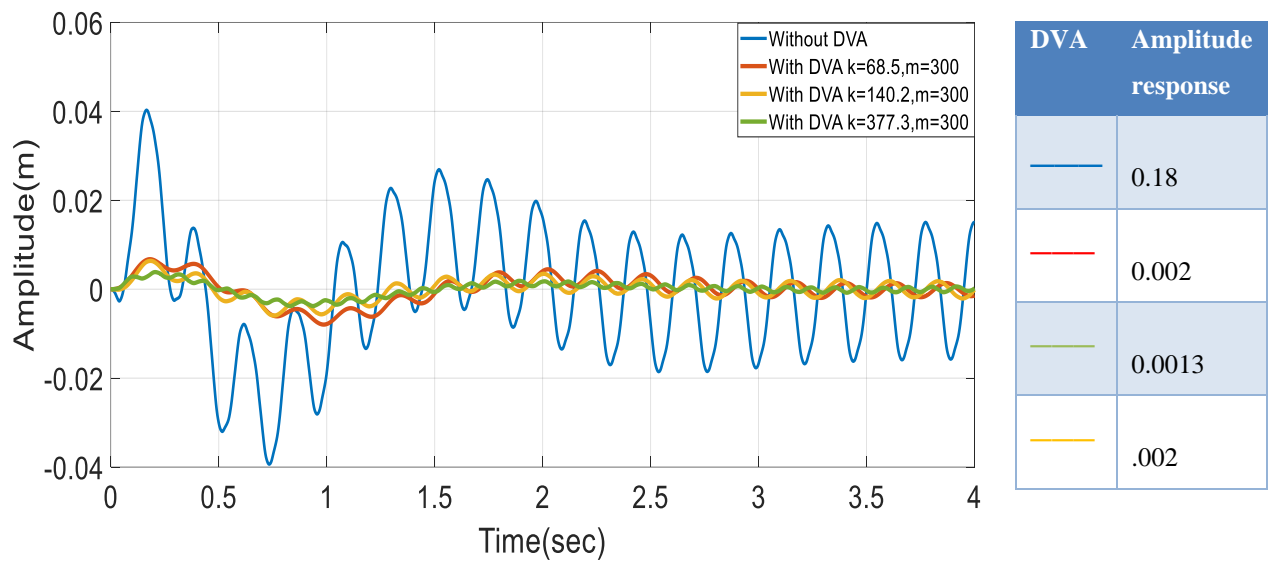


Fig. (5.30) effect of stiffness at pin free with and without DVA at $\omega = 8.1\pi$ rad/sec, $x/l = 1$.

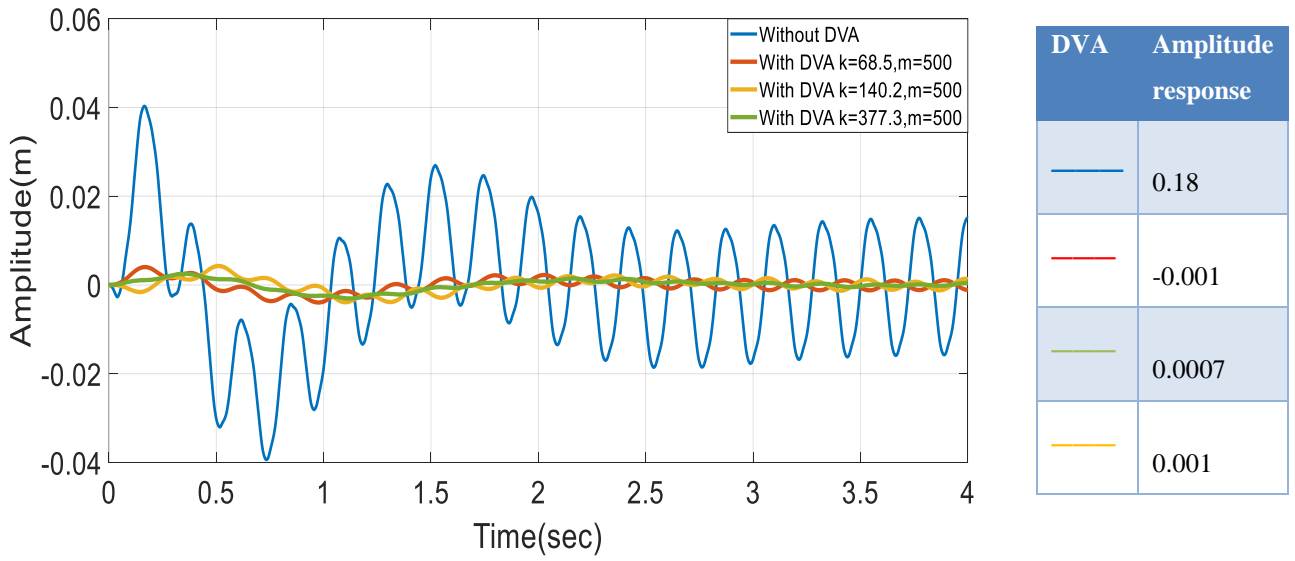


Fig. (5.31) effect of stiffness at pin free with and without DVA at $\omega = 8.1 \pi \text{ rad/sec}$ $x/l = 1$.

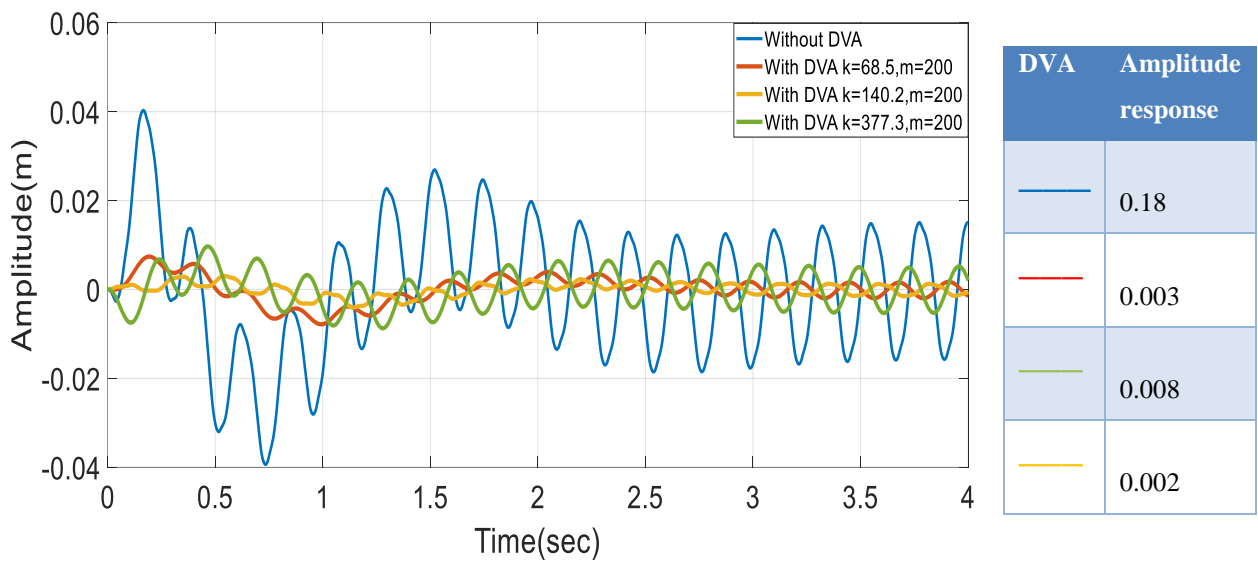


Fig. (5.32) effect of stiffness at pin free with and without DVA at $\omega = 8.1\pi \text{ rad/sec}$, $x / l = 0.5$

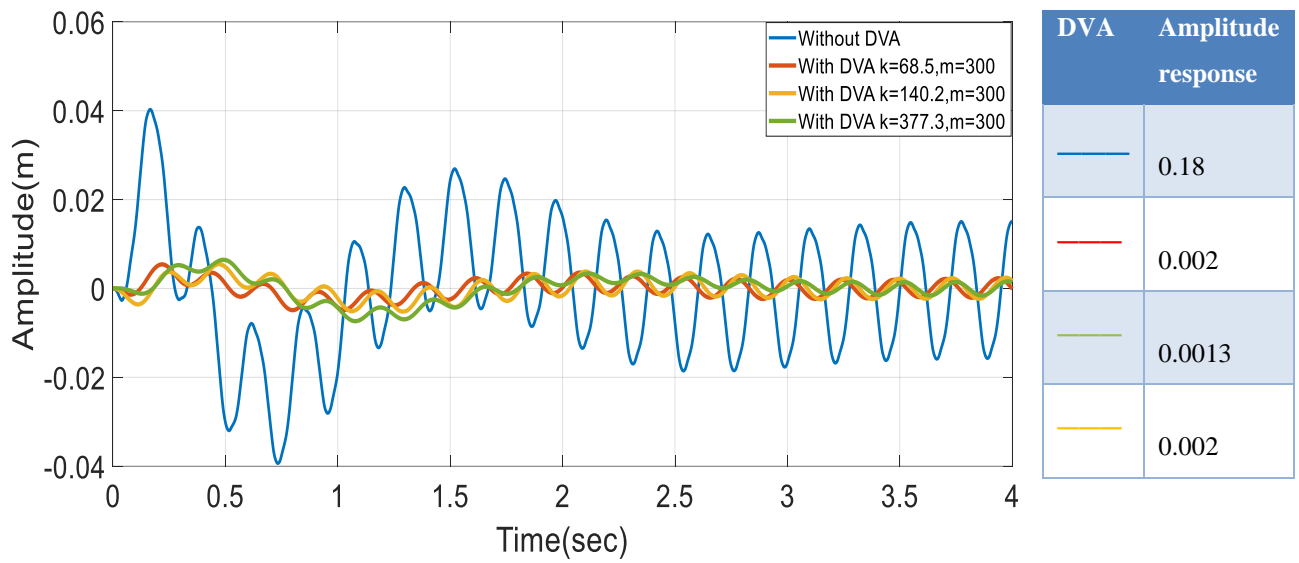


Fig. (5.33) effect of stiffness at pin free with and without DVA at $\omega = 8.1\pi$ rad/sec , $x / l = 0.5$

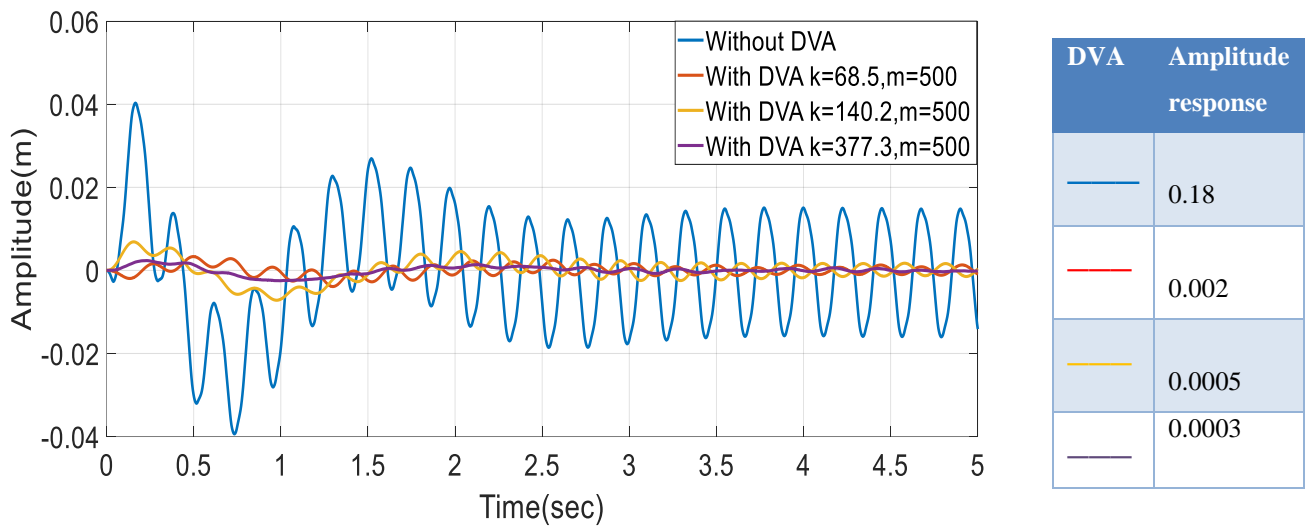


Fig. (5.34) the effect of stiffness at pin free with and without DVA at $\omega = 8.1\pi$ rad/sec, $x / l = 0.5$.

Another location for the DVA of the pinned beam is also studied. Similar conclusions for the other types of boundary conditions where the DVA is attached not at the end of the beam. However, it seems that the magnification in the dynamic response is relatively higher in the pinned beam if compared to the boundary conditions. This can be attributed to how hard the constraint of the beam by its boundary. The harder the constrain, the smaller the magnification in the dynamic response as shown in Figs (5.35-5.37).

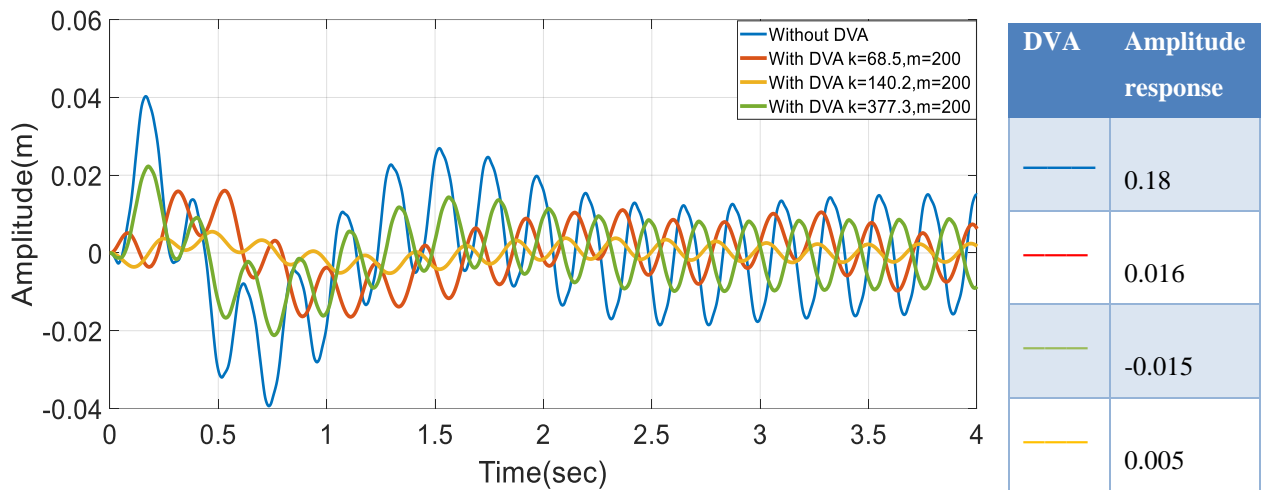


Fig. (5.35) effect of mass of pin free with and without DVA at $\omega = 8.1\pi$ rad/sec , $x / l = 0.337$

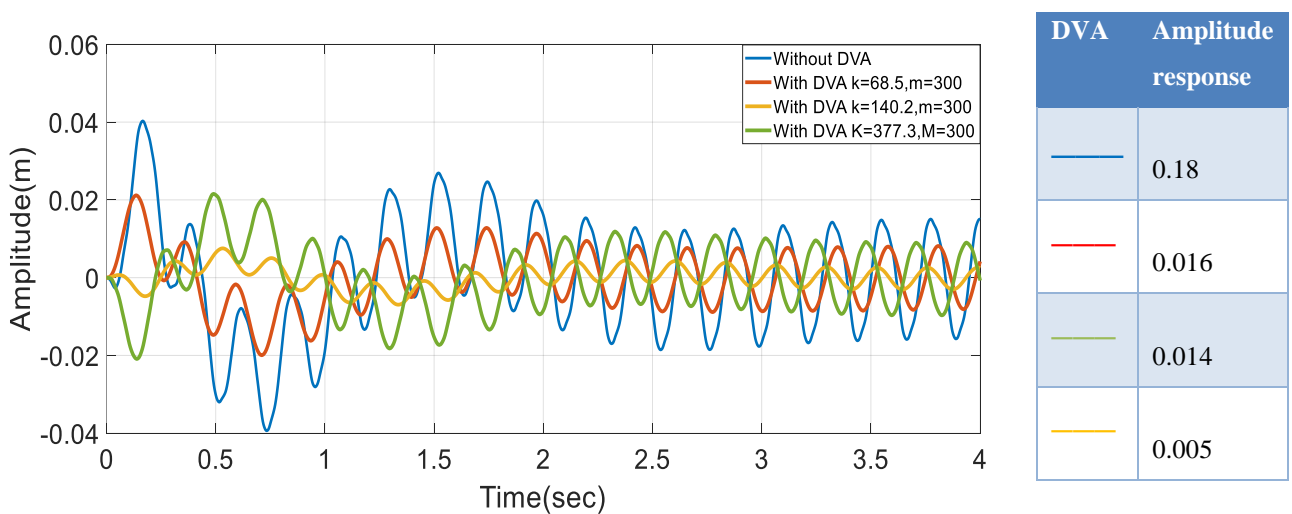


Fig. (5.36) effect of mass of pin free with and without DVA at $\omega = 8.1\pi$ rad/sec x / l = 0.337

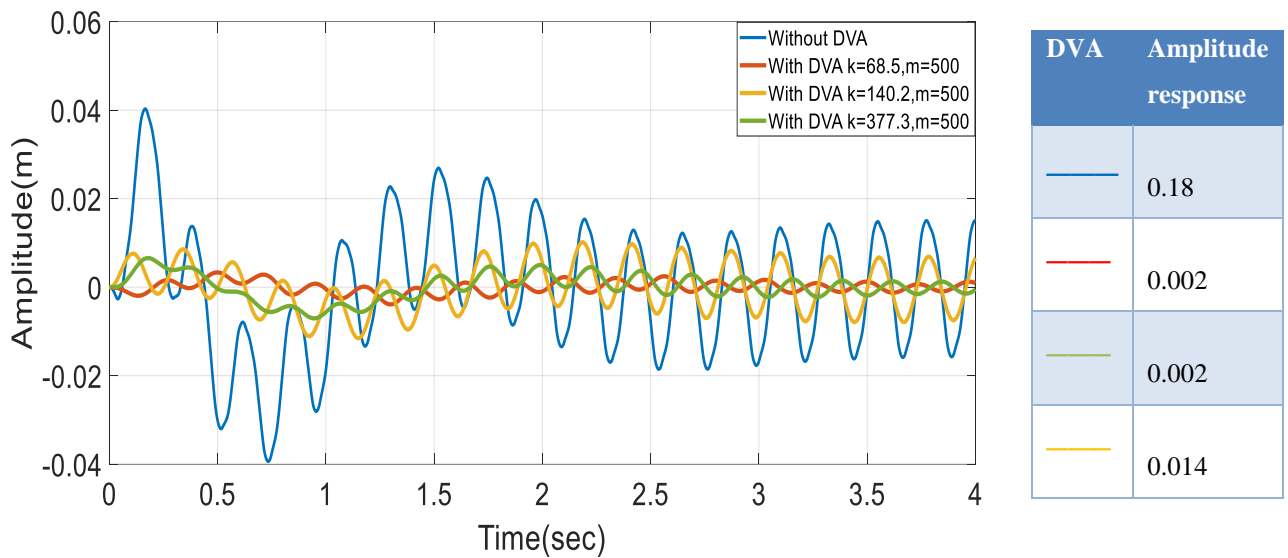


Fig. (5.37) effect of mass of pin free with and without DVA at $\omega = 8.1\pi$ rad/sec, $x / l = 0.337$

5.6.2.1.2 Effect of Mass

Figs. (5.38 through 5.40) quantify effect of mass of DVA on the dynamic response of the pinned beam. The dynamic response of the beam is reduced compared to its response without DVA. It is noted that, within the range of mass and stiffness used in these experiments, there is no common trend for the behavior with increasing or decreasing the stiffness mass of the DVA. That is because the critical values of the DVA parameters that defined the local and local optimal response. However, the results show that band width of the dynamic response (the difference of the upper and lower response at a specific point) is not quite sensitive to the variations of the mass of the DVA at the higher values of the stiffness as shown in Fig. (5.40).

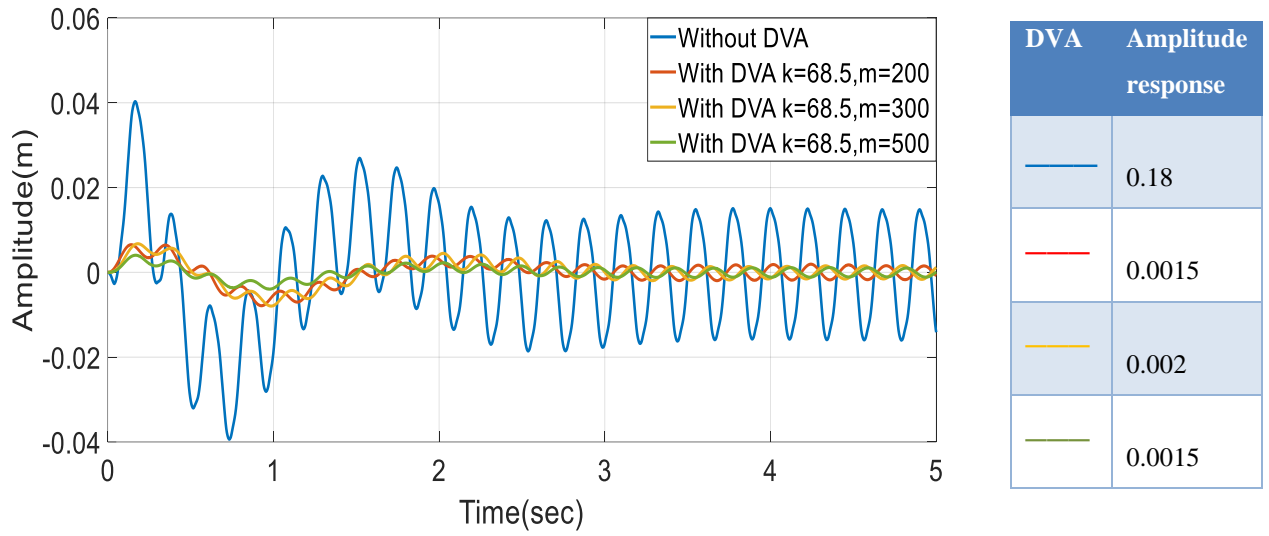


Fig. (5.38) the effect of mass at pin free with and without DVA at $\omega = 8.1\pi$ rad/sec $x/l =$

1

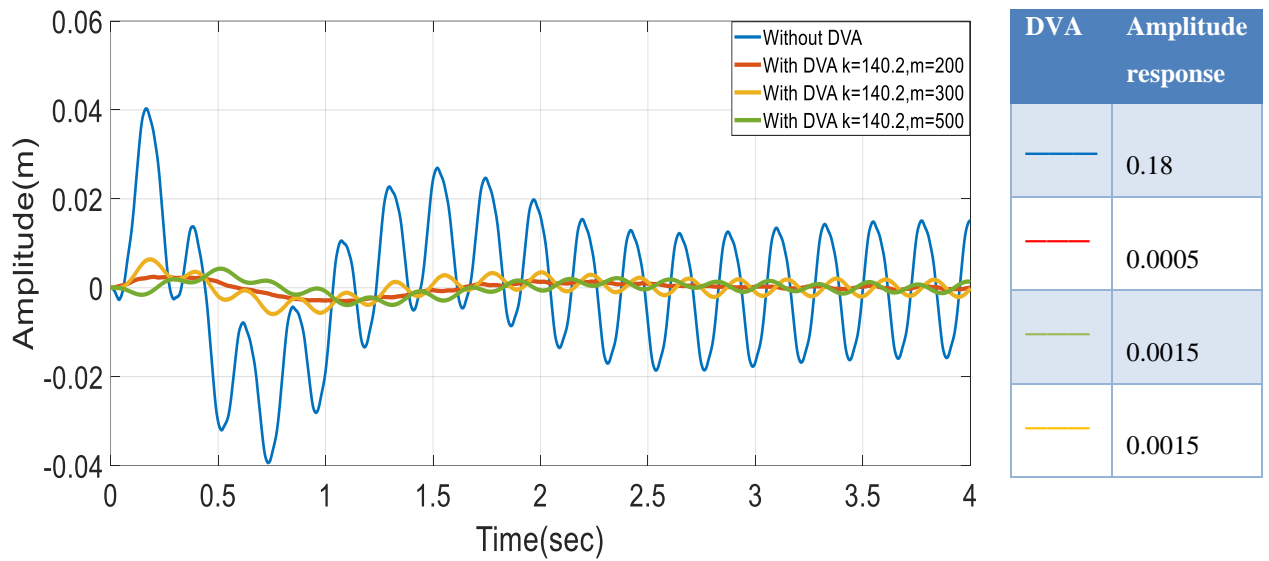


Fig. (5.39) Effect of mass at pin free with and without DVA at $\omega = 8.1\pi$ rad/sec, $x/l = 1$

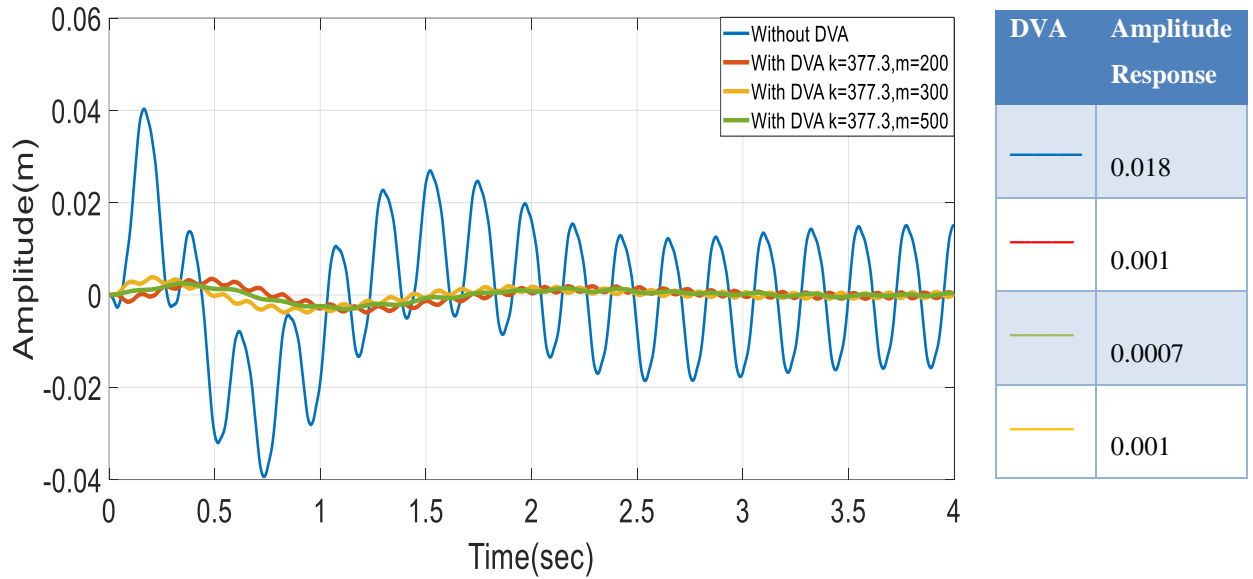


Fig. (5.40) Effect of mass at pin free with and without DVA at $\omega = 8.1\pi$ rad/sec , $x = 1$

DVA locations showed another factor that affect the dynamic response of the pinned beam when the DVA attached at $x/l=0.5$ and $x/l=0.337$ of the beam, respectively. The dynamic response increased as the point at which the DVA is attached get farther from the point of maximum displacement of the pinned beam ($x/l=1$) as shown in Figs (5.41-5.46). The dynamic response become uncontrollable and the dynamic response is unpredictable for the pinned beam specially when the beam is flexible enough where the inertia effect of the other part of the beam become more effective and chaos response might be developed as shown in Fig. (5.46).

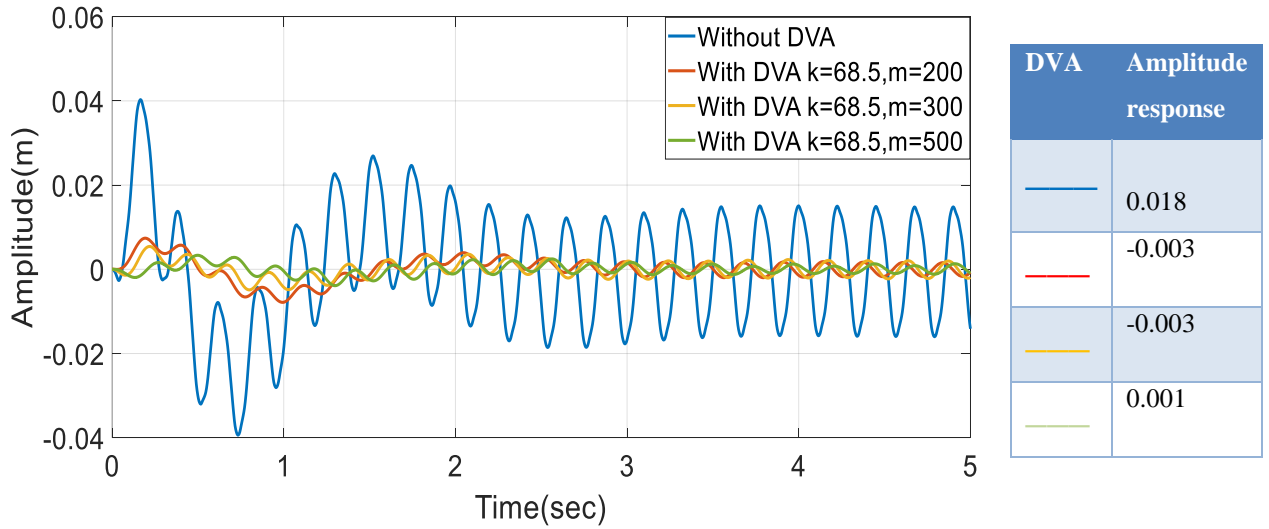


Figure (5.41) the effect of mass at pin free with and without DVA at $\omega = 8.1\pi$ rad/sec , $x / l = 0.5$

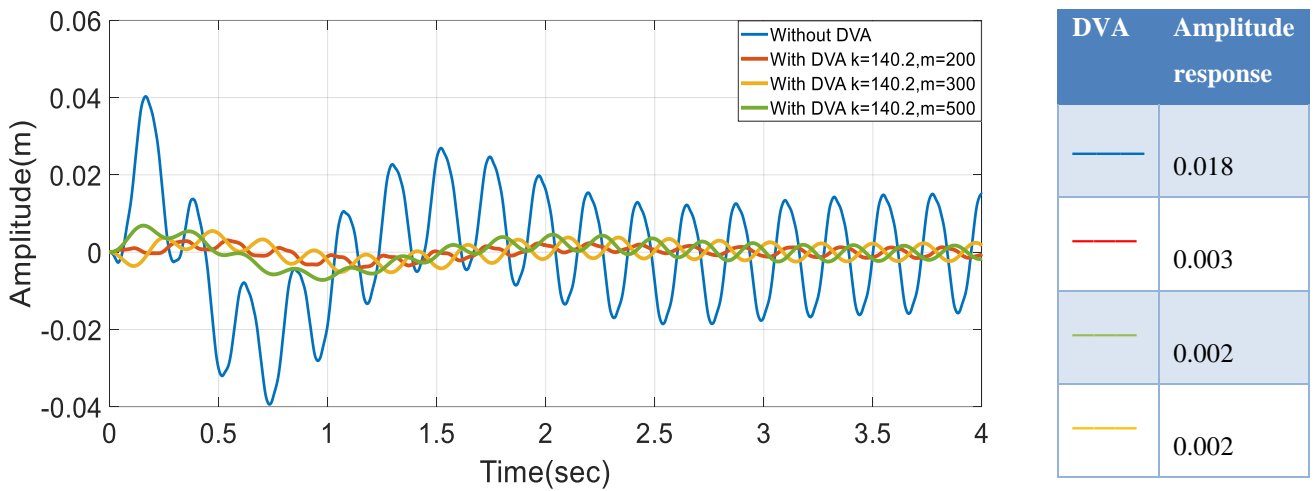
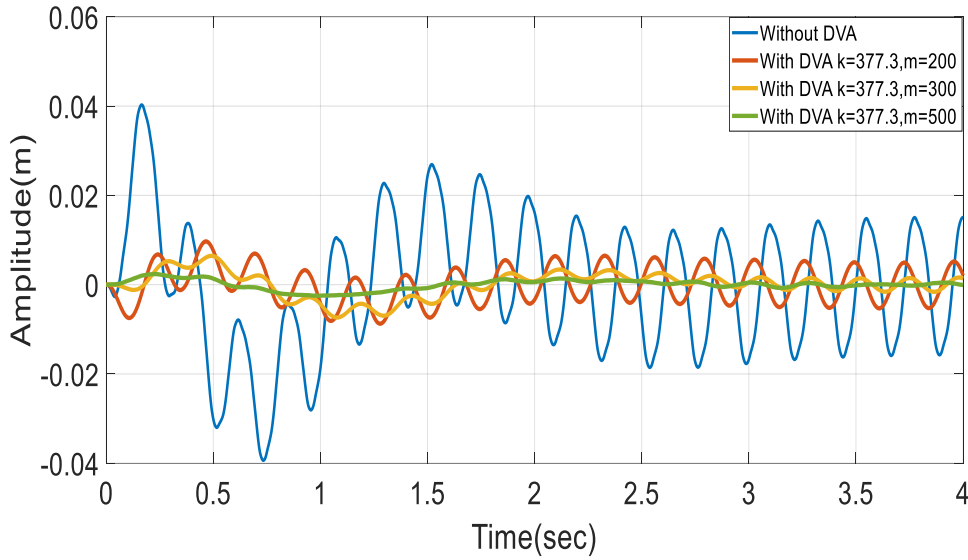
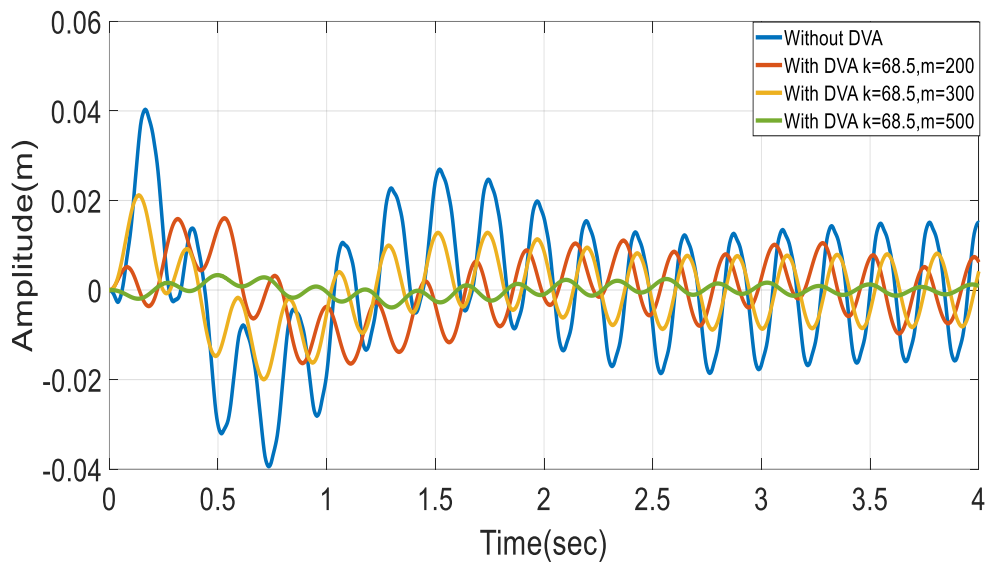


Fig. (5.42) the effect mass at pin free with and without DVA at $\omega = 8.1\pi$ rad/sec , $x / l = 0.5$



DVA	Amplitude response
Without DVA	0.018
With DVA k=377.3, m=200	0.008
With DVA k=377.3, m=300	0.00001
With DVA k=377.3, m=500	0.001

Fig. (5.43) the effect mass at pin free with and without DVA at $\omega = 8.1\pi$ rad/sec, $x / l = 0.5$



DVA	Amplitude response
Without DVA	0.018
With DVA k=68.5, m=200	0.016
With DVA k=68.5, m=300	0.002
With DVA k=68.5, m=500	0.014

Fig. (5.44) the effect of mass at pin free with and without DVA at $\omega = 8.1\pi$ rad/sec, $x / l = 0.377$

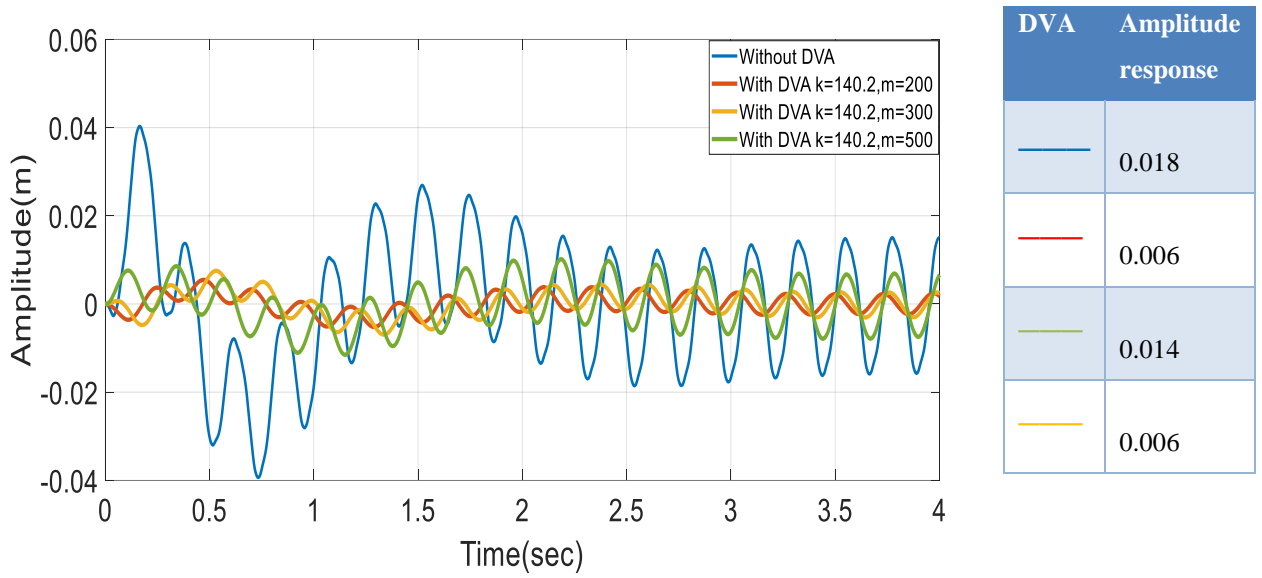


Fig. (5.45) the effect mass at pin free with and without DVA at $\omega = 8.1\pi$ rad/sec, $x / l = 0.337$

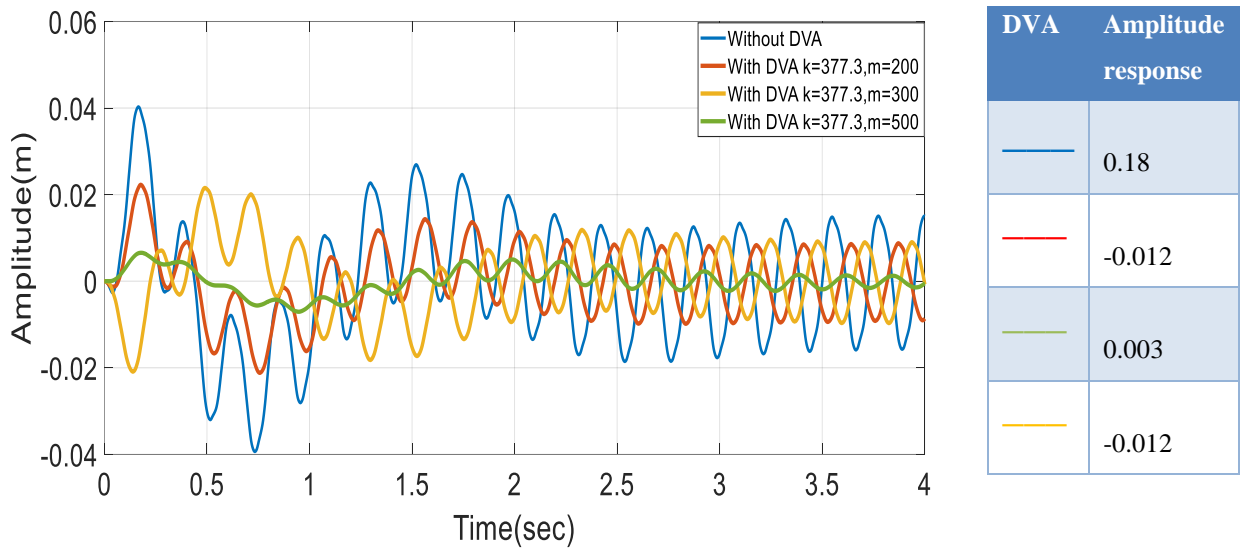


Fig. (5.46) the effect of mass at pin free with and without DVA at $\omega = 8.1\pi$ rad/sec, $x / l = 0.337$

5.6.2.2 Cantilever Boundary Condition

The left-hand side of the cantilever beam is fixed, while the right-hand side is free. Same location of the Dc motor and supporting spring of the beam are kept the same.

5.6.2.2.1 Effect of Stiffness

Table(5.2) demonstrates effect of the stiffness of the DVA on the dynamic response of a beam for four different DVA masses (100, 200, 300,500 gram). First of all, all of the DVA stiffness and mass combinations show a significant impact on the dynamic response of the beam. Regardless of the stiffness and mass values of the DVA, the dynamic response of the beam is reduced compared to its response without DVA.In addition , reducing the stiffness with a DVA mass of 100 grams leads to a decrease in dynamic response, with the better reduction achieved at a stiffness of $k=377.3$ N/m.

Table (5.2) effect of stiffness at cantilever beam with and without DVA at $\omega = 16.5 \pi \text{ rad/sec}$, $x/l = 1$

Effect of Stiffness				
BC	$\omega = 16.5 \pi \text{ rad/sec}$		X/L=1	
	DVA	Mass(m) (g)	Stiffness(K) (N/m)	Ampl.(m)
Cantilever	Without DVA			0.02
	With DVA	100	68.5	0.001
		100	140.2	0.001
		100	377.3	0.0005
		200	68.5	0.001
		200	140.2	0.0005
		200	377.3	0.00001
		300	68.5	0.001
		300	140.2	0.001
		300	377.3	0.0015
		500	68.5	0.001
		500	140.2	0.001
		500	377.3	0.0008

DVA location is also important for this type of boundary condition which need to be studied in details. The next section will discuss effect of DVA location with same stiffness and mass values studied above.

show the dynamic response equivalent to table (5.3) but when the DVA is located at the middle ($x/l=0.5$) instead of ($x/l=1$). In general, similar trend of the dynamic response is noticed when the DVA is attached at the middle of the beam as compared where the DVA is attached at the free end of the beam. The only difference is that the corresponding displacement response is bigger when the DVA attached at the middle.

Table (5.3) effect of stiffness at cantilever beam with and without DVA at $\omega = 16.5 \pi \text{ rad/sec}$, $x/l = 0.5$

Effect of Stiffness				
BC	$\omega = 16.5 \pi \text{ rad/sec}$		X/L=0.5	
Cantilever	DVA	Mass(m) (g)	Stiffness(K) (N/m)	Ampl.(m)
	Without DVA			0.02
	With DVA	200	68.5	0.006
		200	140.2	0.0005
		200	377.3	0.0001
		300	68.5	0.002
		300	140.2	0.003
		300	377.3	0.001

		500	68.5	-0.001
		500	140.2	-0.002
		500	377.3	0.001

5.6.2.2.2 Effect of mass

This effect is implicitly studied in brief in the previous tables. However, detailed explanations are required to demonstrate effect of mass of DVA on the dynamic response of the beam. Tabl(5.4) demonstrates how DVA mass affects the dynamic response of a beam for three different DVA stiffness. Both DVA mass and stiffness variations have a significant impact on the dynamic response of the beam, but to a limited extents. It is noticed that the dynamic response a specific stiffness does not considerably changed the response if compared to the order of the dynamic response without DVA. In other words, the differences in responses are not significant enough within the studied range of the masses in this experimental work.

Table (5.4) effect of mass at cantilever beam with and without DVA at $\omega = 16.5 \pi \text{ rad/sec}$, $x/l = 1$

Effect of mass				
BC	$\omega = 16.5 \pi \text{ rad/sec}$		X/L=1	
Cantilever	DVA	Mass(m) (g)	Stiffness(K) (N/m)	Ampl.(m)
	Without DVA			0.02
	With DVA	100	68.5	0.001
		200	68.5	0.001
		300	68.5	0.0015
		500	68.5	0.001
		100	140.2	0.001
		200	140.2	0.0005
		300	140.2	0.0015
		500	140.2	-0.001
		100	377.3	0.001
		200	377.3	0.0005
		300	377.3	0.0015
		500	377.3	0.001

Table(5.5) show the magnification in the time response due to change the DVA in the middle of the cantilever beam. It important to notice that the combination that give the better reduction in the time response still shows the better reduction among other values even when the DVA is attached at the middle.

5.6.2.3 Fixed-Fixed Boundary Condition

The dimensions of the rectangular Beam 2 are as follows: thickness of $t=0.005\text{m}$, width of $w=0.025\text{m}$, and length of $l=0.84\text{m}$. The boundary conditions are also described in the following subsections. Both sides of the beam are fixed in all directions. Same location of the Dc motor and supporting spring of the beam are kept the same in order to quantify the effect of the boundary conditions in the last section of this chapter.

5.6.2.3.1 Effect of Stiffness

Table(5.5) demonstrates how DVA stiffness affects the dynamic response of a beam for three different DVA masses. First of all, it is important to mention that the old values of the stiffness and some of the mass showed no significant effect on time response of the beam because they are not close enough to the frequency of the beam (30 rad/sec), which represent the best frequency can be attained experimentally just before breaking the requirements of safety for both of the test rig and user.

Next, both DVA stiffness and mass variations have a local significant impact on the dynamic response of the beam. Regardless of the stiffness and mass values of the DVA, the dynamic response of the beam is reduced compared to its response without DVA even in the small order of the time response in order of (10^{-3}).

Table(5.5) the effect of Stiffness at Fixed-fixed beam with and without DVA at $\omega = 30 \text{ rad/sec}$, $x/l = 0.5$

Effect of Stiffness				
BC	$\omega = 30\pi \text{ rad/sec}$		X/L=0.5	
Fixed-Fixed	DVA	Mass(m) (g)	Stiffness(K) (N/m)	Ampl.(m)
	Without DVA			$3.2 * 10^{-3}$
	With DVA	200	427.571	$0.12 * 10^{-3}$
		300	650.34	$0.17 * 10^{-3}$
		200	427.571	$0.18 * 10^{-3}$
		300	650.34	$0.12 * 10^{-3}$
		500	427.571	$0.1 * 10^{-3}$
		500	650.34	$0.12 * 10^{-3}$

5.6.2.3.2 Effect of Mass

Effect of mass is implicitly studied in brief in the previous figures. However, detailed explanations are required to demonstrate effect of mass of DVA on the dynamic response of the beam. Table(5.6) demonstrate how DVA mass affects the dynamic response of a beam for two stiffness of the DVA. As noticed previously, both DVA mass and stiffness variations have a significant impact on the dynamic response of the beam, but to a limited extents.

Regardless of the stiffness and mass values of the DVA, the dynamic response of the beam is reduced compared to its response without DVA.

Table(5.6) the effect of mass at Fixed-fixed beam with and without DVA at $\omega = 30 \text{ rad/sec}$, $x/l = 0.5$

Effect of mass				
BC	$\omega = 30\pi \text{ rad/sec}$		X/L=0.5	
	DVA	Mass(m) (g)	Stiffness(K) (N/m)	Ampl.(m)
Fixed-Fixed	Without DVA			$3.2 * 10^{-3}$
	With DVA	200	427.571	$0.1 * 10^{-3}$
		300	427.571	$0.13 * 10^{-3}$
		500	427.571	$0.38 * 10^{-3}$
		200	650.34	$0.2 * 10^{-3}$
		300	650.34	$0.12 * 10^{-3}$
		500	650.34	$0.2 * 10^{-3}$

Chapter Six

Conclusions and suggestions

CHAPTER SIX

CONCLUSIONS AND RECOMMENDATIONS

6.1 Conclusions

During execution both of the theoretical and experimental part of the DAV system for the lumped mass and beam, respectively, and from obtained the results their discussion in chapter five, the following conclusions can be drawn:

- 1- Both of the mass and stiffness showed a significant effect in reduction the dynamic response. However, this effect varied with the variation of the boundary conditions of the beam and beam geometry.
- 2- The frequency ranges of the optimal designs increase as the mass ratio increases, and the maximum frequency range of 0.510 to 1.022 is attained at a mass ratio and damping ratio of 0.6 and 0.321, respectively.
- 3- Both mass and stiffness have a significant effect on reducing the dynamic response about 97% for the pinned beam, for example.
- 4- Minimal requirements of the DVA parameters can achieve better reduction in the dynamic response if the absorber is located the point of maximum displacement of the beam.

6.2 Recommendations and Suggestions

Many aspects may be concerned with the objectives of the current work in addition to other features that are not considered in the current work. Thus it is possible to suggest the following items as further objectives to be considered for the future consideration.

- 1- Validate the experimental work theoretically by using finite element method.
- 2- Integrate the analytical work with an optimization method to obtain the optimal design of the DVA and its optimal location.
- 3- Use more than one DVA to control the vibration of the beam for different boundary conditions.

References

- [1] Rao, S.S. (2011). *Mechanical Vibrations*. 5th Edition. Pearson
- [2] Zainulabidin, M. H., Jusoh, N. M., Jaini, N., & Kassim, A. S. M. (2016). Effect of tuned absorber location on beam structure vibration by finite element analysis. *ARPJN Journal of Engineering and Applied Sciences*, 11(14), 8585-8591.
- [3] FRANCIS S. TSE, IVAN E. MORSE & ROLLAND T.HINKLE (1978). *Mechanical Vibrations Theory and Applications*. 2nd EDITION. Allyn and Bacon, Inc. 470 Atlantic Avenue, Boston, Massachusetts 02210.
- [4] V.G. Veselago, The electrodynamic of substances with simultaneously negative values of permittivity and permeability, *Sov Phys Usp*, 4 (1968) 509-514.
- [5] Weiglhofer, W. S., & Lakhtakia, A. (Eds.). (2003). *Introduction to complex mediums for optics and electromagnetics* (Vol. 123). SPIE press.
- [6] Altman, J.L.: *Microwave circuits*. Van Nostrand Reinhold, Princeton, NJ, 304 (1964).
- [7] Cui, T. J., Smith, D. R., & Liu, R. (2010). *Metamaterials* (p. 1). Boston, MA, USA:: springer.
- [8] Mendhe, S. E., & Kosta, Y. P. (2011). Metamaterial properties and applications. *International Journal of Information Technology and Knowledge Management*, 4(1), 85-89.
- [9] Tong, X. C. (2018). Electromagnetic Metamaterials and Metadevices. In *Functional Metamaterials and Metadevices* (pp. 39-55). Springer, Cham.

- [10] Kodama, C. H., & Coutu Jr, R. A. (2017). THz Metamaterial Characterization Using THz-TDS. *Terahertz Spectroscopy-A Cutting Edge Technology*.
- [11] Wegener, M. (2011, January). 3D photonic metamaterials and invisibility cloaks: The making of. In *2011 IEEE 24th International Conference on Micro Electro Mechanical Systems* (pp. 1-4). IEEE.
- [12] Turpin, J. P., Bossard, J. A., Morgan, K. L., Werner, D. H., & Werner, P. L. (2014). Reconfigurable and tunable metamaterials: a review of the theory and applications. *International Journal of Antennas and Propagation, 2014*.
- [13] D.R. Smith, W.J. Padilla, D. Vier, S.C. Nemat-Nasser, S. Schultz, Composite medium with simultaneously negative permeability and permittivity, *Phys Rev Lett*, 84 (2000) 4184-4187.
- [14] R. Marques, J. Martel, F. Mesa, F. Medina, Left-handed-media simulation and transmission of EM waves in subwavelength split-ring-resonator-loaded metallic waveguides, *Phys Rev Lett*, 89 (2002) 183901.
- [15] H. Sun, X. Du, P.F. Pai, Theory of metamaterial beams for broadband vibration absorption, *J Intell Mater Syst Struct*, 21 (2010) 1085-1101.
- [16] P.F. Pai, G. Huang, Theory and Design of Acoustic Metamaterial, SPIE, Bellingham, 2016
- [17] J. Li, C. Chan, Double-negative acoustic metamaterial, *Phys Rev E* 70 (2004) 055602.
- [18] Y. Cheng, J. Xu, X. Liu, One-dimensional structured ultrasonic metamaterials with simultaneously negative dynamic density and modulus, *Phys Rev B*, 77 (2008) 045134

- [19] H. Peng, P.F. Pai, H. Deng, Acoustic multi-stopband metamaterial plates design for broadband elastic wave absorption and vibration suppression, *Int J Mech Sci*, 103 (2015) 104-114.
- [20] G. Gantzounis, M. Serra-Garcia, K. Homma, J. Mendoza, C. Daraio, Granular metamaterials for vibration mitigation, *J Appl Phys*, 114 (2013) 093514.
- [21] Lee, C. L., Chen, Y. T., Chung, L. L., & Wang, Y. P. (2006). Optimal design theories and applications of tuned mass dampers. *Engineering structures*, 28(1), 43-53.
- [22] Sladek, J. R., & Klingner, R. E. (1983). Effect of tuned-mass dampers on seismic response. *Journal of structural engineering*, 109(8), 2004-2009.
- [23] Tse, K. T., Kwok, K. C., & Tamura, Y. (2012). Performance and cost evaluation of a smart tuned mass damper for suppressing wind-induced lateral-torsional motion of tall structures. *Journal of Structural Engineering*, 138(4), 514-525.
- [24] Zainulabidin, M. H., & Jaini, N. (2012). Transverse vibration of a beam structure attached with dynamic vibration absorbers: Experimental analysis. *International Journal of Engineering & Technology*, 12(6), 82-86.
- [25] Shi, H., Luo, R., Wu, P., Zeng, J., & Guo, J. (2014). Application of DVA theory in vibration reduction of carbody with suspended equipment for high-speed EMU. *Science China Technological Sciences*, 57(7), 1425-1438.

- [26] Basta, Ehab, Mehdi Ghommem, and Samir Emam. "Flutter control and mitigation of limit cycle oscillations in aircraft wings using distributed vibration absorbers." *Nonlinear Dynamics* 106 (2021): 1975-2003.
- [27] <https://www.linkedin.com/pulse/dynamic-vibration-absorber-case-study-neil-parkinson/>
- [28] Wang, Q., Zhu, Y., & Wang, W. (2019). Optimal design of a dynamic vibration absorber with multi-degree of freedom. *Journal of Sound and Vibration*, 452, 38-50.
- [29] Ko, J. M., & Ni, Y. Q. (2019). Vibration control of building structures using tuned mass dampers: A review. *Journal of Sound and Vibration*, 444, 259-282.
- [30] Sun, H., Du, X., & Pai, P. F. (2010). Theory of metamaterial beams for broadband vibration absorption. *Journal of intelligent material systems and structures*, 21(11), 1085-1101.
- [31] Huang, G. L., & Sun, C. T. (2010). Band gaps in a multiresonator acoustic metamaterial. *Journal of vibration and Acoustics*, 132(3).
- [32] Zainulabidin, M. H., & Jaini, N. (2012). Transverse vibration of a beam structure attached with dynamic vibration absorbers: Experimental analysis. *International Journal of Engineering & Technology*, 12(6), 82-86.
- [33] Gantzounis, G., Serra-Garcia, M., Homma, K., Mendoza, J. M., & Daraio, C. (2013). Granular metamaterials for vibration mitigation. *Journal of Applied Physics*, 114(9), 093514.
- [34] Peng, H., & Pai, P. F. (2014). Acoustic metamaterial plates for elastic wave absorption and structural vibration suppression. *International Journal of Mechanical Sciences*, 89, 350-361.

- [35] Shi, H., Luo, R., Wu, P., Zeng, J., & Guo, J. (2014). Application of DVA theory in vibration reduction of carbody with suspended equipment for high-speed EMU. *Science China Technological Sciences*, 57, 1425-1438.
- [36] Jiang, S. (2015). Finite-element design of metamaterial beams for broadband wave absorption. University of Missouri-Columbia.
- [37] Peng, H., Pai, P. F., & Deng, H. (2015). Acoustic multi-stopband metamaterial plates design for broadband elastic wave absorption and vibration suppression. *International journal of mechanical sciences*, 103, 104-114.
- [38] Cveticanin, L., & Mester, G. (2016). Theory of acoustic metamaterials and metamaterial beams: an overview. *Acta Polytechnica Hungarica*, 13(7), 43-62.
- [39] Liu, Y., Shen, X., Su, X., & Sun, C. T. (2016). Elastic metamaterials with low-frequency passbands based on lattice system with on-site potential. *Journal of Vibration and Acoustics*, 138(2).
- [40] Zainulabidin, M. H., Jusoh, N. M., Jaini, N., & Kassim, A. S. M. (2016). Effect of tuned absorber location on beam structure vibration by finite element analysis. *ARPJN Journal of Engineering and Applied Sciences*, 11(14), 8585-8591.
- [41] Mohamed Salleh, M., & Zaman, I. (2016). Finite element modelling of fixed-fixed end plate attached with vibration absorber. *ARPJN Journal of Engineering and Applied Sciences*, 11(4), 2336-2339.
- [42] Wang, T., Sheng, M. P., Guo, Z. W., & Qin, Q. H. (2017). Acoustic characteristics of damped metamaterial plate with parallel attached resonators. *Archives of Mechanics*, 69(1), 29-52.

- [43] Antoniadis, I., Chatzi, E., Chronopoulos, D., Paradeisiotis, A., Sapountzakis, I., & Konstantopoulos, S. (2017). Low-frequency wide band-gap elastic/acoustic meta-materials using the K-damping concept. arXiv preprint arXiv:1705.00226.
- [44] Li, Y., Baker, E., Reissman, T., Sun, C., & Liu, W. K. (2017). Design of mechanical metamaterials for simultaneous vibration isolation and energy harvesting. *Applied Physics Letters*, 111(25), 251903.
- [45] Sang, S., & Sandgren, E. (2018). Study of two-dimensional acoustic metamaterial based on lattice system. *Journal of Vibration Engineering & Technologies*, 6, 513-521.
- [46] Casalotti, A., El-Borgi, S., & Lacarbonara, W. (2018). Metamaterial beam with embedded nonlinear vibration absorbers. *International Journal of Non-Linear Mechanics*, 98, 32-42.
- [47] Sang, S., Sandgren, E., & Wang, Z. (2018). Wave attenuation and negative refraction of elastic waves in a single-phase elastic metamaterial. *Acta Mechanica*, 229, 2561-2569.
- [48] Johnson, W. R., & Ruzzene, M. (2018, March). Challenges and constraints in the application of resonance-based metamaterials for vibration isolation. In *Health Monitoring of Structural and Biological Systems XII* (Vol. 10600, pp. 489-500). SPIE.
- [49] Dong, G., Li, Q., & Zhang, X. (2019). Vibration attenuation using a nonlinear dynamic vibration absorber with negative stiffness. *International Journal of Applied Electromagnetics and Mechanics*, 59(2), 617-628.
- [50] Ong, W. S., & Zainulabidin, M. H. (2020). Vibration Characteristics of Beam Structure Attached with Vibration Absorbers at its Vibrational Node

and Antinode by Finite Element Analysis. JSE Journal of Science and Engineering,1(1),7-16.

[51] Anigbogu, W., & Bardaweel, H. (2020). A metamaterial-inspired structure for simultaneous vibration attenuation and energy harvesting. Shock and Vibration, 2020, 1-12.

[52] Song, Y., Wen, J., Tian, H., Lu, X., Li, Z., & Feng, L. (2020). Vibration and sound properties of metamaterial sandwich panels with periodically attached resonators: Simulation and experiment study. Journal of Sound and Vibration, 489, 115644.

Shock and Vibration, 2020, 1-12.

[53] Song, Y., Wen, J., Tian, H., Lu, X., Li, Z., & Feng, L. (2020). Vibration and sound properties of metamaterial sandwich panels with periodically attached resonators: Simulation and experiment study. Journal of Sound and Vibration, 489, 115644.

[54] Bao, H., Wu, C., Wang, K., & Yan, B. (2021). An enhanced dual-resonator metamaterial beam for low-frequency vibration suppression. Journal of Applied Physics, 129(9), 095106.

[55] Rupesh Tatte, Vishal Dhende. (2022). VIBRATION ISOLATION OF FIXED-FIXED BEAM USING DYNAMIC VIBRATION ABSORBE. Conference: 3rd National Conference on Recent Trends in Mechanical Engineering (NCRTME-2018).

[56] Haugland, E., & Lundberg, B. (2017). Piezoelectric accelerometers: Principles and applications. IEEE Instrumentation & Measurement Magazine, 20(2), 16-23

[57] Balachandran, B., & Magrab, E. B. (2018). *Vibrations*. Cambridge University Press.

Appendices



Optimal Design of Dynamic Vibration Absorber Based on Harmonic Analysis

Teeb Alhasnawi
Mechanical Engineering Department
University of Babylon
Babylon, Iraq
teeb.basim96@gmail.com

Salwan Obaid Waheed Khafaji
Mechanical Engineering Department
University of Babylon
Babylon, Iraq
eng.salwon.obaid@uobabylon.edu.iq

Abstract— This paper presents a damped dynamic absorber system with an optimal design. In order to build the dynamic absorber for improved performance, the principles of negative stiffness and mass are introduced and discussed in depth together with their physical justification. To meet optimization constraints and acquire the best values for design parameters, harmonic analysis is examined and harmonic response for an external excitation is analytically determined. The optimal damping ratios and frequency ratios for six mass ratios scenarios are simultaneously determined. The findings indicated that damping ratios are crucial variables, even for minor uncertainties. The nonlinear harmonic response was altered by dampening. The best values for ideal damping ratios and frequency ratio must be carefully chosen because they are not independent. Zero response is achieved for the amplitude response when $(\Omega < 0.25)$. Frequency ratio affect the response only in the range of $(0.5 < \Omega < 1.5)$.

Keywords— dynamic absorber, optimization, negative stiffness, negative mass

I. INTRODUCTION

Since many years ago, a numerous effective devices have been introduced. Dynamic vibration absorbers (DVA) are one of the most widely used as vibration control devices due to their efficiency, dependability, and affordability. Since Frahm [1-2] developed the first DVA without damping in 1909. A mass and a spring are traditionally attached to a vibrating body that vibrates harmonically or in a narrowband frequency range as an undamped DVA. A numerous works on optimization design [3-7] and vibration absorber tuning [8-12] have been completed. Some of the above researches are basically worked on positive springs effect. Another concept introduced about the negative stiffness, negative stiffness denotes the reversal of the relationship between external force and displacement in deformed objects. References [13-19] have research reports on the characteristics and stability requirements of the negative stiffness system. The system with negative stiffness (NS) has a higher load-bearing capacity than the system with only positive stiffness, and its natural frequency will also be decreased. By using the buckling of beams under axial load, [20] produced NS around equilibrium and obtained an isolation system by fusing it with a linear positive spring. NS principle was also used for vibration isolation as reported by [21-22] who put forth a new vibration

isolation system in which active control technique was used to achieve NS. [23] studied a passive DVA with a NS mechanism analytically and experimentally. A nonlinear vibration isolator with a negative stiffness mechanism was also studied by [24-26]. The available analytical solution for optimal parameters are time cost, limited in application, and are not valid when design parameters vary in values [27]. There has been little written about the ideal DVA with NS and negative mass (NM) parameters in details, despite the fact that the use of NS in vibration isolation systems has been the subject of extensive research due to its advantages. In this work, principles of negative mass and stiffness are explained along with their physical concepts. Optimal DVA parameters are determined using direct research method by adding a new constraint to the main objectives. Frequency range of the optimal values are studied as well for six cases of different mass ratios.

II. METAMATERIALS NEGATIVE PROPERTIES

A brief introduction about NS and NM are presented to explain their effect on the vibration characteristics

A. Negative Effective Mass

Fig. 1 shows a 2-DOF system exposed to a harmonic excitation. The equations of motion, frequency response functions (FRFs) H_{11} and H_{22} between the response $u_1(t)$ and $u_2(t)$ and the input harmonic force $F(t)$, are given by [7,9]:

$$\begin{bmatrix} m_1 & 0 \\ 0 & m_2 \end{bmatrix} \begin{bmatrix} \ddot{u}_1 \\ \ddot{u}_2 \end{bmatrix} + \begin{bmatrix} k_1 & -k_1 \\ -k_1 & k_1 \end{bmatrix} \begin{bmatrix} u_1 \\ u_2 \end{bmatrix} = \begin{bmatrix} F \\ 0 \end{bmatrix}$$

$$F = F_0 e^{i\Omega t}, \begin{bmatrix} u_1 \\ u_2 \end{bmatrix} = \begin{bmatrix} a_1 \\ a_2 \end{bmatrix} e^{i\Omega t}$$

$$\text{If } n=1, H_{n1} = \frac{a_1}{F_0} = \frac{k_1 - m_2 \Omega^2}{(k_1 - m_1 \Omega^2)(k_1 - m_2 \Omega^2) - k_1^2}$$

$$\text{If } n=2, H_{n1} = \frac{a_2}{F_0} = \frac{k_1}{(k_1 - m_1 \Omega^2)(k_1 - m_2 \Omega^2) - k_1^2}$$

For more convenience, the following terms are simplified as:

$$\frac{F}{m_1} = \frac{F_0}{- \Omega^2 a_1} = m_1 + \frac{m_2}{1 - \Omega^2 / \omega_2^2}, \omega_2 = \sqrt{\frac{k_1}{m_2}}$$

where m_1 and m_2 are the principal and absorber masses, respectively. F is the excitation harmonic forces applied at the principal mass. u_1 and u_2 are the degrees of freedom of principal and absorber mass, respectively. Ω is the excitation



LETTER OF ACCEPTANCE

Date: Monday, June 19, 2023
Paper ID: HCNAS_008

Dear Author,

On behalf of the HCNAS-23 Scientific Committee, and based on our (Reviewers' Evaluation, Scientific Committee Decision, and Guest Editors' Approval), we are pleased to inform you that your paper entitled

Experimental Evaluation of Dynamic Vibration Absorbers for Vibration Suppression in Beam Structure

Written by

Teeb Basim Abbas and Salwan Obaid Waheed Khafaji

Has been accepted in HCNAS Conference and selected to be processed for possible publication in AIP Conference Proceedings (ISSN: 0094-243X, 1551-7616). We have accepted your paper based on our initial technical checking, the positive double-blind reviews and your Paper's Scope and Subject. Remember that your paper in Camera Ready Version should accurately follow our reviewer comments and the technical notes. The publication Schedule of the accepted paper will be provided after passing the Internal Check of AIP Editors. The paper should not contain plagiarism (it that date (more than 15%), and the Camera Ready version should follow our conference Rules and AIP Ethics and Guidelines. Publication time depends on Publication Queue on AIP, and we will provide you with the required information after we finalize all selected Papers for our Conference and present the accepted papers at the conference session.

Thank you for considering this Conference as a venue for your work

Sincerely yours

Signature of Prof. Dr. Shuzhuan Sharma, Conference Guest Editor

Signature of Prof. Dr. Mohammad I. Mohammed, Chair of Scientific Committee

CAUTION: This Acceptance Letter is Made by ICAT (Special Session) Conference Guest Editors. All Approval and other Inquiries should be addressed to Conference Editorial Board and Editors Committee, as all accepted Papers will be Processed for Possible Publication in the AIP Conference Proceedings upon the Final Decision upon Publish of your Paper will be Made by AIP Publication Editors Only after Review the Paper Contents and Writing Quality.



Experimental Evaluation of Dynamic Vibration Absorbers for Vibration Suppression in Beam Structure

Teeb Basim Abbas^{1,2,a)} and Salwan Obaid Waheed Khafaji³

¹ MSC student at Mechanical Engineering Department, University of Babylon, Babylon

² Teaching Assistant at Almustaqbal University, Babylon

³ Mechanical Engineering Department, University of Babylon, Babylon.

^{a)} Corresponding author: teeb.abbas.engh421@student.uobabylon, Teeb.basim@uomus.edu.iq

Abstract. The efficiency of dynamic vibration absorbers (DVAs) in reducing vibrations in beam structures is experimentally assessed in this research. The dynamic vibration absorbers are small devices added to a structure, that use a mass-spring-damper system calibrated to the natural frequency of the structure to reduce vibration levels. The experimental examination included the addition of these absorbers to a beam structure and the measurement of the levels of vibrations under various circumstances. The dynamic behavior of a beam is examined experimentally under two boundary conditions (pinned-free, cantilever), with different configurations of the dynamic vibration absorbers' design parameters and placements along the beam. External vibrations are applied to the beam, and their amplitude is measured both with and without the absorbers. Investigations are conducted on the effects of the absorber's mass, stiffness, and locations. The findings demonstrated that adding DVAs to the beam structure greatly reduced vibration levels, especially at the beam natural frequency. Both mass and stiffness significantly reduce the dynamic response (from, for instance, 0.018m to 0.00652m). However, this effect changes based on the boundary conditions. If the DVA is situated at the point of maximum displacement, the minimal needs of the DVA parameters can better reduce the dynamic response.

Keywords. Dynamic vibration absorber, beam, experimental investigation, dynamic response.

INTRODUCTION

Vibration is a pervasive phenomenon in human activities. Light waves vibrate to enable vision, while eardrums vibrate to facilitate hearing. In engineering, the effects of vibration are considered in the design of machines, buildings, turbines, and engines. Most vibrations are considered undesirable due to their negative consequences such as elevated stress levels, energy loss, fatigue, reduced efficiency, and others. Excessive vibration in a system often leads to disruption, discomfort, damage, or even destruction. To prevent such outcomes in machinery or structures, it is necessary to control unwanted vibrations. One effective solution is to use what they called by Metamaterials for vibration attenuation [1-3]. One of the promising methods for vibration attenuation of the structure is using dynamic vibration absorbers (DVA) that provide a counter-back motion to eliminate vibration. This traditional DVA is only applicable to systems with one degree of freedom. [4,5] Consequently, its use is constrained. The development of vibration absorbers dates back to 1909. The first vibration absorber developed by Den Hartog consists of a second mass-spring device, similarly modeled as a mass-spring system, is attached to the main device and keeps it from vibrating at the same frequency as the sinusoidal force occurring on the main device. There is a well-known solution to this well-known vibrational problem. The main mass's vibration amplitude cannot be made zero at the driving frequency if damping is added to the absorber, but the system's sensitivity to changes in the forcing frequency reduces[6]. Wu looked at how an absorber's helical spring's inertia affected a beam's ability to dynamically respond



Experimental Evaluation of the Performance of Dynamic Vibration Absorbers for Vibration Mitigation in Beam Structures

T.B.Abbas¹ S.O. Waheed^{2,3}

1. MSC student at Mechanical Engineering Department, University of Babylon, Babylon,, e-mail.account

teeb.abbas.engh421@student.uobabylon.edu.iq

Teaching Assistant at Almustaqbal University, Babylon, e-mail.account

Teeb.basim@uomus.edu.iq

2. Mechanical Engineering Department, University of Babylon, Babylon,, e-mail.account.

eng.salwon.obaid@uobabylon.edu.iq

Abstract- In this study, experiments are used to evaluate the effectiveness of dynamic vibration absorbers (DVAs) in minimizing vibrations in beam structures. The dynamic vibration absorbers are modest additions to a structure that employ a mass-spring system tuned to the natural frequency of the structure to lower vibration levels. These absorbers were added to a beam construction as part of the experimental investigation, and the vibration levels under various conditions were measured. Under the pinned-free boundary, the dynamic behavior of a beam is experimentally investigated with various combinations of the design parameters (mass and spring) and locations of the dynamic vibration absorbers. The beam is subjected to external vibrations, and both with and without the absorbers, its amplitude is measured. According to the results, adding DVAs to the beam structure significantly reduced vibration levels, particularly closer to the natural frequency of the beam. The dynamic response is greatly reduced by mass and stiffness (from, for example, 0.018m to 0.00052m). However, depending on the DVA location, this effect can change. The minimal requirements of the DVA parameters can better reduce the dynamic response if the DVA is positioned at the point of maximum displacement for each corresponding mode.

Keywords: Dynamic vibration absorber, beam, Experimental investigation, dynamic response

1. INTRODUCTION

A common occurrence in human activity is vibration. Eardrums vibrate to permit hearing, while light waves vibrate to enable vision. The effects of vibration are taken into account when designing machinery, structures, turbines, and engines in engineering. Due to their detrimental effects, such as increased stress levels, energy loss, weariness, and decreased efficiency, the majority of vibrations are regarded as undesirable. When a system vibrates excessively, it frequently causes interruption, pain, harm, or even destruction. Unwanted vibrations must be managed if such results in machinery or structures are to be avoided. Utilizing what they refer to as Metamaterials for vibration reduction is one efficient remedy [1-3]. Utilizing dynamic vibration absorbers (DVA), which offer a counter-back motion to remove vibration, is one of the method's promising for vibration attenuation of the structure. Systems with a single degree of freedom are the only ones that can use this conventional DVA[4,5]. As a result, its utility is limited. Vibration absorbers were first created in 1909. Den Hartog's first vibration damper is made up of a second mass-spring device that is connected to the first device and prevents it from vibrating at the same frequency as the sinusoidal force acting on the primary device. This well-known vibrational issue has a well-known solution. If damping is added to the absorber, the main mass's vibration amplitude cannot be rendered zero at the driving frequency, but the system's sensitivity to changes in the forcing frequency decreases[6]. Wu investigated the effect of the inertia of the helical spring of an absorber on the dynamic response of a beam to a changing load[7]. Foda and Albassam studied vibration absorbers for beam structures with three different end conditions. Simple support, free, and clamped termination circumstances are applicable[8]. For beam vibration under point or dispersed harmonic stimulation, Wong et al. studied a DVA that combines translational and rotational type absorbers[9]. A structure's DVA will react to an external stimulation by applying some force in the

الخلاصة

تستخدم مخمدات الاهتزاز الديناميكية بشكل واسع لتقليل الاهتزازات للأنظمة الميكانيكية. تبحث هذه الدراسة فعالية المخمدات الديناميكية في تقليل الاهتزازات لكلا من انظمة مركزة (Lumped) وعتبه (beam) لشروط حدودية مختلفة. تضمنت هذه الدراسة جزئيين. تم في الجزء الاول تطوير موديل الرياضي للنظام الاول واطافة مبدئي المرونة السالبة والكتلة السالبة. درس تأثير عوامل مختلفة على الاستجابة الديناميكية للأنظمة اعلاه. استخدمت طريقة بسيطة وسهلة مباشرة لإيجاد التصميم الامثل لستة حالات مختلفة. بينت النتائج النظرية بأن الاستجابة الديناميكية للنظام الاساسي تقل بشكل كبير بزيادة نسبة التخميد. لم تكن الاستجابة الديناميكية حساسة جدا للتغيير في نسب التخميد للمخمد مقارنة بما يقابله للنظام الاساسي. ان التغييرات في قيم نسب الكتلة والتردد لم تؤثر على الاستجابة الديناميكية عندما تكون نسبة التردد اقل من ٠,٢٥. بالإضافة الى ذلك، الفرق في الاستجابة الترددية للنظام الاساسي اقل عند القيم الواطئة من نسب التردد وتزداد بشكل كبير عندما تصل هذه النسبة الى ١,٥. ان مديات التردد للتصميم الامثل تزداد بزيادة نسب الكتلة وان اقصى مدى للتردد من ٠,٢٢-١,٥ يحصل عندما تكون نسبة التردد ونسبة التخميد ٠,٦ و ٠,٣٢١ على التوالي.

اما في الجزء الثاني، فقد اجريت عدة تجارب مختبرية لتحليل الاستجابة الديناميكية لعتبة مع وبدون المخمد الديناميكي وثلاث حالات من الشروط الحدودية (pinned-free, cantilever, and fixed-fixed). سلط حمل خارجي ديناميكي وتم قياس الاستجابة للعتبة عند مواقع مختلفة على طولها باستخدام المعجلات. بينت النتائج العملية بانه كل من كتلة المخمد والسريرك لهما تأثير كبير في تقليل الاستجابة الديناميكية للعتبة بنسبة تخفيض وصلت الى ٩٧%. ان المتطلبات الاقل للمخمد يمكن ان تحقق افضل تقليل بالاستجابة الديناميكية للمخمد عندما يقع المخمد عند النقطة التي تحقق اعلى ازاحه للعتبة.



جمهورية العراق
وزارة التعليم العالي والبحث العلمي
جامعة بابل / كلية الهندسة
قسم الهندسة الميكانيكية

رسالة

تأثير مخر اهتزاز ديناميكي على خصائص الاهتزاز لعنبة تحت ظروف مختلفة

مقدمة إلى جامعة بابل / كلية الهندسة وهي جزء من متطلبات نيل شهادة
الماجستير في الهندسة / الهندسة الميكانيكية / تطبيقي

أعدت من قبل

طيب باسم عباس حمزه

بأشراف

الاستاذ الدكتور : سلوان عبيد وحيد خفاجي

١٤٤٤ هـ

٢٠٢٣ م